Investigation of two solid sample introduction techniques for the analysis of biological, environmental, and pharmaceutical samples by inductively coupled plasma spectrometry

Rebecca Lam

Department of Chemistry
McGill University
Montreal, Québec, Canada

November 2006

A Thesis submitted to McGill University in partial fulfilment of the requirements of the degree of Doctor of Philosophy

© Rebecca Lam, 2006

Library and Archives Canada

Published Heritage Branch

395 Wellington Street
Ottawa ON K1A 0N4
Canada

Bibliothèque et Archives Canada

Direction du Patrimoine de l'édition

395, rue Wellington
Ottawa ON K1A 0N4
Canada

Your file Votre référence
ISBN: 978-0-494-32202-4
Our file Notre référence
ISBN: 978-0-494-32202-4

NOTICE:
The author has granted a non-exclusive license allowing Library and Archives Canada to reproduce, publish, archive, preserve, conserve, communicate to the public by telecommunication or on the Internet, loan, distribute and sell theses worldwide, for commercial or non-commercial purposes, in microform, paper, electronic and/or any other formats.

The author retains copyright ownership and moral rights in this thesis. Neither the thesis nor substantial extracts from it may be printed or otherwise reproduced without the author's permission.

AVIS:
L'auteur a accordé une licence non exclusive permettant à la Bibliothèque et Archives Canada de reproduire, publier, archiver, sauvegarder, conserver, transmettre au public par télécommunication ou par l'Internet, prêter, distribuer et vendre des thèses partout dans le monde, à des fins commerciales ou autres, sur support microforme, papier, électronique et/ou autres formats.

L'auteur conserve la propriété du droit d'auteur et des droits moraux qui protège cette thèse. Ni la thèse ni des extraits substantiels de celle-ci ne doivent être imprimés ou autrement reproduits sans son autorisation.

In compliance with the Canadian Privacy Act some supporting forms may have been removed from this thesis.

While these forms may be included in the document page count, their removal does not represent any loss of content from the thesis.

Conformément à la loi canadienne sur la protection de la vie privée, quelques formulaires secondaires ont été enlevés de cette thèse.

Bien que ces formulaires aient inclus dans la pagination, il n'y aura aucun contenu manquant.

Canada

Abstract

In this thesis, new approaches to direct trace metals analysis of solid samples by inductively coupled plasma spectroscopy were investigated using laser ablation and thermal vaporization systems for solid sample introduction of biological, environmental, and pharmaceutical samples.

Laser ablation with inductively coupled plasma atomic emission spectroscopy (ICP-AES) and inductively coupled plasma mass spectrometry (ICP-MS) was applied to pharmaceutical tablets. Precision of analysis depended on laser parameters and could be improved using signal ratios. The feasibility of using laser ablation-ICP-MS for detecting natural levels of mercury along a single human hair strand was also demonstrated.

As well, the use of an induction-heating electrothermal vaporizer (IH-ETV) coupled to an ICP-MS was successful in determining mercury concentrations in a single human hair strand. Methodologies for multielement analysis of powdered hair were also explored using IH-ETV-ICP-MS. While calibration by reference hair materials showed promise, calibration methods by liquid standards were not suitable for any element. Detection limits achieved for most elements were below natural levels found in human hair.

IH-ETV-ICP-AES was also applied to the analysis of analyte-laden chromatographic powder. This study showed potential problems that may arise due to the methodology taken to analyze such materials. Finally, recommendations for future investigations and methodologies for laser ablation and thermal vaporization are discussed.

Résumé

Cette thèse décrit de nouvelles techniques d'analyse de métaux en traces dans des échantillons solides par la spectroscopie à plasma induit. Les recherches des systèmes d'ablation laser et de vaporisation thermique ont étés élaborées pour l'analyse d'échantillons biologiques, environnementaux, et pharmaceutiques à l'état solide.

L'ablation laser couplée à un spectromètre d'émission atomique à plasma induit (ICP-AES) ainsi que couplé à un spectromètre de masse à plasma induit (ICP-MS) ont été utilisées pour l'analyse de comprimés pharmaceutiques. La précision dépend des paramètres du laser et peut être améliorée grâce aux rapports de signaux. Nous avons aussi démontré que l'ablation laser couplée à l'ICP-MS peut être utilisée pour la détection de mercure a des niveaux naturels dans un brin de cheveu.

De même, le vaporisateur électrothermique à chauffage induit (IH-ETV) couplé à l'ICP-MS permet la détection et le dosage quantitatif du mercure à de très faibles concentrations (naturelles) dans un brin de cheveu. La possibilité d'utiliser ce dispositif affin de doser d'autres éléments dans des cheveux en poudre a aussi été examinée. Il a été démontré que les étalons de références certifiés (cheveux en poudre) pouvaient être utilisés pour l'étalonnage alors que les étalons liquides ne convenaient pas. Ce dispositif permet la détection d'éléments à des concentrations plus basses que ce que l'on retrouve normalement dans les cheveux.

L'IH-ETV couplé à l'ICP-AES a aussi été utilisé pour faire l'analyse multi-élémentaire de matériel chromatographique. Cette étude met en évidence plusieurs problèmes qui peuvent survenir en raison des méthodes de préparation des échantillons.

Finalement, les recommandations pour les recherches futures sont formulées et les méthodologies pour l'ablation laser et la vaporisation thermique sont discutées.

Contributions to original knowledge

1. The application of laser ablation for ICP analysis of pharmaceutical tablets was evaluated. Precision depended on the laser's parameters and could be improved from 12–31% to 1–6 % with internal standardization.
2. LA-ICP-MS was demonstrated to be able to detect natural levels of Hg in a single human hair strand, as well as temporal changes in Hg concentrations along the hair strand.
3. A method for the quantification of mercury in a single human hair strand using IH-ETV-ICP-MS was developed. No sample preparation was required, and the results achieved by external standardization with certified reference materials were comparable with a reference method.
4. The multielement analysis of powdered hair samples was investigated using IH-ETV-ICP-MS. Detection limits achieved were sufficient to detect As, Cd, Cu, Pb and Zn at natural levels.
5. Using IH-ETV-ICP-AES, the direct analysis of 8-hydroxyquinolate metal complexes adsorbed on chromatographic powder (silica gel) was shown for the first time. The shape of the time profile and the magnitude of an analyte's signal are affected by other analytes and the silica gel matrix.

Contributions of authors

In addition to the introduction and conclusions, the contents of this Thesis are presented as three published manuscripts (Chapters 2–4), and two additional thesis chapters (Chapters 6 and 7) that are being prepared for submission to peer-reviewed journals. Appendix A reports on an additional project while Appendices B–D include additional experimental details in support of these chapters.

Prof. Eric D. Salin of McGill University supervised all of the work presented, and was available for project guidance and direction throughout.

The experiments described in Chapters 2, 5 and 6 were designed, conducted, and interpreted by the author under the supervision of Dr. Salin. The text in Chapter 2 has been published as the following manuscript:

"Analysis of pharmaceutical tablets by laser ablation inductively coupled plasma atomic emission spectrometry and mass spectrometry (LA-ICP-AES and LA-ICP-MS)", Rebecca Lam and Eric D. Salin, Journal of Analytical Atomic Spectrometry, 2004, 19(7), 938-940.

Experiments described in Chapter 3 were designed by the author. They were either carried out by the author herself or by Madeleine Jensen-Fontaine, an undergraduate student under the immediate supervision of the author. Dr. Hing Man Chan (then a professor with the McGill University School of Dietetics and Human Nutrition) and Melissa Legrand (a graduate student under his direction) offered their expertise in discussions of hair analysis. Melissa Legrand also performed the collection and the digestion of the hair sample studied. The work is presented in the following manuscript:

"Direct detection of mercury in single human hair strands by laser ablation inductively coupled plasma mass spectrometry (LA-ICP-MS)", Melissa Legrand, Rebecca Lam, Madeleine Jensen-Fontaine, Eric D. Salin, and Hing Man Chan, Journal of Analytical Atomic Spectrometry, 2004, 19(10), 1287-1288.

The author designed and performed all experiments and data treatment presented in Chapter 4. Josiane P. Lafleur, an undergraduate student, had performed a preliminary study leading to this work and offered helpful discussion. Dr. Chan again contributed his expertise in hair analysis. This work has been published and appears in the following manuscript:

"Induction heating-electrothermal vaporization for direct mercury analysis of a single human hair strand by inductively coupled plasma mass spectrometry", Josiane P. Lafleur, Rebecca Lam, Hing Man Chan, and Eric D. Salin, Journal of Analytical Atomic Spectrometry, 2005, 20(12), 1315-1317.

The author of this doctoral thesis wrote the text that appears in the three published manuscripts, while the listed co-authors aided in the editing process. These manuscripts are reproduced with the permission of The Royal Society of Chemistry (RSC). Waivers obtained from the RSC and the listed co-authors may be found in Appendix E.

Acknowledgements

This thesis is the result of five (at times, seemingly long) years of work that would have been impossible without the help of the following people.

First and foremost, I would like to thank my thesis supervisor, Dr. Eric Salin. The opportunity to go to conferences, as well as his utmost patience with my work habits were genuinely appreciated. My self-confidence has grown enormously under his guidance and friendship, to which I am forever grateful.

I would also like to thank Dr. David Burns and Dr. Joan Power of the Chemistry Department for providing feedback on my research at the yearly seminars. Members of the department's technical staff (Fred Kluck, Bill Bastian, Rick Rossi and Georges Kopp) also deserve many thanks for fixing the various things that have gone wrong over the years. Thanks to Chantal Marotte for taking care of the administrative side of graduate studies.

Thank you to all of the members of the Salin lab over the past five years for your friendship and moral support. Special thanks go to Julie Asselin and Jian Min Ren for their assistance with the ETV, Isabelle Levesque for her expertise with the construction of the digital ETV controller, and Madeleine Jensen-Fontaine and Josiane Lafleur for their contributions to the hair projects.

A heartfelt 'thank you' goes to Rob, who endured my late work hours and rants. He made me realize that sometimes, there are more important things than lab work.

Finally, thank you to my family for always encouraging me to pursue my dreams.

Table of contents

Table of figures

Table of tables

Chapter 1 Introduction

1.1 The importance of trace metal analysis

The knowledge of chemical composition plays an important role in all aspects of daily life. Specifically, metals can have a large impact due to their effects on the environment, toxicological properties, and the role they play in sustaining many biological systems. The extent of pollution and its transport can be followed from the concentrations of metals found in the environment [1]. The metal concentrations in a human body or any living organism can be used to assess illness, nutrition or toxic exposure [2, 3] in addition to revealing the underlying mechanisms of biological reactions [4, 5]. Determination of the elemental composition can verify the safety of our water supply [6] and foodstuffs [7]. Quality control in industry often depends on finding trace contamination, such as in the manufacture of semiconductors [8]. Trace metal analysis has even found use in forensics [9] and art authentication [10].

1.1.1 Common methods of metals analysis

Spectrochemical analysis dates back to the late 1800s, when Gustav Kirchoff and Robert Bunsen demonstrated that metals could be identified and quantified by the colours and intensities they produced when sprinkled into a flame. Flame photometers had become commercially available by the 1950s, when flame instruments had grown in popularity for metals analysis.

In modern flame instruments, a solution of the sample is nebulized into the flame where atomization and ionization occur in the 2000°C environment. Detection is either

achieved by atomic emission spectroscopy (AES), atomic fluorescence spectroscopy (AFS), or most commonly in current commercial systems, atomic absorption spectroscopy (AAS). Precision is typically 1% RSD (relative standard deviation) with detection limits from the parts per million to parts per billion range for many elements.

Historically, arc, spark, and X-ray fluorescence systems were the first instruments that were able to directly sample solid materials for atomic spectroscopy. Arc and spark discharges have been used since the 1920s for qualitative and quantitative atomic emission spectroscopy, while X-ray fluorescence gained wide use in the 1950s. These multielement methods are described in more detail in section 1.3.

In the 1970s, commercial instruments using a graphite furnace with atomic absorption spectroscopy (GF-AAS) were introduced. By heating the graphite furnace in which the few microlitres of solubilized sample is placed, thermal vaporization is used to atomize the sample. When compared to flame systems, enhanced sensitivity and detection limits that are a magnitude lower are seen with furnace systems. Since the radiation source for the absorption measurement is usually a hollow cathode lamp, GF-AAS is predominantly a single element technique.

In some situations, the unique physical or chemical properties of an element can lead to the development of specialized methods. Mercury is one such case, due to its low vapor pressure at room temperature. In the cold-vapor atomic absorption spectroscopy (CV-AAS) technique, any mercury present in the sample is first oxidized to Hg^{2+}, typically using a mixture HNO_3 and H_2SO_4. The Hg^{2+} is then reduced to elemental Hg^0 with $SnCl_2$. The elemental Hg^0 vapor is swept into a long-pass cell where the atomic absorption is measured at 253.7 nm, where detection limits down to the parts per billion level are achievable. Modern mercury analyzers that automate the reduction and detection

steps in CV-AAS are common in laboratories where mercury analyses are performed on a routine basis. Systems using atomic fluorescence detection have also been commercialized.

In the past 25 years, multielement metal analysis has become routine due to the evolution and commercialization of inductively coupled plasma (ICP) instruments. Review articles on the applications of ICP instruments show the wide variety of samples that can be analyzed, such as geological materials, environmental samples, and biological matter [11-13].

There are several characteristics of ICP instrumentation that make it advantageous over the other mentioned methods for metals analysis. For trace analysis, advances in electronics and engineering have made detection limits on the order of parts per trillion possible for ICP instruments. The large linear dynamic range and high sensitivity of ICP instruments have served well in determining both minor and trace elements in various samples. At least 70 elements can be quantified by ICP. Fast sample throughput is possible since as many as 20–30 elements can be determined in a single sample analysis of a few minutes. The multielement capability also allows the use of calibration methodologies such as internal standardization, as well as isotope determination with mass detectors.

1.1.2 Inductively coupled plasma instrumentation

Inductively coupled plasma instrumentation is comprised of three parts: the sample introduction system, the inductively coupled plasma (ICP), and either a mass or optical detection system. In this section, the ICP and detectors will be discussed, while sample introduction systems will be examined in more detail in section 1.2.

1.1.2.1 The inductively coupled plasma

The housing for the ICP is a quartz torch that sits inside an induction coil powered by a radio-frequency (RF) generator (0.5–2 kW of power at (usually) 27 or 41 MHz). The torch is made of three concentric quartz tubes. The outer tubes facilitate the flow of argon that support the eventual plasma discharge, while the innermost tube serves as a pathway for analyte to be introduced to the plasma. When argon flows through the torch, the RF generator creates a high current flow in the coil. A spark introduces electrons into the argon gas flow. As these electrons are accelerated in the magnetic field produced by the coil, inelastic collisions with argon atoms result in collisionally-induced ionization. The argon ions and the released electrons undergo further collisions, until a stable plasma is formed when the rate of ionization equals the rate of recombination.

The plasma, a partially ionized gas discharge, is formed at atmospheric pressure. It is analogous to a flame, but achieves higher gas temperatures (4500–8000°C) and electron temperatures (8000–10000°C). At these high temperatures, the role of the plasma in an ICP instrument is to atomize, excite and ionize a sample. Since argon gas is typically used to form the plasma, the plasma itself is a chemically inert environment that reduces the formation of oxides. Self-absorption and self-reversal effects that may be present in other atomizers are not encountered in plasmas.

1.1.2.2 Optical detection

The ICP was first developed as an excitation source for atomic emission spectrometry in the 1960s [14-16]. In the plasma, excited atoms or ions will emit light of characteristic wavelengths upon relaxation. The intensity of the emitted light is proportional to the analyte concentration. Modern inductively coupled plasma atomic

emission spectrometers (ICP-AES) typically use a Czerny-Turner arrangement with an echelle grating to separate the wavelengths and a cross-dispersion element to separate overlapping orders. A two-dimensional array-based detector, such as a charge-coupled device, measures the emitted light.

Detection limits for ICP-AES for most elements are in the parts per billion level. Array-based detectors allow simultaneous detection of numerous emission wavelengths. Problems encountered in ICP-AES analysis include spectral overlap of atomic lines and molecular band species, and shifts in the background continuum emission due to the sample matrix.

1.1.2.3 Mass detection

The first interfacing of an argon plasma with a mass detector was achieved in 1980 [17]. The atmospheric pressure plasma is interfaced to the mass detector, which is under vacuum, by a sampler and a skimmer cone. Both cones are metal (typically nickel or platinum) and contain a small orifice in the middle to allow the passage of plasma gas. The region between the cones is under 0.1–1 torr in pressure. The fraction of the gas that passes through the skimmer cone enters a chamber maintained at the pressure of the mass spectrometer (10^{-5} – 10^{-7} torr). In this chamber, the gas passes through a series of ion lenses that focus the positive ions into a narrow beam, while at the same time preventing the transmission of neutral atoms and photons to the detector.

The focused ions then go through a mass analyzer that separates the ions by their mass to charge ratio. A scanning quadrupole is the most common type of mass analyzer used in commercial ICP-MS systems due to its fast scanning properties and low cost. An electron multiplier detector is then used on either a pulse count or analog mode to detect

the number of ions. Other variations of ICP-MS systems available include time-of-flight instruments and high-resolution magnetic sector instruments with single or multiple-collector arrangements.

ICP-MS can achieve better detection limits than ICP-AES, with detection limits in the parts per trillion. Isotopic analysis is also possible. However, interferences may arise from spectral overlaps, while matrix effects from the sample can enhance or suppress the analyte signal.

1.2 Sample introduction for atomic spectroscopy

1.2.1 Conventional sample introduction

For analysis by commercial ICP instrumentation, the samples are conventionally required to be in a solution form. This also holds true for other instruments for metals analysis such as commercial flame-AAS or flame-AES systems, GF-AAS and CV-AAS mercury analyzers.

In a commercial ICP instrument, the sample is usually pumped into a nebulizer that converts the solution into an aerosol. A spray chamber is used to segregate the droplets, allowing only the fine droplets to be swept into the central channel of the ICP torch. In the plasma, the sample aerosol is desolvated, atomized, and finally ionized for detection. Pneumatic nebulizers, using concentric or cross-flow arrangements, are the most common type used. Ultrasonic nebulizers [18] and direct injection nebulizers [19] have also been used for the analysis of solution samples. A detailed review of nebulizers and the processes that affect the transport of sample aerosol is available in the literature [20].

Solution nebulization offers several advantages. A solution sample is homogenous in composition and allows for dilution if necessary. Several calibration methodologies are available for solution samples, which include external standards, standard additions, and internal standard calibration. Standard reference solutions are easy to make or are commercially available. A survey of commercially available pneumatic nebulizers and spray chambers showed that precision of analysis was typically 1% RSD [21].

1.2.2 The need for solid sample introduction methods

While solution nebulization offers advantages, it is not perfect. Nebulizers can clog if the solution sample has a high dissolved solids content or any undissolved particles. Since large droplets are removed from the sample aerosol before reaching the plasma, transport efficiency is generally limited to 1% [21]. In addition, spectral interferences in ICP-MS systems become a problem due to polyatomic ions that can be formed from solvent.

Many sample types, such as soils and foodstuffs, are in the solid form. In the case of solids, a sample preparation step is required to either digest the solid matrix of the sample, or to extract the analytes of interest from the matrix to obtain a sample in solution form. This requirement can add many disadvantages.

First, such a sample preparation step can be laborious and time consuming. While a typical analysis of a solution by ICP can be completed within minutes, the sample preparation step can take many hours. To completely release the metals from the sample matrix, a complex procedure may be require. An example is provided by Lachas *et al.* for the preparation of coal samples [22]. Samples are first ashed in concentrated H_2SO_4 to digest the organic matrix. The resulting mixture is heated on a hot plate for three hours, followed by further heating in a furnace. Then, the mixture is treated with $HClO_4$ and HF, and heated again to dryness. Finally, the residue is dissolved in dilute HNO_3 for analysis by ICP spectrometry. This example demonstrates the multi-step process that is often required in the preparation of solid samples.

Microwave extraction is often employed to decrease the sample digestion time. For the coal samples mentioned in the previous paragraph, a microwave procedure using

HNO_3 requires only fifteen minutes of heating time. However, in this case, the samples also required filtration and a one-hour period of cool-down time to prevent loss of analytes upon removal from the microwave.

Due to the time required for chemical sample preparation, analyses can be expensive in terms of the labor required to perform the task. It can also be costly in terms of additional equipment and space for fumehoods, furnaces and microwave digestors, in addition to storage space required for the samples themselves during the many steps. Pure and ultrapure reagents used during sample preparation or for preconditioning of sample storage containers can also quickly add to the overall cost per sample.

Hazards to the environment and to the workplace personnel also increase with the use of solvents in sample preparation. The use of concentrated $HClO_4$ or HF, for example, requires extra safety precautions. The production, use and disposal of solvents are energy-consuming and place a burden on the environment.

Every extra step in handling the sample increases the risk of sample contamination from the reagents or improperly prepared sample containers. The potential for human error is also increased with each extra step of sample handling. Analyte loss may also become a problem, from either improper sample transfer from one container to another or the loss of volatile analytes during heated digestion/extraction procedures.

One strategy to eliminate the need for the digestion or extraction of the sample is to use slurry nebulization [23, 24]. In this method, minor sample preparation is still required as samples need to be powdered. An aqueous dispersion of the fine powder is then nebulized into the ICP instrument, in a similar manner to solution nebulization. Slurries have also been used for atomic absorption analysis by graphite furnace [25]. However, for successful analysis, the slurry requires a complete, uniform dispersion and a

correct particle size distribution [26]. Consequently, this method may not be suitable for all solid samples.

Ideally, a technique where the solid sample can be placed "as is" directly into an instrument with no sample pretreatment is needed. Solid sample introduction methods, where the sample digestion/extraction step is eliminated, pose many advantages. Overall analysis time is reduced, increasing sample throughput for routine analyses. The ability to have a result within minutes can provide rapid feedback when it is a question of toxicity or quality control. The analysis procedure is also simplified and less labor-intensive, potentially reducing the overall cost per sample. The risk of contamination of sample and analyte loss is reduced. The elimination of solvents makes solid sample introduction more environmentally friendly and fits with the current drive towards green chemistry.

1.3 Solid sample analysis systems

There exist several methods of direct analysis for solid samples, where little to no sample preparation is required. The following sections discuss the most common solid sample analysis methods that have been historically used or still exist today as stand-alone systems.

1.3.1 Dc Arc spectroscopy

A dc arc device typically consists of two electrodes, both commonly made of graphite. One cup-shaped electrode contains the solid sample in the form of a powder while the other acts as a counter electrode. An arc, a high direct current (approximately 10 A) low voltage (10–50 V) continuous electrical discharge, forms between two conducting electrodes. The current through the graphite heats the cup and vaporizes the sample while the plasma (arc) excites the analytes that are carried from the cup into the plasma. Originally the emitted light intensity was detected using a photographic plate. Later, detection with photomultipliers was used.

While there is still some development of novel arc systems [27], arc spectroscopy has fallen from routine use today due to sample requirements, precision, and calibration issues [28]. The arc does not necessarily contact the electrode in the same place from one analysis to another. This "arc wander" causes different portions of the electrode to be sampled, resulting in poor precision for replicates of the same sample. This also limits the use of arc ablation for analyses requiring high spatial resolution, restricting arc ablation to homogenous samples. Calibration is also a problem, as the energy dissipated in the arc (and therefore analyte emission intensity) depends on the sample matrix.

1.3.2 Spark spectroscopy

In spark ablation, the sample itself is used as an electrode. Metal samples can be ground flat, while powders can be pressed as a pellet. The spark is an intermittent high-voltage (1–10 kV) low-current (1–10 mA) electrical discharge that is formed between a counter electrode and the sample. This spark, lasting a few microseconds, vaporizes small portions of the sample's surface.

Like arc ablation sources, spark sources can be coupled with simple atomic emission detection systems. Detection is most commonly carried out using a polychromator with photomultiplier tubes. Spark systems are still made commercially by several companies, and are commonly found in foundries and metal-casting facilities. The majority of spark systems sold are used for routine analysis of iron, aluminum and copper alloys, where detection limits down to 10 ppm are achieved for elements in steel [29].

Spark ablation is more precise than arc ablation, since the sample is sampled by successive discharges that strike many different locations on the samples surface during one analysis. Unlike arcs, intermittent sparks propagate in the same direction instead of "wandering". However, the amount of material sampled may change with sparking time. Correction for the change in mass vaporized from one analysis to another must be done with the use of an internal standard [30]. As in arc ablation, the samples themselves must be conductive or mixed with a conductive binder. Its detection limit also restricts its use for trace analyses.

1.3.3 X-ray fluorescence

In X-ray fluorescence spectroscopy (XRF), a source of X-rays is used irradiate the sample. The most common source of X-rays is the X-ray tube, an evacuated tube containing a tungsten filament cathode and an anode containing a target metal (such as molybdenum or tungsten). Electrons produced at the cathode are accelerated by a potential as high as 100 kV towards the target metal. Upon collision, part of the energy beam is converted to primary X-rays. These primary X-rays are used to irradiate a sample.

When the atoms in the sample absorb the X-rays, an electron from the inner energy shell of the atom may be ejected. An electron from a higher energy shell immediately drops down to fill the void, with the excess energy emitted as fluorescent X-rays. These fluorescent X-rays are emitted with characteristic energies that can be used to identify the elements present in the sample.

Two different detection configurations are commonly used in commercial instruments. In wavelength-dispersive XRF, dispersion is achieved using diffraction crystals in a multi-channel arrangement with gas flow counters or scintillation counters for simultaneous multielement detection. In energy-dispersive XRF, a semiconductor transducer such as a Si(Li) lithium-drifted silicon detector acts as both the dispersive element and detector.

Chemical analysis by X-ray was first applied to minerals by Hadding in 1922 [31]. Improvements to XRF instrumentation and applications is still actively pursued, as covered in a review by Potts *et al.* [32]. Portable XRF systems have also been developed for field use [33]. The technique is ideal for major and minor element determination,

where it is often used for geological applications. Detection limits for a variety of elements in silicate rocks are reported to range from 9–300 ppm [34]. In addition to geological applications, XRF has also found clinical use [35]. Toribara *et al.* reported a precision of 1% and detection limits in the low parts per million range for the analysis of single human hair strands [36].

The main advantages of XRF include multielement detection and preservation of the sample since the radiation does not destroy it. However, XRF can suffer from matrix effects as the fluorescent X-rays can be reabsorbed by the sample. While precision of this technique can as good as solution nebulization methods, the technique is limited for trace analysis by its relatively poor detection limits. XRF is also not sensitive for light elements.

Though not as widely used as XRF, other similar radiative techniques for solid samples exist. Particle-induced X-ray emission (PIXE) [37] and neutron activation analysis (NAA) [38] are techniques in which solid samples are bombarded with ion beams or neutrons to determine their trace metal concentrations.

1.3.4 Laser induced breakdown spectroscopy

Laser induced breakdown spectroscopy (LIBS) employs a laser as both a sampling and excitation tool. A laser pulse is fired at the sample, causing local heating of the material at the impact spot. The localized heating results in the ejection of a small amount of sample material, containing solid particles, liquid drops and atomic vapor. The interactions between the laser pulse and the free atoms cause a small, hot plasma (duration 5–20 ns) to form at the focus of the laser, either at the sample's surface or

directly into the sample. Within this mini-plasma, the sample's atoms are excited and emit light. Therefore, the sampling, excitation and (possibly) ionization steps occur within the same step of the process. The emitted light is then measured by an optical detection system.

Nd:YAG lasers are commonly used as they are compact. A high power density (minimum 1–10 MW cm^{-2}) is a requirement for generating the laser plasma. Consequently, the fundamental wavelength of 1064 nm is typically used since it provides high power density. Methods of spectral resolution include filters or spectrometer-based systems. Photomultipliers and array detectors have been used. A review of the effects of instrument design on quantitative analysis by LIBS is covered by Tognoni *et al.* [39].

In another review article, Lee covered recent applications of LIBS [40]. St-Onge *et al.* reported the use of LIBS for zinc alloy analysis, achieving detection limits of 10–500 ppm for Al, Cu, Fe, Pb and Sn with an average RSD of 13% [41]. Capitelli *et al.* report detection limits ranging from 30–100 ppm for the analysis of soils, while comparisons with ICP analyses only showed partial agreement [42].

The *in-situ* analysis simplifies the equipment required (only a laser for sampling and an atomic emission detector). The technique can also be applied to solids, liquids, and gaseous samples. The use of fibre optics in the optical detection system allows for remote analysis, an advantage for the analysis of chemically hazardous samples. The potentially compact size of the laser and the detection system allows LIBS to be used in field-portable instrumentation.

However, the amounts of sample vaporized and plasma properties (such as temperature and electron density) are strongly dependent on the laser pulse and the physical properties of the sample itself. These limitations can affect precision and

accuracy. Matrix effects are pronounced in LIBS since the laser both ablates and excites the sample. In general, applications of LIBS show detection limits in the parts per million range, which is insufficient for trace metal analysis.

1.3.5 Graphite furnace-atomic absorption spectroscopy

The graphite furnace system was developed as an alternative to flame systems for the analysis of solutions. The analysis of solid samples by GF-AAS was first proposed by L'vov in 1959. [43] A common commercial design involves a graphite furnace tube of Massmann design [44] (approximately 5 cm in length, 1 cm diameter) in which a solid sample is placed by a spatula. As an alternative, the solid sample may be placed in a sample "boat" that is then placed inside the furnace. Slurry sampling has also been investigated [25].

The graphite tube is held tightly in a pair of precisely machined graphite contact electrodes. Current is applied to the electrodes and the graphite furnace is heated ohmically to vaporize and atomize the sample. A temperature program can be applied to first ash an organic matrix at a low temperature before atomizing the sample at a final temperature of 2000–3000°C. Absorption of the vaporized analytes is then measured.

Reviews of solid sampling with both laboratory-built and commercial GF-AAS instruments are available [45-48]. Precision of GF-AAS analysis of nickel-based alloys was found to range from 7–25%, depending on the element [49]. Schron *et al.* found that the solid matrix of geological or ceramic material greatly affected absorption signal, while achieving detection limits ranging from 0.006–150 ppm [50].

One problem seen with solid sampling-GF-AAS is that incomplete atomization of samples can lead to molecular interferences in absorption measurements. The method is also usually restricted to single element analysis and has a relatively short linear calibration range. Poor precision may result due to inhomogeneity of samples, since only small samples (typically 0.1–10 mg) can be placed in the furnace.

1.4 Solid sample introduction techniques for ICP

Hybrid (or hyphenated) methods involve coupling technologies in order to combine the best features from each component. The resulting combined instrumentation may achieve capabilities not possible by the individual subsystems.

The coupling of certain solid sampling methods with ICP instrumentation is such a case. Advantages offered by ICP instruments have provided impetus for researchers to adapt existing solid sample systems or to develop new solid sample introduction technology for use with ICP instruments. In this case, the role of the solid sample introduction system is to break down a portion of sample through ablation, serve as a direct means for placing the solid sample into the plasma of the ICP, or to vaporize the sample through a thermal process. The ICP serves as the atomizer and excitation system and the detection systems is/are conventional.

1.4.1 Arc nebulization

Arc discharges similar to those in arc spectroscopy systems have been described for use as a sample introduction systems for ICP instrumentation. Rusak reported detection limits in the parts per million range for Mg in geological samples by arc-ICP-AES [51]. Jiang *et al.* reported that oxide interferences seen with conventional solution analysis were not seen with solids analysis by arc-ICP-MS, with detection limits also in the parts per million range [52, 53]. Samples analyzed by this method are required to be conductive or made conductive by embedding in a conductive matrix.

1.4.2 Spark ablation

In 1976, Human *et al.* first showed that a conventional high voltage spark discharge setup could be used as a sample introduction device for ICP-AES analysis of copper in aluminum alloys and iron in brass [54]. As with spark spectroscopy, samples need to be conductive or mixed with conducting powder for analysis [55]. The use of spark discharge with ICP-MS was demonstrated by Ivanovic *et al.* in 1992 [56]. They showed that analysis of copper alloy standards containing trace elements with concentration ranges from 0.75–125 ppm produced linear calibration curves. They also reported that internal standardization procedures were not required, as in spark spectroscopy. Spark ablation devices have even been developed commercially as sample introduction accessories for ICP instruments.

1.4.3 Laser ablation

Like LIBS, laser ablation (LA) uses a laser as the sampling method. However, the role of the laser is not to form a localized plasma, but to ablate a portion of the solid sample to produce some transportable material in the form of vapor and small particulates. A crater is formed in the sample if the laser is fired at one spot, while trenches are formed if the laser is continuously fired while the beam is moved with respect to the sample. The ablated vapor and particulate are swept by an inert carrier gas to the ICP for atomization and detection. A good correlation exists between the ablated sample mass and the analytical signal of the detector since the material is usually completely vaporized in the atomization step, independently of the ablation step by the laser.

In commercially available laser ablation systems, the lasers are typically operated in the UV wavelength range. Frequency multiplied Nd:YAG lasers (213, 266 nm) and excimer lasers (157, 193 and 308 nm) are commonly used as shorter wavelengths offer higher energies for efficient bond breaking of the solid sample [57]. Samples are placed on a translation stage, so that the *x-y* position of sample with respect to the laser as well as the laser's focus can be controlled. The optical pathway of a laser ablation system often includes a microscope or a CCD camera with a monitor so that the user can visually observe the laser sampling process. Through a computer interface, the user can control the laser frequency along with the laser power.

The first use of laser ablation with a flame atomic absorption system for the analysis of nickel-based alloys was reported by Kantor *et al.* in 1976 [58]. Laser sampling for graphite furnace AAS has also been documented [59]. When commerical ICP technology was emerging in the 1980s, Gray reported the use of laser ablation as a sample introduction method for ICP-MS [60] while Darke *et al.* later reported the use of laser ablation with ICP-AES detection [61]. Since then, laser ablation has grown to be a popular method for direct sample introduction into ICP instruments, with several manufacturers offering commercial laser ablation systems.

Unlike arc or spark ablation devices, lasers can be used to ablate a wide variety of organic or inorganic materials, regardless of their physical properties. Little sample preparation, if any, is required. Little sample is needed as the laser can remove spots of material 10–100 micron in diameter from the sample (equivalent to less than a microgram of sample). Due to the ability of the laser to focus on specific locations on the sample, this technique offers high spatial resolution.

Review articles have shown that laser ablation in recent years has been applied to a wide variety of samples [57, 62-64]. Biological analyses have included fish otholiths [65] and human fingernails [66], while laser ablation has been used for analysis of tree rings in environmental analyses [67]. Metallurgical and geological applications still dominate the field of laser ablation. Lichte reported that using LA-ICP-MS for the analysis of rocks, an accuracy of 5% and a detection limit of 0.01 ppm for many elements could be achieved [68].

Calibration is a problem when using laser ablation with ICP instrumentation. To compensate for variations in laser output between shots and therefore differences in the amount of sample ablated, internal standardization is often required. This requires doping the sample or using naturally occurring element present in the sample. To avoid matrix interference, calibration using matrix-matched standards is often required. However, such standards may not exist for the matrix of interest or are difficult to synthesize.

Approaches using a tandem liquid calibration methodology, where a liquid standard solution is simultaneously introduced to the ICP, have also been attempted [69]. Leach *et al.* reported measured concentrations using a tandem methodology that were within 8% of the certified values for a steel reference material [70]. However, in an ICP-MS system, using solutions can introduce polyatomic interferences from the solvent if a wet aerosol is used. Overall sensitivity can also be decreased due to the dilution in the gas flow with the tandem setup.

1.4.4 Electrothermal vaporization

The first electrothermal vaporizers (ETV) used as a solid sample introduction device for ICP instruments were modified from graphite furnaces manufactured for GF-AAS systems. In this case, the role of the furnace is not to completely atomize the sample, but to vaporize it for atomization in the plasma. ETV units have also been sold as a sample introduction device for their ICP instruments.

The use of electrothermal vaporization to introduce samples into an ICP offers several advantages. With no solvent used, the plasma should ionize the dry sample vapor released from the ETV more efficiently than nebulized sample solutions. The elimination of solvents also reduces the polyatomic interferences that may be seen in ICP-MS. The detection limits of ETV-ICP-MS have been found to be 10-fold better than those obtained by conventional solution ICP-MS [71].

Reviews of solid sampling with ETV-ICP-MS is available [72, 73]. Calibration by standard additions was necessary for accurate determination of toxic metals in some biological samples [74], while others report that external standards using solid reference materials was sufficient [73]. Precision is generally reported to be in the range of 5–15%.

1.4.5 Direct sample insertion

"Direct sample insertion" (DSI) is when a sample, either liquid or solid, is placed in a sample-carrying probe that is then inserted directly into an atomizer such as a flame or a plasma. In the literature, the term is generally applied to insertion into a plasma. Sample carrying probes have been made of graphite cups or rods, metal cups, or wire

loops. Insertion into the plasma can be done manually or through an automated drive mechanism.

Unlike solution nebulization and external vaporization methods, DSI achieves 100% transport efficiency. High signal intensities are achieved, and the short analysis time would mean less background noise is integrated into the analyte signal. This would lead to better detection limits than other methods.

The probe design can be changed in terms of its geometry and composition. The probes are also disposable, minimizing sample contamination from run to run. Since the vaporization occurs in the plasma of the ICP instrument, an external device such as a laser or ETV is not required, making this technique relatively inexpensive.

To avoid quenching the plasma, the samples must be relatively small. Also, the sample must also be dry and pyrolyzed to remove any organic material. Lack of precise alignment of the sample support with respect to the torch can affect the precision. The temperature of vaporization cannot be controlled, and carbide formation can be a problem for ICP-AES.

The method was first described for flame atomization. Direct sample insertion of a screw rod impregnated with powdered rock samples into an acetylene flame was demonstrated by Govindaraju in 1974 [75]. The atomic absorption signal for lead was measured. RSD was found to be 5–15%, with a detection limit of 1 ppm. Solid samples placed on tantalum boats for direct insertion into a flame for AAS analysis have also been described [76].

Instrumentation and applications of DSI with ICP instruments have been covered extensively in two review papers [77, 78]. Salin and Horlick first described the DSI as a device to introduce milligrams of powders and solids and microlitre volumes of liquids to

an ICP-AES [79]. Their manually driven device required extinguishing and relighting the plasma between runs. Shortly after, Sommers and Ohls [80] reported a pneumatically driven device that propelled the DSI probe into the plasma, allowing continuous plasma operation. While most literature reports the use of DSI with ICP-AES, applications with ICP-MS have also been documented [81, 82]. DSI has been used on a variety of solid samples, including plant material [83, 84], sediments [85], and metal alloys [86]. For these applications, detection limits range from low parts per billion to low parts per million for samples ranging in 0.2–250 mg in size.

1.4.6 Induction-heating electrothermal vaporizer

The induction heating electrothermal vaporizer (IH-ETV) was designed to take advantage of the best features of ETV and DSI designs – the *ex-situ* heating of ETV and the non-contact heating of DSI probes. The IH-ETV was first demonstrated for ICP-MS by Goltz and Salin in 1987 [87]. The cup is inserted into the center of an induction coil to which a maximum of 1.5 kW radio-frequency power at 13.1 MHz is applied, causing eddy currents in the graphite. These currents cause heating of the graphite cup.

As the cup is rapidly heated, the sample is vaporized. The graphite cup is contained in a glass or quartz sample chamber. An inert carrier gas enters through the bottom of the chamber and carries the vaporized sample to the ICP instrument. In Goltz and Salin's paper, the IH-ETV was used to introduce 5–300 μl samples of multielement solutions that were dried and then vaporized as dry aerosols. They achieved a 3–30 fold improvement in detection limits with this method when compared with traditional solution nebulization.

Goltz *et al.* also investigated the use of IH-ETV with ICP-AES [88]. Using multi-element standards, they showed a 2–3 order of magnitude improvement in detection limits over solution nebulization. They also showed the feasibility of using the method to analyze extracts of acid-digested reference materials.

Rybak and Salin further characterized the IH-ETV system used by Goltz *et al.*, showing that linear temperature control was possible was well as a fast heating time that was independent of the final temperature [89]. Their results also showed that a secondary gas such as SF_6 could be mixed with the argon carrier gas in order to improve vaporization or transport efficiency of analytes.

Since the cup is heated by non-contact means, there is no requirement for expensive, precisely machined contact parts as with traditional electrothermal vaporizers. The sample cup itself can be customized in shape and size to suit a particular sample. Commercially available graphite cups used for arc systems can be used, or cups can be machined from graphite rods using a lathe. The ability to have a large cup offers space for both the sample and potential reagents. By using a larger sample, IH-ETV can potentially offer better detection limits and minimization of inhomogeneity effects. The disposable nature of the cups and non-contact heating also minimizes the risk of contamination from sample to sample from reused electrodes. The interchangeability and removal of the cups from the IH-ETV system allows a batch of samples to be prepared ahead of time. Online chemical reactions (*e.g.,* by the addition of oxygen) can be performed without fear of eroding parts since the vaporized material does not come in contact with any metal part.

If argon is used as the carrier gas, arcing can occur between the graphite cup and the glass chamber at high power. The arcing can disrupt the stability of the plasma in an ICP instrument, affecting precision and signal-to-noise ratio. Also, arcing can erode the

graphite cups. Rybak *et al.* reported that mixing N_2, O_2, HCl or SF_6 with the argon carrier gas can eliminate arcing [89]. Ren *et al.* found that arcing could be eliminated by using a quartz sample chamber instead of glass along with introducing water vapor in the argon carrier gas by means of a sparger [90].

Other applications of this particular system have included slurries of soil and sediment reference materials [91] and analytes spiked on cellulose filters by ICP-AES [92]. Recently, Ludke *et al.* reported a similar IH-ETV system for the analyses of aerosol particles by time-of-flight ICP-MS [93]. While the design of IH-ETV can accommodate the direct analyses of solid samples such as soils or powders, analytical results have not been reported yet.

1.5 Objectives

One goal of this thesis is the development of novel methods of direct solid sample analysis. By eliminating the traditional sample digestion/extraction step, these methods are faster – an advantage in a routine analysis setting in an industrial, clinical, or environmental laboratory. Hybrid methods of solid sampling using ICP instrumentation were chosen for the advantages outlined in section 1.1.1. These new methods include exploring the feasibility of IH-ETV for direct solids analysis.

It is also a goal of this thesis to determine metals in samples that have not been widely studied in their solid form. The majority of solid sampling methods to date have been developed for metallurgical and geological samples. This thesis focuses on samples containing predominantly organic matrices – whether biological in nature such as human hair, or non-biological such as pharmaceutical tablets with a microcrystalline cellulose matrix or toxic metals adsorbed on octadecyl-silica based chromatographic powder.

1.6 Thesis Outline

Chapter 2 describes the use of laser ablation with inductively coupled plasma instrumentation for the analysis of pharmaceutical tablets. Two methods of laser sampling are compared, and detection limits for ICP-AES and ICP-MS are reported.

Chapter 3 presents the application of laser ablation with ICP-MS to detect mercury along a single human hair strand.

Chapter 4 demonstrates the use of IH-ETV with ICP-MS for the determination of total mercury in single human hair strands. The method described is validated against a reference method.

Chapter 5 expands on the work presented in the previous chapter to include the multielement determination of powdered human hair using IH-ETV-ICP-MS. Calibration strategies are also presented.

Chapter 6 evaluates the use of IH-ETV-ICP-AES for the analysis of analyte-laden chromatographic material.

Chapter 7 summarizes the knowledge gained from the laser ablation and IH-ETV studies carried on the samples described in the previous chapters. Conclusions are made, along with a discussion of future directions for these methods.

1.7 References

1. O. T. Butler, J. M. Cook, C. F. Harrington, S. J. Hill, J. Rieuwerts and D. L. Miles, *Journal of Analytical Atomic Spectrometry*, 2005, **20**, 130-157.

2. J. Savory and M. R. Wills, *Clinical Chemistry (Washington, DC, United States)*, 1992, **38**, 1565-1573.

3. F. T. Fitzgerald and L. M. Tierney, Jr., *Advances in Internal Medicine*, 1984, **30**, 337-358.

4. J. Savory and M. M. Herman, *Annals of Clinical and Laboratory Science*, 1999, **29**, 118-126.

5. A. Sanz-Medel, *Pure and Applied Chemistry*, 1998, **70**, 2281-2285.

6. G. F. Nordberg, *Environmental Toxicology and Chemistry*, 1990, **9**, 887-894.

7. K. Pyrzynska, *Critical Reviews in Analytical Chemistry*, 2004, **34**, 69-83.

8. J. M. Collard and Y. Kishi, *Special Publication - Royal Society of Chemistry*, 2005, **301**, 317-333.

9. A. Ulrich, C. Moor, H. Vonmont, H.-R. Jordi and M. Lory, *Analytical and Bioanalytical Chemistry*, 2004, **378**, 1059-1068.

10. W. Devos, C. Moor and P. Lienemann, *Journal of Analytical Atomic Spectrometry*, 1999, **14**, 621-626.

11. K. L. Linge, *Geostandards and Geoanalytical Research*, 2005, **29**, 7-22.

12. K. Wrobel, K. DeNicola, K. Wrobel and J. Caruso, *Advances in Mass Spectrometry*, 2004, **16**, 229-273.

13. J. S. Becker, *Canadian Journal of Analytical Sciences and Spectroscopy*, 2002, **47**, 98-108.

14. S. Greenfield, I. L. Jones and C. T. Berry, *Analyst*, 1964, **89**, 713-720.

15. G. W. Dickinson and V. A. Fassel, *Analytical Chemistry*, 1969, **41**, 1021-1024.

16. R. H. Wendt and V. A. Fassel, *Anal. Chem.*, 1965, **37**, 920-922.

17. R. S. Houk, V. A. Fassel, G. D. Flesch, H. J. Svec, A. L. Gray and C. E. Taylor, *Analytical Chemistry*, 1980, **52**, 2283-2289.

18. C. E. Taylor and T. L. Floyd, *Applied Spectroscopy*, 1981, **35**, 408-413.

19. D. R. Wiederin, F. G. Smith and R. S. Houk, *Analytical Chemistry*, 1991, **63**, 219-225.

20. J. Mora, S. Maestre, V. Hernandis and J. L. Todoli, *TrAC, Trends in Analytical Chemistry*, 2003, **22**, 123-132.

21. F. J. M. J. Maessen, P. Coevert and J. Balke, *Analytical Chemistry*, 1984, **56**, 899-903.

22. H. Lachas, R. Richaud, A. A. Herod, D. R. Dugwell, R. Kandiyoti and K. E. Jarvis, *Analyst (Cambridge, United Kingdom)*, 1999, **124**, 177-184.

23. J. G. Williams, A. L. Gray, P. Norman and L. Ebdon, *Journal of Analytical Atomic Spectrometry*, 1987, **2**, 469-472.

24. L. Ebdon, M. Foulkes and K. Sutton, *Journal of Analytical Atomic Spectrometry*, 1997, **12**, 213-229.

25. N. J. Miller-Ihli, *Journal of Analytical Atomic Spectrometry*, 1997, **12**, 205-212.

26. P. Goodall, M. E. Foulkes and L. Ebdon, *Spectrochimica Acta, Part B: Atomic Spectroscopy*, 1993, **48B**, 1563-1577.

27. Z. Zhou, K. Zhou, X. Hou and H. Luo, *Applied Spectroscopy Reviews*, 2005, **40**, 165-184.

28. L. H. Ahrens and S. R. Taylor, *Spectrochemical Analysis; A Treatise on the d-c Arc Analysis of Geological and Related Materials*. 1961.

29. V. B. E. Thomsen, *Modern spectrochemical analysis of metals : an introduction for users of arc/spark instrumentation*, ASM International, Materials Park, OH. 1996.

30. J. S. Beaty and R. J. Belmore, *Journal of Testing and Evaluation*, 1984, **12**, 212-219.

31. A. Hadding, *Zeitschrift fur Anorganische und Allgemeine Chemie*, 1922, **122**, 195-200.

32. P. J. Potts, A. T. Ellis, P. Kregsamer, C. Streli, C. Vanhoof, M. West and P. Wobrauschek, *Journal of Analytical Atomic Spectrometry*, 2005, **20**, 1124-1154.

33. X. Hou, Y. He and B. T. Jones, *Applied Spectroscopy Reviews*, 2004, **39**, 1-25.

34. J. A. Anzelmo and J. R. Lindsay, *Journal of Chemical Education*, 1987, **64**, A200, A202-A204.

35. J. Boerjesson and S. Mattsson, *X-Ray Spectrometry*, 2004, 487-515.

36. T. Y. Toribara, D. A. Jackson, W. R. French, A. C. Thompson and J. M. Jaklevic, *Analytical chemistry*, 1982, **54**, 1844-1849.

37. H. J. Annegarn and S. Bauman, *Nuclear Instruments & Methods in Physics Research, Section B: Beam Interactions with Materials and Atoms*, 1990, **B49**, 264-270.

38. A. Moauro, P. L. Carconi and S. Casadio, *Journal of Radioanalytical and Nuclear Chemistry*, 1997, **216**, 171-178.

39. E. Tognoni, V. Palleschi, M. Corsi and G. Cristoforetti, *Spectrochimica Acta, Part B: Atomic Spectroscopy*, 2002, **57B**, 1115-1130.

40. W.-B. Lee, J. Wu, Y.-I. Lee and J. Sneddon, *Applied Spectroscopy Reviews*, 2004, **39**, 27-97.

41. L. St-Onge, M. Sabsabi and P. Cielo, *Journal of Analytical Atomic Spectrometry*, 1997, **12**, 997-1004.

42. F. Capitelli, F. Colao, M. R. Provenzano, R. Fantoni, G. Brunetti and N. Senesi, *Geoderma*, 2002, **106**, 45-62.

43. B. V. L'Vov, *Inzhener.-Fiz. Zhur., Akad. Nauk Belorus. S.S.R.*, 1959, **2**, 44-52.

44. H. Massmann, *Spectrochimica Acta, Part B: Atomic Spectroscopy*, 1968, **23**, 215-226.

45. F. J. Langmyhr and G. Wibetoe, *Progress in Analytical Atomic Spectroscopy*, 1985, **8**, 193-256.

46. C. Bendicho and T. C. De Loos-Vollebregt, *Journal of Analytical Atomic Spectrometry*, 1991, **6**, 353-374.

47. U. Kurfurst, *Solid Sample Analysis: Direct and Slurry Sampling using GF-AAS and ETV-ICP*. 1997.

48. R. E. Sturgeon, *Spectrochimica Acta, Part B: Atomic Spectroscopy*, 1989, **44B**, 1209-1220.

49. J. Y. Marks, G. G. Welcher and R. J. Spellman, *Applied Spectroscopy*, 1977, **31**, 9-11.

50. W. Schron, A. Liebmann and G. Nimmerfall, *Fresenius' Journal of Analytical Chemistry*, 2000, **366**, 79-88.

51. D. A. Rusak, R. L. Litteral, B. W. Smith and J. D. Winefordner, *Talanta*, 1997, **44**, 1987-1993.

52. S. J. Jiang and R. S. Houk, *Analytical Chemistry*, 1986, **58**, 1739-1743.

53. S. J. Jiang and R. S. Houk, *Spectrochimica Acta, Part B: Atomic Spectroscopy*, 1987, **42B**, 93-100.

54. H. G. C. Human, R. H. Scott, A. R. Oakes and C. D. West, *Analyst (Cambridge, United Kingdom)*, 1976, **101**, 265-271.

55. A. Aziz, J. A. C. Broekaert, K. Laqua and F. Leis, *Spectrochimica Acta, Part B: Atomic Spectroscopy*, 1984, **39B**, 1091-1103.

56. K. A. Ivanovic, D. M. Coleman, F. W. Kunz and D. Schuetzle, *Applied Spectroscopy*, 1992, **46**, 894-899.

57. R. E. Russo, X. Mao, H. Liu, J. Gonzalez and S. S. Mao, *Talanta*, 2002, **57**, 425-451.

58. T. Kantor, L. Polos, P. Fodor and E. Pungor, *Talanta*, 1976, **23**, 585-586.

59. K. Dittrich and R. Wennrich, *Spectrochimica Acta, Part B: Atomic Spectroscopy*, 1980, **35B**, 731-740.

60. A. L. Gray, *Analyst (Cambridge, United Kingdom)*, 1985, **110**, 551-556.

61. S. A. Darke, S. E. Long, C. J. Pickford and J. F. Tyson, *Journal of Analytical Atomic Spectrometry*, 1989, **4**, 715-719.

62. S. F. Durrant and N. I. Ward, *Journal of Analytical Atomic Spectrometry*, 2005, **20**, 821-829.

63. S. F. Durrant, *Journal of Analytical Atomic Spectrometry*, 1999, **14**, 1385-1403.

64. D. Guenther and B. Hattendorf, *TrAC, Trends in Analytical Chemistry*, 2005, **24**, 255-265.

65. P. M. Outridge, S. R. Chenery, J. A. Babaluk and J. D. Reist, *Environmental Geology (Berlin, Germany)*, 2002, **42**, 891-899.

66. I. Rodushkin and M. D. Axelsson, *Science of the Total Environment*, 2003, **305**, 23-39.

67. S. A. Watmough, T. C. Hutchinson and R. D. Evans, *Journal of Environmental Quality*, 1998, **27**, 1087-1094.

68. F. E. Lichte, *Analytical Chemistry*, 1995, **67**, 2479-2485.

69. M. Thompson, S. Chenery and L. Brett, *Journal of Analytical Atomic Spectrometry*, 1989, **4**, 11-16.

70. J. J. Leach, L. A. Allen, D. B. Aeschliman and R. S. Houk, *Analytical Chemistry*, 1999, **71**, 440-445.

71. C. J. Park, J. C. Van Loon, P. Arrowsmith and J. B. French, *Analytical Chemistry*, 1987, **59**, 2191-2196.

72. A. Martin-Esteban and B. Slowikowski, *Critical Reviews in Analytical Chemistry*, 2003, **33**, 43-55.

73. L. Moens, P. Verrept, S. Boonen, F. Vanhaecke and R. Dams, *Spectrochimica Acta, Part B: Atomic Spectroscopy*, 1995, **50B**, 463-475.

74. A. Aziz, J. A. C. Broekaert and F. Leis, *Spectrochimica Acta, Part B: Atomic Spectroscopy*, 1982, **37B**, 369-379.

75. K. Govindaraju, G. Mevelle and C. Chouard, *Analytical Chemistry*, 1974, **46**, 1672-1675.

76. J. T. Cheng and W. F. Agnew, *Atomic Absorption Newsletter*, 1974, **13**, 123-124.

77. R. Sing, *Spectrochimica Acta, Part B: Atomic Spectroscopy*, 1999, **54B**, 411-441.

78. V. Karanassios and G. Horlick, *Spectrochimica Acta Reviews*, 1990, **13**, 89-166.

79. E. D. Salin and G. Horlick, *Analytical Chemistry*, 1979, **51**, 2284-2286.

80. D. Sommer and K. Ohls, *Fresenius' Zeitschrift fuer Analytische Chemie*, 1980, **304**, 97-103.

81. L. Blain, E. D. Salin and D. W. Boomer, *Journal of Analytical Atomic Spectrometry*, 1989, **4**, 721-725.

82. G. E. M. Hall, J. C. Pelchat, D. W. Boomer and M. Powell, *Journal of Analytical Atomic Spectrometry*, 1988, **3**, 791-797.

83. M. E. Rybak, P. Hatsis, E. D. Salin and K. Thurbide, *Tappi Journal*, 2001, **84**, 102.

84. M. Abdullah and H. Haraguchi, *Analytical Chemistry*, 1985, **57**, 2059-2064.

85. L. Blain and E. D. Salin, *Spectrochimica Acta, Part B: Atomic Spectroscopy*, 1992, **47B**, 205-217.

86. C. W. McLeod, P. A. Clarke and D. J. Mowthorpe, *Spectrochimica Acta, Part B: Atomic Spectroscopy*, 1986, **41B**, 63-71.

87. D. M. Goltz and E. D. Salin, *Journal of Analytical Atomic Spectrometry*, 1997, **12**, 1175-1180.

88. D. M. Goltz, C. D. Skinner and E. D. Salin, *Spectrochimica Acta, Part B: Atomic Spectroscopy*, 1998, **53B**, 1139-1147.

89. M. E. Rybak and E. D. Salin, *Spectrochimica Acta, Part B: Atomic Spectroscopy*, 2001, **56B**, 289-307.

90. J. M. Ren, M. E. Rybak and E. D. Salin, *Journal of Analytical Atomic Spectrometry*, 2003, **18**, 485-486.

91. M. E. Rybak and E. D. Salin, *Applied Spectroscopy*, 2001, **55**, 816-821.

92. E. D. Salin and J. M. Ren, *Journal of Analytical Atomic Spectrometry*, 2003, **18**, 953-954.

93. C. Luedke, J. Skole, K. Taubner and M. Kriews, *Spectrochimica Acta, Part B: Atomic Spectroscopy*, 2005, **60B**, 1412-1422.

Chapter 2 Analysis of Pharmaceutical Tablets by Laser Ablation Inductively Coupled Plasma Atomic Emission Spectrometry and Mass Spectrometry (LA-ICP-AES and LA-ICP-MS)

One focus of the thesis is solid-sample methods using ICP instrumentation for samples that have not been widely explored, such as metals in pharmaceutical tablets of organic matrix. As an undergraduate research project, I had once explored the feasibility of laser ablation inductively coupled plasma atomic emission spectrometry (LA-ICP-AES) for the analysis of dietary supplements. The study showed potential for the method, but the store-bought zinc tablets used in these experiments were not ideal samples in terms of homogeneity or surface shape. Using custom-made pharmaceutical tablets of known specification instead, I revisited the analyses for potential application in the pharmaceutical industry.

The manuscript presented in this chapter has been previously published in the *Journal of Analytical Atomic Spectrometry*, 2004, 19(7), 938-940.

A schematic of the laser ablation system along with images of the ablated tablets are provided in Appendix B.

2.1 Abstract

Laser ablation was studied with inductively coupled plasma atomic emission spectrometry (LA-ICP-AES) and with inductively coupled mass spectrometry (LA-ICP-MS) for the analysis of pharmaceutical tablets (10% and 20% Neusilin). For spot analysis with LA-ICP-AES, precision ranged from 12–31% relative standard deviation (RSD), but improved to 1–6% when ratios of signals were used. For continuous scanning, the precision ranged from 1–7 % RSD. Weaker laser conditions required for ICP-MS gave precisions of 47–61% RSD (29% when signal ratios were used). Under unoptimized conditions, the detection limits for LA-ICP-AES of tablets were 70 $\mu g\ g^{-1}$ for Al and 20 $\mu g\ g^{-1}$ for Mg. The detection limits for LA-ICP-MS were 40 $\mu g\ g^{-1}$ for Al and 6 $\mu g\ g^{-1}$ for Mg. These results suggest that LA-ICP spectroscopy may find application in tablet analysis.

2.2 Introduction

Laser ablation (LA) has been used as a technique for solid sample introduction into an inductively coupled plasma (ICP) instrument in a variety of applications [1, 2]. While used extensively in the environmental, geological and metallurgical fields, little exploration regarding the application of LA for tablet analysis has been done in the pharmaceutical industry.

Traditionally, the analysis of pharmaceutical tablets has been done by high-performance liquid chromatography (HPLC). Sample dissolution is required, and it may take hours before results are obtained. Using laser ablation with inductively coupled plasma atomic emission spectrometry (ICP-AES) or inductively coupled plasma mass spectrometry (ICP-MS) for tablet analysis eliminates the need for sample preparation and allows results to be obtained in minutes. There are often metallic species (e.g. K, Mg, Fe) only present in the active ingredient, a matrix ingredient or in a tablet coating, making selective detection by atomic spectrometry possible. LA-ICP spectrometry has also been used for analysis of powdered organic and inorganic material in a tightly pressed pellet form [3-7], suggesting that analysis of pharmaceutical tablets is feasible. For example, there is the potential for quantitative determination or probing tablet uniformity.

Lasers have been demonstrated as a potential analysis tool for tablets by laser-induced breakdown spectroscopy (LIBS) [8, 9]. Theoretically, LA should have several advantages over LIBS. Since the ablation and atomization steps are independent of each other, instrumental parameters can be optimized for each separately. Also, the separate sampling and excitation processes in LA lead to different physical processes. In LIBS, where there is only one energy source, there is competition between the ablation and the

excitation processes as they occur at the same place and approximate time frame. The competition between processes would appear to make LIBS more susceptible to matrix effects. This is not a problem specifically with LA, since the effect of variable ablation can be minimized by using an internal standard (or a major matrix species) and calculating the ratio of the analyte and standard signals.

2.3 Experimental

2.3.1 Instrumentation

All tests were performed with a CETAC LSX-100 laser ablation system (CETAC Technologies, Omaha, NE, USA) coupled with either a Thermo Jarrell-Ash IRIS ICP-AES (Thermo Elemental, Franklin, MA, USA) or a Perkin-Elmer SCIEX ELAN 6000 ICP-MS (SCIEX, Concord, Ontario, Canada). In-house Teflon adapters were used to connect the laser ablation system to the glass cyclonic spray chamber of the ICP-AES or directly to the injector tube of the torch assembly of the ICP-MS. The operating conditions and data acquisition parameters for both instruments are given in Table 2-1.

The laser ablation system was equipped with a Q-switched frequency quadrupled Nd:YAG laser system, operating at 266 nm. The beam profile of the laser was 1 mm Gaussian with an 8-12 ns pulse duration. The position and focus of the laser with respect to the sample was varied by an *x-y-z* translation stage that moved the sample cell. Argon was used as the carrier gas to the ICP instrument.

Table 2-1 Instrument operating parameters

ICP-AES	
Instrument	TJA IRIS
RF power	1350 W
Plasma gas flow rate	14 l min^{-1} Ar
Auxiliary gas flow rate	1 l min^{-1} Ar
Carrier gas flow rate	1 l min^{-1} Ar
Acquisition time	45 s for single spot sampling 115 s for scanning sampling
Integration time	0.25 s for single spot sampling 0.3 s for scanning sampling
ICP-MS	
Instrument	PE SCIEX Elan 6000
RF power	1000 W
Sampling and skimmer cones	Nickel
Plasma gas flow rate	15 l min^{-1} Ar
Auxiliary gas flow rate	1.2 l min^{-1} Ar
Carrier gas flow rate	0.8 l min^{-1} Ar
Detector mode	Analog
Acquisition mode	Peak hopping
Sweeps per reading	1
Readings per replicate	300
Replicates	1
MCA channels	1 for both Al and Mg
Dwell time	200 ms for Al, 200 ms for Mg
Total acquisition time	120 s for single spot sampling

Two methods to probe a sample for bulk analysis by laser ablation were tested. The single spot method involved firing the laser at a fixed site for a fixed number of laser pulses, resulting in a single ablation crater. Continuous scanning involved moving the sample relative to the laser in an *x-y* plane such that an ablation trench is formed.

2.3.2 Samples

The uncoated tablet formulation consisted of either 10% or 20% by weight magnesium aluminosilicate (Neusilin type UFL_2, Fuji Chemical Industry Co., Ltd, Toyama, Japan) in a microcrystalline cellulose (MCC) matrix (Avicel PH 102, FMC BioPolymer, Philadelphia, PA, USA). Tablet weight was 300 mg, compressed at 3000 psig (ca. 21 MPa) into a 12/32" (0.94 cm) diameter flat-faced round shape. For Neusilin type UFL_2, the chemical composition is $Al_2O_3 \cdot MgO \cdot 1.7SiO_2 \cdot xH_2O$ where $x < 7$. Assuming $x = 7$, the 10% tablets contained about 14600 μg g^{-1} of Al and 6600 μg g^{-1} of Mg. Particle sizes were less than 45 μm for Neusilin and on average 100 μm for Avicel. While these particular tablets are not commercially available, MCC is a common tablet matrix and the specifications are typical of pharmaceutical tablets [10].

2.4 Results and Discussion

To determine the reproducibility of the laser ablation system combined with the ICP-AES under the given conditions, a polished piece of pure copper metal was ablated. Laser ablation of pure metals is generally reproducible and can be used as an indicator of the laser power precision.

Fifty laser shots were fired at a rate of 10 Hz to form uniform craters of approximately 100 μm in diameter. For nine random sites, the integrated transient peak areas for the Cu 327.4 nm emission line were compared to give a relative standard deviation (RSD) of 3%. Mao *et al.* reported 2% RSD for the ablation of copper under similar conditions [11]. Monitoring 63 m/z (Cu) in LA-ICP-MS, the RSD between nine sites using one laser shot per site was determined to be 9%.

The continuous scanning method of sampling was also tested with the copper disc and ICP-AES. An even-walled trench with a rounded bottom was produced with a trench width of approximately 100 μm. The Cu 327.4 nm emission signal was recorded every 0.25 seconds for 60 seconds. Using the data points recorded after 30 seconds into the data acquisition process (when the signal stabilized), the RSD was determined to be 4% for this sampling method.

2.4.1 Single spot ablation of tablets

There were usually two parts to the ablation crater when either 25 or 50 laser shots were fired on a site at 10 Hz – the deep center hole where the main laser contact occurred and the outer edge around the hole where additional particles broke from the tablet

surface. The diameter of the center hole was typically around 75 μm while the outer edge ranged from 300–500 μm. The outer edge was generally more uniform in shape when the laser was defocused below the surface of the tablet, compared to when the laser was focused on the tablet surface. When the laser energy was reduced from 1.8 mJ to about 0.8 mJ, the outer crater edge was smaller and more circular.

Figure 2-1 shows examples of the transient signals obtained for spot analysis. A laser energy of 0.9 mJ and 25 laser pulses were typical parameters needed to obtain a large transient signal with ICP-AES, while just 0.5 mJ and 2 laser pulses were sufficient for a large signal with ICP-MS.

Figure 2-1 Transient signals for spot analysis of tablets with (a) ICP-AES detection and (b) ICP-MS detection

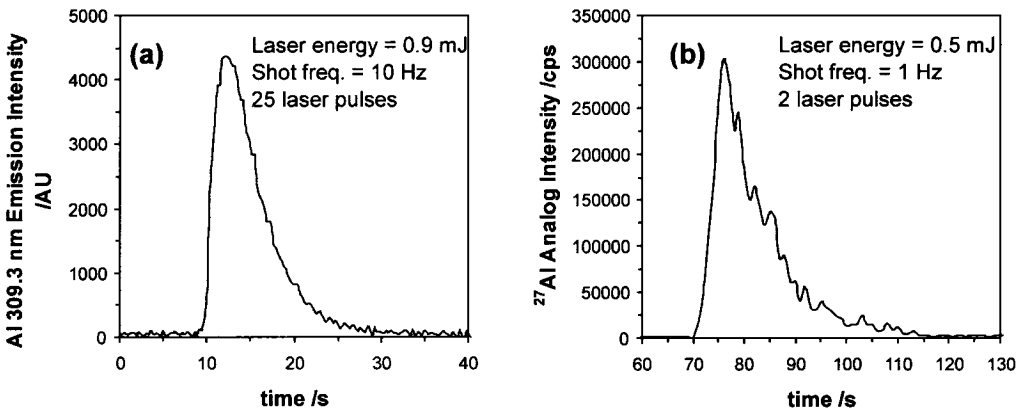

Table 2-2 shows the precision of site-to-site analysis within a 20% Neusilin tablet with ICP-AES detection. The integrated transient peaks for the Al 309.3 nm and Mg 282.5 nm emission lines were used to calculate the RSD. For a laser energy range of 0.8–1.8 mJ, 25–50 laser pulses, focusing the laser 0–3 mm below the tablet surface, the RSD values ranged from 12–30% for Al and 14–31% for Mg. This is comparable with the 10–

20% range reported for tablet analysis using LIBS [9]. Generally, focusing the laser below the surface of the tablet by 2 mm produced better precision. This correlates with the more uniform craters observed when the laser was defocused. The precision observed may reflect non-representative sampling due to the laser spot size relative to the particle sizes or local homogeneities, as well as variability in the ablation process from site to site.

Table 2-2 Single spot method of tablet analysis (20% Neusilin)

With ICP-AES detection:						
Laser pulses (at 10Hz)	Laser power	Sites sampled on tablet	Laser focus	RSD Al (309.3 nm)	RSD Mg (285.5 nm)	RSD ratio (Mg:Al)
50	1.8 mJ	9	at surface	27%	25%	3%
50	1.8 mJ	9	2 mm below surface	20%	21%	2%
25	1.8 mJ	9	at surface	30%	31%	6%
25	1.8 mJ	8	2 mm below surface	14%	14%	2%
25	0.8 mJ	13	at surface	22%	23%	3%
25	0.8 mJ	13	2 mm below surface	13%	17%	4%
25	0.8 mJ	5	at surface	17%	20%	3%
25	0.8 mJ	5	1 mm below surface	23%	24%	1%
25	0.8 mJ	5	2 mm below surface	12%	14%	3%
25	0.8 mJ	5	3 mm below surface	23%	24%	3%
With ICP-MS detection:						
Laser pulses (at 1 Hz)	Laser power	Sites sampled on tablet	Laser focus	RSD ^{27}Al	RSD ^{24}Mg	RSD ratio (Mg:Al)
2	0.5 mJ	6	2 mm below surface	47%	61%	29%

When an internal standards approach was applied and the ratio of the Al 309.3 nm emission intensity to the Mg 285.2 nm emission intensity was determined under each set of conditions, the RSD varied from 1–6%. This suggests that it may be possible to use a matrix element as an internal standard to correct for variation in the amount sampled from site to site.

The results with ICP-MS detection for a 20% Neusilin tablet are also shown in Table 2-2. When the same laser parameters used with AES detection were applied, the signal from the MS for 27 m/z (Al) and 24 m/z (Mg) were saturated. Fewer laser shots and reduced laser energy were used to obtain a signal in the range of the instrument. Two laser shots and a reduced laser energy (0.5 mJ) firing at 1 Hz were sufficient to produce a large transient signal. However, a crater was not visually distinguishable on the tablet surface with only two laser shots. The RSDs for Al and Mg were 47% and 61% respectively, while using the signal ratio of Mg to Al improved the RSD to 29%. Either lower concentrations or monitoring the signal of less abundant isotopes is needed for more precise tablet analysis by LA-ICP-MS.

A calibration curve was constructed using a blank, a 10% Neusilin tablet, and a 20% Neusilin tablet. The average transient peak areas of the Al 309.3 nm and Mg 285.2 nm emission lines from the ablation with ICP-AES detection of the tablets (laser energy of 1.8 mJ, 25 shots per site, laser focused 2 mm below the surface) was used. The integrated baseline signals for Al and Mg were used as the blank values. The plot shows that the response curve is linear in the given concentration range (R^2 = 0.964 for Al, R^2 = 0.988 for Mg), and it would be expected to be linear down to the detection limit.

The detection limits for LA-ICP-AES were determined to be 70 $\mu g\ g^{-1}$ for Al and 20 $\mu g\ g^{-1}$ for Mg, while the detection limits for LA-ICP-MS were 40 $\mu g\ g^{-1}$ for Al and 6 $\mu g\ g^{-1}$ for Mg. These detection limits are for the analytes in solid form under unoptimized operating conditions for laser ablation.

2.4.2 Continuous ablation of tablets

The continuous scanning method was tested on the 10% Neusilin tablets using LA-ICP-AES. The Al 309.3 nm spectral line was monitored at an integration time of 0.25 seconds using an average laser energy of 2 mJ firing at a rate of 10 Hz.

The ablation trenches on the tablet surface had uneven walls with a width of approximately 75 μm. The trenches produced at the lower scan rates of 10 and 20 μm s^{-1} were more uniform in appearance than those produced at the higher scan rates of 50 and 150 μm s^{-1}. Some of the surface near the trenches produced at the higher scan rates also appear to have partially broken down. This type of breakdown was not observed to be as extensive with the lower scan rates. Also, at the highest scan rate, a row of individual ablation craters was observed instead of a trench.

The time scans for scan rates of 10, 20, 50, and 150 μm s^{-1} are shown in Figure 2-2. A 25 s moving average was applied to smooth the data. As seen in Figure 2-2, the signals initially spiked before reaching a plateau. This probably reflects the large particles that came off the surface with the initial laser pulses. Increasing the scan rate increased the signal intensity, as more fresh material was ablated at the faster rate. The RSD was calculated from the data points beginning 50 s after the start of data acquisition, where the emission signal appeared to be most stable. For the four scan rates tested, the RSD was determined to be 3%, 1%, 7%, and 6% respectively. This is better than the 12–30% RSD found for the Al signal in spot analysis. Scanning gives better results than spot analysis since a more representative portion of the material is sampled, and may be useful for probing tablet uniformity.

Figure 2-2 Effect of laser scan rates on analyte signal and RSD. (A) 10 μm s^{-1}, (B) 20 μm s^{-1}, (C) 50 μm s^{-1}, and (D) 150 μm s^{-1}

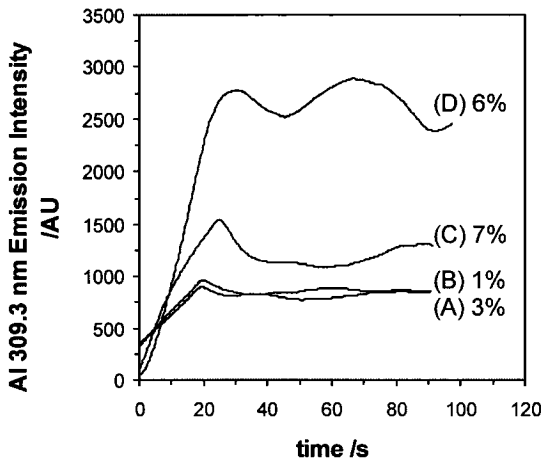

2.5 Acknowledgments

The authors wish to thank CETAC Technologies for the use of an LSX-100 Laser Ablation System, Dr. Scott McGeorge of Transition Technologies for set-up and operational assistance, and the Natural Sciences and Engineering Research Council of Canada for financial support.

2.6 References

1. S. F. Durrant, Journal of Analytical Atomic Spectrometry, 1999, **14**, 1385-1403.

2. R. E. Russo, X. Mao, H. Liu, J. Gonzalez and S. S. Mao, Talanta, 2002, **57**, 425-451.

3. A. A. Van Heuzen and J. B. W. Morsink, Spectrochimica Acta, Part B: Atomic Spectroscopy, 1991, **46B**, 1819-1828.

4. W. T. Perkins, N. J. G. Pearce and T. E. Jeffries, Geochimica et Cosmochimica Acta, 1993, **57**, 475-482.

5. A. Raith and R. C. Hutton, Fresenius' Journal of Analytical Chemistry, 1994, **350**, 242-246.

6. S. A. Baker, M. Bi, R. Q. Aucelio, B. W. Smith and J. D. Wineforder, Journal of Analytical Atomic Spectrometry, 1999, **14**, 19-26.

7. O. V. Borisov, C. J. Bannochie and R. E. Russo, Applied Spectroscopy, 2001, **55**, 1304-1311.

8. M. D. Mowery, R. Sing, J. Kirsch, A. Razaghi, S. Bechard and R. A. Reed, Pharmaceutical and Biomedical Analysis, 2002, **28**, 935-943.

9. L. St-Onge, E. Kwong, M. Sabasi and E. B. Vadas, Spectrochimica Acta Part B: Atomic Spectroscopy, 2002, **57B**, 1131-1140.

10. H. A. Lieberman, L. Lachman and J. B. Schwartz, eds., Pharmaceutical dosage forms: tablets, Marcel Dekker, Inc., New York. 1989.

11. X. Mao, O. V. Borisov and R. E. Russo, *Spectrochimica Acta Part B: Atomic Spectroscopy*, 1998, **53B**, 731-739.

Chapter 3 Direct Detection of Mercury in Single Human Hair Strands by Laser Ablation Inductively Coupled Plasma Mass Spectrometry (LA-ICP-MS)

While I was completing the laser ablation studies on pharmaceutical tablets, Prof. Hing Man (Laurie) Chan (then of the McGill University School of Dietetics and Nutrition) expressed interest in developing new methods of analysis for hair. In particular, he was interested in determining mercury levels in hair since it is now used as an indicator of mercury exposure from diet. However, the conventional method being used in his laboratory for determining mercury levels along a hair strand required tedious sample preparation and did not provide the rapid feedback he desired. Approximately 100 hair strands per individual were required, making assessments in large monitoring programs more difficult. The method was also limited to a resolution of 1-cm segments along the hair strand.

A direct method of hair analysis with minimal sample preparation and minimal sample size was sought. Due to direct sampling ability and high spatial resolution of the laser, the opportunity was taken to explore the potential use of LA-ICP-MS for the rapid detection of mercury along a single human hair strand.

The manuscript presented in this chapter has been previously published in the *Journal of Analytical Atomic Spectrometry*, 2004, 19(10), 1287-1288.

Operating parameters for the laser ablation system and the ICP-MS can be found in Appendix C.

3.1 Abstract

Single shot laser ablation ICP-MS has demonstrated the potential to detect Hg in single human hairs with a resolution corresponding to less than one day of growth and with a detection limit of approximately 0.2 $\mu g\ g^{-1}$.

3.2 Introduction

Mercury, a metallic element that occurs naturally in the environment, has long been recognized as toxic. Damage to the kidneys, liver, brain, and particularly the central nervous system are some of the effects of acute and chronic mercury poisoning [1]. Methylmercury, the most toxic form of mercury, bioaccumulates along the aquatic food chain and is ingested by humans when fish is part of the diet. The ingested methylmercury enters the bloodstream and is then incorporated into hair as it grows.

Hair is a convenient biomarker of exposure since hair collection is less invasive than sampling blood. Hair samples are easy to store, and no medical training is required for hair collection. Variations in metal intake over time are translated into variations in metal concentrations along a hair strand; thus hair provides a record of exposure. Measuring Hg in hair samples is an established biomonitoring technique used in many epidemiological studies [2].

Airey reported an average Hg concentration in hair of 1.2 $\mu g\ g^{-1}$ for Canada and 2.4 $\mu g\ g^{-1}$ for the United States [3], while other studies report averages ranging from 0.3–1.0 $\mu g\ g^{-1}$ for US populations [2].

The most widely used technique for measuring mercury in hair samples is a wet digestion followed by cold vapor atomic absorption spectrometry (CV-AAS) detection, such as the protocol outlined by Farant *et al* [4]. A digestion protocol lengthens the time needed for analysis, and may introduce contamination or analyte loss. In order to determine the concentration along the length of the hair, the hair strand has to be cut into segments and digested individually. It is difficult to analyze segments smaller than one centimeter, due to the minimum amount of sample required. For example, 100 one-

centimeter segments (and therefore 100 hair strands) may be needed to obtain the 10 mg sample size for analysis by CV-AAS detection. Assuming hair grows one cm per month, the time resolution for this technique is therefore limited to a monthly scale.

Proton-induced x-ray emission photometry (PIXE) [5] and x-ray fluorescence (XRF) [6] have been used to directly sample along the length of single hair strands. These techniques are capable of spatial resolutions of millimeters of hair. However, the instrumentation required for PIXE does not make it attractive for routine hair analysis, while the Hg detection limits of 3 to 5 $\mu g\ g^{-1}$ for XRF [7] are not sufficient for detecting natural levels in hair.

Laser ablation inductively coupled plasma mass spectrometry (LA-ICP-MS) appears to be suited for hair analysis. No sample digestion or hair segmenting is required since the laser samples directly. Only a small sample is needed, and analysis is rapid (less than a minute), providing the potential for high sample throughput. The laser beam can also be traversed along the length of the hair, with the spatial resolution to produce ablation craters tens of microns wide. The high spatial resolution allows the sampling of individual hair strands, where thickness usually ranges from 40 to 120 μm for human scalp hair [8]. The resolution also allows the potential for monitoring trace metals along the hair strand on a daily level – something not yet demonstrated with other techniques. Lastly, ICP-MS is capable of multielemental analysis and detection limits needed for tracking $\mu g\ g^{-1}$ levels of trace metals in hair.

The first analysis of hair by LA-ICP-MS was reported by Durrant and Ward [9]. They did not sample the hair strands directly; rather they ground the hair into a powder and analyzed the pressed pellets. Recently, Rodushkin and Axelsson showed that LA-

ICP-MS analysis using continuous ablation across a flattened wisp of hair at a spatial resolution of 2.5 mm gave distributions of elements along the hair (concentrations ranging from 0.1 to 4000 $\mu g\ g^{-1}$) [10]. Russo *et al.* have already demonstrated that current laser technology can produce ablation craters in individual hair strands, though they did not report any analytical results [11]. Our objective was to demonstrate the applicability of LA-ICP-MS for determination of Hg levels in single hair strands.

3.3 Experimental

Hair samples were analyzed by a CETAC LSX-100 laser ablation system (CETAC Technologies, Omaha, NE, USA) coupled with a Perkin-Elmer ELAN 6000 ICP-MS (SCIEX, Concord, Ontario, Canada). An in-house adapter made of Teflon was used to connect the LSX-100 directly to the injector tube of the torch assembly of the ELAN 6000. A glass sample holder for aligning the single hair strands straight in the sample cell was also constructed in-house. The sample holder consisted of a microscope slide with four parallel trenches of 120 μm width, spaced 5 mm apart. Tape was used to secure the ends of the hair samples to the sample holder.

The LSX-100 was equipped with a Q-switched frequency quadrupled Nd:YAG laser system, operating at 266 nm. The beam profile of the laser was 1 mm Gaussian with an 8-12 ns pulse width. A translation stage varied the position of the sample cell in the X, Y and Z directions to adjust the focus and position of the laser with respect to the sample. The ablated sample was carried into the ICP-MS by an argon gas stream.

In these experiments, single sites along the hair strand were sampled. The laser was held in a fixed position as the laser was fired, forming an ablation crater in the sample. The ICP-MS was not optimized for laser ablation but was instead optimized with conventional nebulization-based conditions of power and flows, and all experiments were run under these conditions. However, optimization with solids for laser ablation should improve the results.

Human scalp hair was collected from residents of Grand Manan, a fishing community in New Brunswick, Canada. The hair was collected following the procedure established by the First Nations and Inuit Health Lab of Health Canada (FNIHL) [12].

Stainless steel scissors were used to cut a 2.5 mm in diameter bundle of hair as close to the scalp as possible. All samples were collected from the back of the head then stored in polyethylene bags. One-centimeter segments of hair were base-digested [4] and Hg concentration was determined by CV-AAS at the FNIHL. The first centimeter of hair closest to the scalp from one particular individual had an average concentration of Hg of 3.63 $\mu g\ g^{-1}$. The hair samples from this individual were straight and brown, and were used for all experiments.

3.4 Results and Discussion

Using a single laser pulse at a power of 1.5 mJ, the craters formed were approximately 50 μm wide and were not deep enough to go completely through the hair strand. Craters made along a hair strand are shown in Figure 3-1. Assuming a growth rate of 1 cm per month, a sampling size of 50 μm would correspond to roughly 4 hours of growth. Sampling at this spatial/time resolution should be able to generate daily record of Hg exposure.

Figure 3-1 Ablation craters resulting from single laser shots at 1.5 mJ, spaced about 100 μm apart along a hair strand

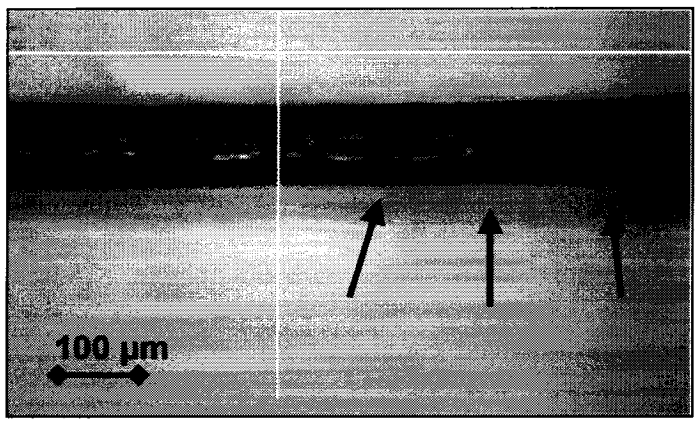

A single laser shot on the hair strand produced a pronounced signal at the ^{202}Hg mass in the ICP-MS. The adjacent 205 mass was also monitored during the analysis as a reference. There should be no signal observed there since the only isotope present at that mass is Tl. Its natural concentration in hair is quite low (less than 5 ng g^{-1}) [13], and it would not be expected to contribute a detectable signal. There was indeed no peak observed at the 205 mass, indicating that the ^{202}Hg peak is not an artifact of the laser firing (i.e. a pressure pulse). Experiments with other fibers indicated that there was no

trace amount of Hg in the system. Signal peaks of approximately 12 s were observed and smoothed with a 101 point moving average, which corresponded to roughly 10 seconds. Under these sampling conditions, the detection limit (3σ) for Hg using LA-ICP-MS was determined to be 0.2 μg g^{-1} at the 99% confidence level (assuming a Hg concentration of 3.63 μg g^{-1} in that sample). The benchmark dose used by the United States Environmental Protection Agency (USEPA) for risk assessment is at 11 μg g^{-1}. An uncertainty factor (UF) of 10 is used to establish the Reference Dose [2]. This detection limit is five times lower than the Reference Dose, *i.e.* the minimum risk level, and should be sufficient to monitor Hg in hair for risk assessment purpose.

As with other solid sample analysis techniques, laser ablation provides challenges with respect to calibration. One problem is the variability that can occur in the sampling process, even under the same nominal laser parameters. One way to minimize this problem would be to use a variation of the calibration technique of internal standards. In this case, all calculations are made relative to the signal of an element with a homogenous concentration across the matrix.

In biological samples, C and S have been used as internal standards for LA-ICP-MS. For our experiments, the mass of ^{34}S was chosen since it made a larger signal than ^{13}C. Sulfur is found in hair due to its inclusion in several amino acids: cysteine, methionine and cysteic acid [14]. According to the literature, the sulfur concentration (*e.g.* 47 700 ± 4100 (S.D.) μg g^{-1} reported for a Swedish population) is constant both between hair samples and within the same hair strand [10].

Sites 150 μm apart along a single hair strand were ablated with a single laser shot at 1.5 mJ over a length of 600 μm or about two days of growth. The laser precision was

initially established by firing consecutive shots at a pure copper disc, where a 7% relative standard deviation (RSD) was observed. Along the hair strand, an RSD of 6% was obtained for ^{34}S, suggesting that sulfur may be a suitable internal standard for calibration. Using the area under the transient peaks, the ^{202}Hg to ^{34}S ratio was calculated for these sites along the single strand of hair. The change in this ratio along the hair strand is shown in Figure 3-2. The level of Hg in this individual appears to be decreasing further from the root end of the hair. This means an increase in Hg during the two-day time frame since hair grows out from the root end. The use of signal ratios from LA-ICP-MS data appears to be useful in determining changes in concentration over the length of a hair strand and may help reconstruct daily records of exposure.

Figure 3-2 Ratio of ^{202}Hg to ^{34}S signals along a hair strand, with 0 μm as the root end

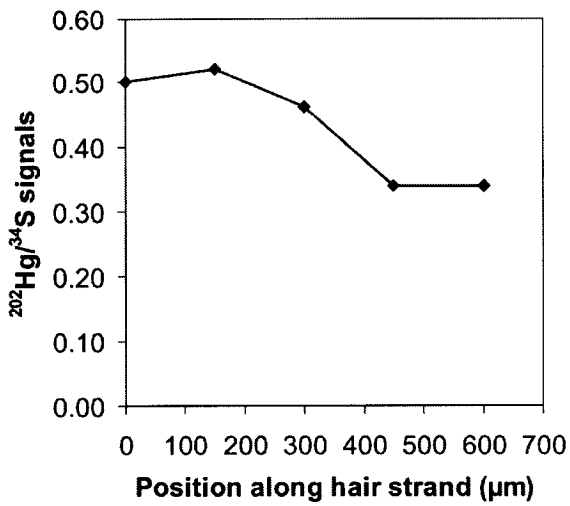

3.5 References

1. ATSDR, *Toxicological profile for mercury*, U.S. Department of Health and Human Services, Public Health Service, Atlanta, GA, 1999.

2. USNRC, *Toxicological effects of methylmercury*, National Academy Press, Washington, DC. 2000.

3. D. Airey, *Science of the Total Environment*, 1983, **31**, 157-180.

4. J. P. Farant, D. Brissette, L. Moncion, L. Bigras and A. Chartrand, *Journal of Analytical Toxicology*, 1981, **5**, 47-51.

5. V. Valkovic, D. Miljanic, R. M. Wheeler, R. B. Liebert, T. Zabel and G. C. Phillips, *Nature (London, United Kingdom)*, 1973, **243**, 543-544.

6. T. Y. Toribara, D. A. Jackson, W. R. French, A. C. Thompson and J. M. Jaklevic, *Analytical Chemistry*, 1982, **54**, 1844-1849.

7. E. Cernichiari, T. Y. Toribara, L. Liang, D. O. Marsh, M. W. Berlin, G. J. Myers, C. Cox, C. F. Shamlaye, O. Choisy and et al., *Neurotoxicology*, 1995, **16**, 613-627.

8. C. R. Robbins, *Chemical and physical behavior of human hair*, Springer-Verlag, New York. 2002.

9. S. F. Durrant and N. I. Ward, *Food Chemistry*, 1994, **49**, 317-323.

10. I. Rodushkin and M. D. Axelsson, *Science of the Total Environment*, 2003, **305**, 23-39.

11. R. E. Russo, G. L. Klunder, P. Grant and B. D. Andresen, *Applied Physics A: Materials Science & Processing*, 1999, **69**, S895-S897.

12. L. Bigras, *First Nations and Inuit Health Laboratory Internal Report*. 1998.

13. J. F. Maurice, G. Wibetoe and K.-E. Sjastad, *Journal of Analytical Atomic Spectrometry*, 2002, **17**, 485-490.

14. S. A. Katz and A. Chatt, *Hair analysis: applications in the biomedical and environmental sciences*, VCH Publishers, New York, NY. 1988.

Chapter 4 Induction heating-electrothermal vaporization for direct mercury analysis of a single human hair strand by inductively coupled plasma mass spectrometry

While LA-ICP-MS provided the necessary spatial resolution and detection limits to be successful in detecting natural levels of mercury present in a single human hair strand, quantification became a problem. Ideally, this requires well-characterized single hair strands. However, hair strands are not currently available as certified reference materials, nor did I have access to hair strands that were calibrated to the resolution achievable by the laser ablation system. Technical limitations in the particular commercial laser ablation system being used (poor control in the power of single laser shots, lack of fine-tuning in *x-y* position of the sample with respect to the laser) also made it difficult to develop laser ablation as a routine method.

I had first investigated traditional electrothermal vaporization for potential use in speciation analysis. By the final round of this work, the induction-heating electrothermal vaporizer (IH-ETV) was being evaluated for this application. However, due to similar research by another group, this work was not pursued. The progress of this project is reported in Appendix A. It was then decided that the IH-ETV would be a suitable sample introduction system for the quantification of mercury in a hair strand – the entire hair strand could be directly vaporized into an ICP-MS without any sample digestion. The main problem of this system (arcing) had been recently solved by another member of the group.* This would allow for rapid screening of hair samples from individuals where mercury exposure from diet or the environment was of immediate concern.

This investigation would also explore the feasibility of using IH-ETV for direct vaporization of a solid matrix, whereas previous applications had only reported analytical results for solutions, slurries or analyte deposits.

The manuscript presented in this chapter has been previously published in the *Journal of Analytical Atomic Spectrometry*, 2005, 20(12), 1315–1317.

Please note that the DMA-80 Direct Mercury Analyzer (Milestone Inc.) was omitted from the Introduction section (4.2) of this chapter. While the manufacturer provides an application note for direct analysis of hair samples, there are currently no peer-reviewed articles examining the performance of this instrument.

Due to the space restrictions set by the journal, some experimental details were omitted from the manuscript. They can be found in Appendix D.

[*] J. M. Ren, M. E. Rybak and E. D. Salin, *Journal of Analytical Atomic Spectrometry*, 2003, 18, 485-486.

4.1 Abstract

It was demonstrated that a single human hair strand can be analyzed for total mercury using an induction heating-electrothermal vaporizer with ICP-MS detection, achieving a detection limit of 20 pg or 30 ng g^{-1} (based on a 0.6 mg sample).

4.2 Introduction

There is a growing concern about mercury from environmental and dietary sources and its effects on human health. For example, populations where fish is a dietary staple may be at risk due to mercury levels present in fish tissue. In many epidemiological studies, hair has been used as a biomarker because the mercury in the bloodstream is incorporated into the hair structure as it grows. Natural mercury concentrations in hair range from 0.3 to 1.0 $\mu g\ g^{-1}$ for typical North American populations [1]. Since hair grows at roughly one cm per month, it is possible to track mercury exposure along the length of the hair. Hair samples are also more convenient to collect and store when compared to blood samples.

The most widely used methods of determining mercury in hair involve a digestion protocol followed by detection using either cold-vapor atomic absorption (CV-AAS), cold-vapor fluorescence spectroscopy (CV-AFS), or inductively coupled plasma mass spectrometry (ICP-MS) [2]. However, a digestion step is time consuming (typically hours) and may result in sample contamination or analyte loss. These methods also require about 5–10 mg of hair; 100 hair strands may be needed to achieve this amount.

X-ray fluorescence [3], particle induced X-ray emission spectroscopy [4], and laser ablation-ICP-MS [5] have been used to directly analyze human hair strands for mercury. While there is little sample preparation required, X-ray fluorescence has relatively high detection limits, particle induced X-ray spectrometry is expensive and LA-ICP-MS often has calibration problems. Recently, commercial mercury analyzers have been used for direct analysis of solid hair samples. These instruments integrate a methodology called combustion-gold amalgamation-atomic absorption spectroscopy (C-G-AAS) that uses

sample combustion with a catalyst, mercury collection with gold amalgamation, then detection by CV-AAS. This technique has been successfully applied to the analysis of powdered human hair, horse fur, and single human hair strands [6, 7]. However, some sample preparation can still be required, as the addition of modifiers to the hair sample may be needed to absorb combustion by-products.

We report an alternate method using an induction heating-electrothermal vaporizer (IH-ETV) that requires only simple, direct sample vaporization followed by detection. In an IH-ETV, a graphite cup containing the sample is inductively heated at a user-set temperature. The vaporized analyte is transported to a detector (an ICP-MS in our case) by a carrier gas. An advantage of this set-up is the reduction of the risk of contamination due to the non-contact heating environment and the ability to interchange the graphite sample cup. Furthermore, no sample preparation is required. There is also the potential for multi-elemental analysis and excellent detection limits with ICP-MS, the vaporization temperature is easily controlled, and the inexpensive graphite cups can be customized in shape and size to suit a particular sample. In previous work, the IH-ETV has been used to vaporize soil slurries and cellulose filters [8, 9]. Our objective in this project is to show that IH-ETV-ICP-MS can be used to rapidly determine mercury in a single hair strand.

4.3 Experimental

4.3.1 Instrumentation

The IH-ETV system used in this study, a modified LECO Model 521 induction furnace (LECO, St. Joseph, MI, USA), has been previously described in detail [10-12]. To eliminate the risk of arcing, the glass sample chamber was replaced with one made of quartz and the argon carrier gas was passed through a sparger containing distilled deionized water [13]. Commercially available graphite cups along with boiler caps were used (type S-16 and BC-1, Bay Carbon Inc., Bay City, MI, USA). The vaporized samples were carried in the argon stream to a Perkin-Elmer SCIEX Elan 6000 ICP-MS system (SCIEX, Concord, ON, Canada) through PTFE tubing at a flow rate of 0.5 l min^{-1}. Typical operating values were used for the other parameters of the ICP-MS.

4.3.2 Samples and standards

The hair samples came from women living in the village of Brasilia Legal, Brazil. Details of this population and hair collection procedures are described elsewhere [14]. For this study, hair strands collected from four individuals were cut to a 12-cm length from the root end and weighed to the nearest 0.01 mg. As part of two other interdisciplinary projects, the mercury concentrations of 12-cm segments of these hair strands were previously determined by CV-AAS and C-GA-AAS [7, 14].

Calibration using the external standards methodology was undertaken with Hg standard solutions and with a hair certified reference material (CRM). Mercury calibration solutions were prepared in a 1% HNO_3 matrix from a 1000 μg g^{-1} Hg stock

solution (SCP Science, Baie D'Urfé, QC, Canada) on the same day of analysis. The CRM, BCR 397 (IRMM, Belgium), was composed of powdered human hair. The samples or standards (one coiled hair strand, 10 μl of solution, or up to 1 mg of CRM) were placed inside a graphite cup, then covered with a boiler cap and heated to approximately 800°C. A boiler cap is a graphite lid that fits over the sample cup. The cap prevents the unvaporized sample from escaping from the cup when the carrier gas and heating is applied, while a small hole at the top of the cap allows the vaporized sample to exit.

The same graphite cup and boiler cap were used for all samples in a given day, and then changed daily. Blanks (empty graphite cup) were checked routinely. No problems with sample carryover were seen. The ^{197}Au isotope was also monitored as a background signal. Total analysis time for a sample was less than two minutes.

4.4 Results and discussion

Typical ^{202}Hg transient profiles from a hair strand, powdered hair CRM and a mercury calibration solution with approximately the same peak area are overlaid in Figure 4-1. The graphite cup was heated for 40 seconds (data acquisition started 10 s before the beginning of the heating step). The hair strand and the powdered hair CRM show similar peak shapes, though a minor distinction can be made between the steepness of the leading edges. This is probably due to different heating rates between the hair strand and the powdered hair. The entire hair strand touched the walls of the cup and was vaporized quickly, while the some of the hair rested on other hair and was momentarily insulated. The slight differences in peak heights show that height is not useful for accurate quantification. However, the peak areas are the same, indicating that powdered hair is a suitable calibration material for hair strands if peak areas are used.

Figure 4-1 Transient profiles of ^{202}Hg for various types of samples

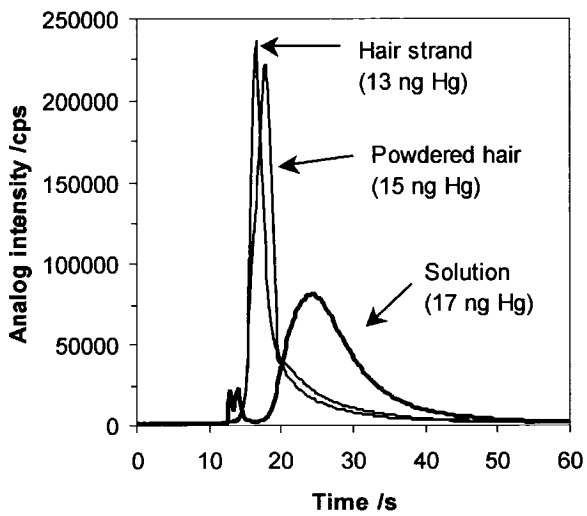

In contrast to the hair matrices, the transient profile of the mercury solution shows two distinct sets of peaks for ^{202}Hg. Infrared measurements have shown that it takes roughly 10 s after power has been applied to the induction coil for the cup to reach 80% of its final temperature setting. Therefore when the cup was heated, the water in the solution immediately vaporized. The water probably carried some of the mercury, resulting in the small peak at the beginning of the profile, while the rest of the mercury came off as a broad peak afterwards. There may be two possible reasons for the broad peak shape of the solution when compared to the peaks for the hair. First, it was observed that the solution permeated into the graphite cup, and it may have taken longer for it to be released when heated. Second, it may be due to different thermal properties of the forms of mercury present in the samples (organic mercury bound to sulfur in the hair matrices versus inorganic mercury in the solution). One last observation can be made about the liquid calibration peak area - it was less than that of the hair strand and the powdered hair. The peaks areas for mercury solutions were consistently low when cups containing mercury solution were not immediately analyzed. Experiments show that the loss of mercury is time-dependent and reheating of the cup at higher temperatures did not result in further mercury release. This indicates that there was some analyte loss, probably due to evaporation. Therefore mercury solutions are unsuitable for external standards calibration of hair strands.

An external standards calibration plot was constructed using the peak areas of the transient signals for the blank, and roughly 0.5 mg and 1 mg of the CRM. Using a linear least squares regression, R^2 greater than 0.999 were routinely achieved. In Table 4-1, the total mercury concentrations determined for the hair strands by external standards using the powdered CRM are compared with an estimate previously determined by CV-AAS

using the protocol described by Farant *et al* [15]. When the concentrations of the four hair strand samples (11 total replicates) from IH-ETV-ICP-MS were plotted against the concentrations estimated by CV-AAS, a slope of 1.03 and R^2 of 0.95 were obtained. At less than 4% relative standard deviation (RSD), precision for hair strand analysis was comparable to that of C-G-AAS and CV-AAS methods [6, 15]. On average, the percent recovery was 110%.

Table 4-1 Determination of mercury concentrations in hair strands

Sample ID	Hg by CV-AAS ($\mu g\ g^{-1}$)	Mean Hg by IH-ETV-ICP-MS ($\mu g\ g^{-1} \pm$ SD)*	% RSD	% Recovery
BL529	3.9	3.94 ± 0.03	0.8	101
BL565	8.2	10.5 ± 0.3	2	128
BL591	13.8	13.6 ± 0.3	4	99
BL442	13.9	15.51 ± 0.08	0.5	112

*n = 3, except n = 2 for BL529

The detection limit (3σ) achieved by this method was 20 pg of Hg, or the equivalent of 30 ng g^{-1} for a 12 cm strand of hair (0.6 mg, 1 cm of hair = 0.05 mg). This detection limit also means that only 0.4 cm (corresponding to about two weeks of growth) or roughly 0.02 mg of hair is needed to detect a natural mercury level of 1 μg g^{-1}. As a consequence, just one hair strand is sufficient to estimate mercury levels in an individual – much less hair than the 100 strands that may be required for traditional methods with a digestion step.

We have demonstrated that IH-ETV-ICP-MS can easily determine mercury concentrations in a single hair strand, using external standards calibration with powdered hair CRMs. The results were comparable to that of CV-AAS, but were obtained more

quickly and required a smaller sample size – making IH-ETV-ICP-MS a possibility for routine hair analysis for mercury. In the future, with the controllable temperature of the IH-ETV and the multi-element capability of the ICP-MS, we hope to determine other elements in human hair.

4.5 Acknowledgments

We thank C. Passos and D. Mergler of the Centre d'Etudes des Interactions Biologiques entre la Santé et l'Environnement (CINBIOSE) at l'Université du Québec à Montréal for providing the hair samples. Scholarship support from the Natural Sciences and Engineering Research Council (NSERC) and the Fonds de Recherche sur la Nature et les Technologies (FQRNT) is gratefully acknowledged by JPL.

4.6 References

1. USNRC, *Toxicological Effects of Methylmercury*, National Academy Press, Washington, D.C. 2000.

2. U. S. Gill, H. M. Schwartz and L. Bigras, *Archives of Environmental Contamination and Toxicology*, 2002, **43**, 466-472.

3. T. Y. Toribara and D. A. Jackson, *Analytical Chemistry*, 1982, **54**, 1844-1849.

4. V. Valkovic, D. Miljanic, R. M. Wheeler, R. B. Liebert, T. Zabel and G. C. Phillips, *Nature*, 1973, **111**, 251-252.

5. M. Legrand, R. Lam, M. Jensen-Fontaine, E. D. Salin and H. M. Chan, *Journal of Analytical Atomic Spectrometry*, 2004, **19**, 1287-1288.

6. J. V. Cizdziel and S. Gerstenberger, *Talanta*, 2004, **64**, 918-921.

7. M. Legrand, C. J. S. Passos, D. Mergler and H. M. Chan, *Environmental Science and Technology*, 2005, **39**, 4594-4598.

8. M. E. Rybak and E. D. Salin, *Applied Spectroscopy*, 2001, **55**, 816-821.

9. E. D. Salin and J. M. Ren, *Journal of Analytical Atomic Spectrometry*, 2003, **18**, 953-954.

10. D. M. Goltz, C. D. Skinner and E. D. Salin, *Spectrochimica Acta, Part B: Atomic Spectroscopy*, 1998, **53B**, 1139-1147.

11. D. M. Goltz and E. D. Salin, *Journal of Analytical Atomic Spectrometry*, 1997, **12**, 1175-1180.

12. M. E. Rybak and E. D. Salin, *Spectrochimica Acta, Part B: Atomic Spectroscopy*, 2001, **56B**, 289-307.

13. J. M. Ren, M. E. Rybak and E. D. Salin, *Journal of Analytical Atomic Spectrometry*, 2003, **18**, 485-486.

14. C. J. Passos, D. Mergler, E. Gaspar, S. Morais, M. Lucotte, F. Larribe, R. Davidson and S. de Grosbois, *Environmental Research*, 2003, **93**, 123-130.

15. J. P. Farant, D. Brissette, L. Moncion, L. Bigras and A. Chartrand, *Journal of Analytical Toxicology*, 1981, **5**, 47-51.

Chapter 5 Multielement analysis of human hair by induction-heating electrothermal vaporization inductively coupled plasma mass spectrometry (IH-ETV-ICP-MS)

The previous chapter described mercury determination by IH-ETV-ICP-MS using a relatively low vaporization temperature of about 800°C. Mercury has a unique chemistry making it particularly attractive for a thermal vaporization technique.

However, since the ICP-MS has multielement capabilities and the IH-ETV can achieve higher vaporization temperatures, the application of IH-ETV-ICP-MS was expanded to include other elements that may be found in hair. For example, other toxic metals such as arsenic and lead can be used to monitor for toxicity and environmental exposure in a similar fashion as mercury is used. The levels of other elements in hair may be linked to nutrition and disease. This chapter describes use of IH-ETV-ICP-MS for the direct multielement analysis of powdered hair materials.

5.1 Abstract

Conventional methods of hair analysis, using instruments such as inductively coupled plasma mass spectrometry (ICP-MS), require a digestion step that has many disadvantages. Instead, we explore the feasibility of using an induction heating-electrothermal vaporizer (IH-ETV) with ICP-MS for direct multielement determination of sub-microgram amounts of solid hair material.

As, Cd, Cu, Hg, Pb and Zn were determined using powdered hair standard reference materials. Transient ICP-MS profiles reveal that powdered hair SRMs and hair strands have the same analyte signal shapes, while solution profiles do not match. External standards calibration using SRMs gives results that agree with the certified values, with the precision of determination ranging from 9–54%. External standards calibration using solutions standards or by a standard additions approach did not give accurate results due to the different temporal response. Absolute detection limits ranged from 0.01–8 ng, low enough to determine natural levels of metals in a single human hair strand.

5.2 Introduction

The use of hair samples as indicators of metals concentration in the human body has gained recent interest in environmental, clinical, and forensics fields. For example, studies have investigated the use of hair samples for the determination of levels of mercury intoxication [1], for monitoring workplace exposure to heavy metals [2], and for potentially discriminating sick and healthy patients [3, 4].

A common approach to simultaneous multielement analysis of hair samples is by inductively coupled plasma atomic emission spectroscopy (ICP-AES) or inductively coupled plasma mass spectrometry (ICP-MS) [5-7]. Conventional ICP analyses using nebulization require samples to be in a solution form, thus hair strands need to be digested prior to analysis. Digestion protocols for hair samples can be laborious, sometimes involving overnight digestion [4] or treatment multiple steps [6]. These protocols can lead to sample contamination or analyte loss.

Several multielement methods of direct hair analysis have been proposed in the literature. While X-ray fluorescence has a precision of 1% for hair analysis, its relatively poor detection limits (in the parts per million range) restricts the number of elements that can be naturally detected in hair [8]. Neutron activation analysis has also been used for multielement analysis of hair samples [9], but the cost and accessibility of the instrumentation does not make it attractive for routine use. Laser ablation with ICP-MS [10, 11] and direct sample insertion with ICP-AES [12] have been investigated for multielement hair analysis.

Hair analysis using an electrothermal vaporizer (ETV) as a solid sample introduction system for an ICP instrument has been demonstrated [13-15]. However, the

typical ETV design using a graphite furnace tube does not allow for easy insertion of solid hair samples. For example, techniques of placing hair samples into the ETV may include embedding hair strands in glue or tape [13]. Introduction of samples to ETV systems can also been done as slurries. However, slurry methods such as the one described by Chen *et al.* [15] for hair analysis can be as laborious as hair digestion procedures.

In the previous work shown in Chapter 4, the use of an induction heating electrothermal vaporizer (IH-ETV) with ICP-MS was successful in determining mercury concentrations in single human hair strands [16]. However, the multielement capability of ICP-MS was not fully exploited nor explored. In this paper, we investigate the use of IH-ETV-ICP-MS for multielement analysis of human hair. The IH-ETV design offers advantages over the traditional ETV design, such as interchangeable sample cups, ease of use and large potential sample volumes. The removal of the sample cup from the system also allows for easy and rapid sample placement.

5.3 Experimental

5.3.1 Samples and standards

As calibrated hair strands are not yet available as reference materials, powdered hair certified reference materials were used. Three different materials were examined: BCR 397 (Institute for Reference Materials and Measurements, Belgium), NIES 13 (National Institute for Environmental Studies, Japan), and IAEA 086 (International Atomic Energy Agency, Austria). The reference materials were homogenized by manual shaking prior to being weighed (analytical balance readability = ± 0.01 mg; standard deviation 0.02 mg). To approximate the equivalent mass of a 12-cm strand of hair, 0.30–1.00 mg of reference material were used per analysis.

Multielement standard solutions containing As, Cd, Cu, Hg, Pb, and Zn were prepared on the day of analysis from dilutions of single element 1000 $\mu g\, g^{-1}$ stock solutions (2–5% HNO_3 matrix, SCP Science, Baie D'Urfé, Quebec, Canada or Fisher Scientific, Nepean, Ontario, Canada). Dilutions were done using 1% HNO_3, which was made from stock trace metal grade HNO_3 (Fisher Scientific, Nepean, Ontario, Canada) in 18 MΩ distilled deionized water (Milli-Q water system, Millipore Corp., Bedford, MA, USA).

5.3.2 Instrumentation

The IH-ETV system used in this study, a modified LECO Model 521 induction furnace with a full forward power of 1.5 kW (LECO, St. Joseph, MI, USA) and a quartz sample chamber, has been previously described in detail [17-20]. As in the previous study with

mercury, water vapour was introduced into the carrier gas through a sparger containing distilled deionized water to reduce the risk of arcing within the sample chamber [16].

Commercially available graphite sample cups (type S-3 cup mounted on a separate S-1 pedestal, Bay Carbon, Bay City, MI, USA) were used. A boiler cap (type BC-1, Bay Carbon) was also used as a lid in order to contain the sample within the cup. The specifications of the parts of the graphite cup assembly are given in Figure 5-1. Before use, new graphite cups were cleaned by heating at full RF power (approximately 1400°C inside the cup) for 60 seconds to remove any possible contamination. Samples or standards placed in the cup were heated at full RF power for a total of 60 seconds. A separate drying step was not implemented for liquid standards. Cups were reheated at full RF power between runs to ensure no sample carryover.

The vaporized samples were analyzed using a Perkin-Elmer Elan 6000 ICP-MS (SCIEX, Concord, ON, Canada) connected to the IH-ETV through a 90 cm piece PTFE tubing (1/4" o.d., 1/8" i.d., Cole-Parmer, Anjou, QC, Canada). The ICP-MS parameters are summarized in Table 5-1. Due to the range of analyte masses examined and their concentrations in the reference hair materials (0.5 to 199 $\mu g\ g^{-1}$), the Elan 6000 Autolens and Dual Stage detector features were used.

Figure 5-1 Dimensions of the graphite sample holder: (A) cup, (B) pedestal, and (C) boiler cap (not drawn to scale)

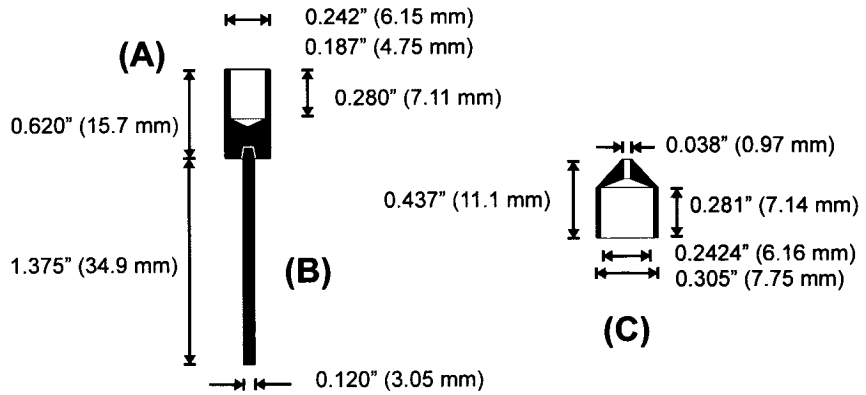

Table 5-1 ICP-MS operating parameters

ICP-MS	
RF power	1100 W
Sampling and skimmer cones	Nickel
Plasma gas flow rate	15 l min^{-1} Ar
Auxiliary gas flow rate	1.2 l min^{-1} Ar
Carrier gas flow rate	0.5 l min^{-1} Ar
Signal measuring parameters	
Detector mode	Dual (pulse and analog modes)
Autolens	On
Acquisition mode	Peak hopping
Sweeps per reading	1
Readings per replicate	600
Replicates	1
MCA channels	1
Dwell time	25 ms per isotope
Total acquisition time	105 s
Isotopes measured	^{63}Cu, ^{66}Zn, ^{75}As, ^{111}Cd, ^{197}Au, ^{202}Hg and ^{208}Pb

5.4 Results and Discussion

5.4.1 Temperature calibration

In this study, commercially available graphite cups were used instead of graphite cups machined in-house. The commercial cups generally have thicker walls than those that are machined. It was expected that there might be a loss of sensitivity due to the use of thicker walls that would provide slower heating rates. It was felt that this disadvantage was offset by the precision improvement that was to be expected by using manufactured rather than hand-made electrodes. Initial experiments were performed using the same type of commercially available graphite cup as in the previous mercury study (type S-16, Bay Carbon) [16]. However, the maximum temperatures that were obtained at full RF power were approximately 1400°C for the outside of the cup and 1200°C for the inside bottom of the cup. While these temperatures are sufficient to vaporize a volatile element such as mercury, they were not high enough for even moderately volatile elements such as zinc or lead.

Subsequent experiments were performed using S-3 type cups, which were of same general dimensions except they have thinner walls. Of the commercially available graphite cups offered by Bay Carbon that can be fitted with boiler caps, the S-3 cups achieve the highest temperatures. The temperature calibration of these cups and the IH-ETV system was performed using temperature-indicating lacquers (rated at 111°C, 302°C, 649°C, Omega Engineering Inc., Stamford, CT, USA) and pellets (rated at 107°C and 816°C) applied to the outside and to the inside of the graphite cups. The results are shown in Figure 5-2.

Figure 5-2 Temperature calibration of the graphite cup and boiler cap

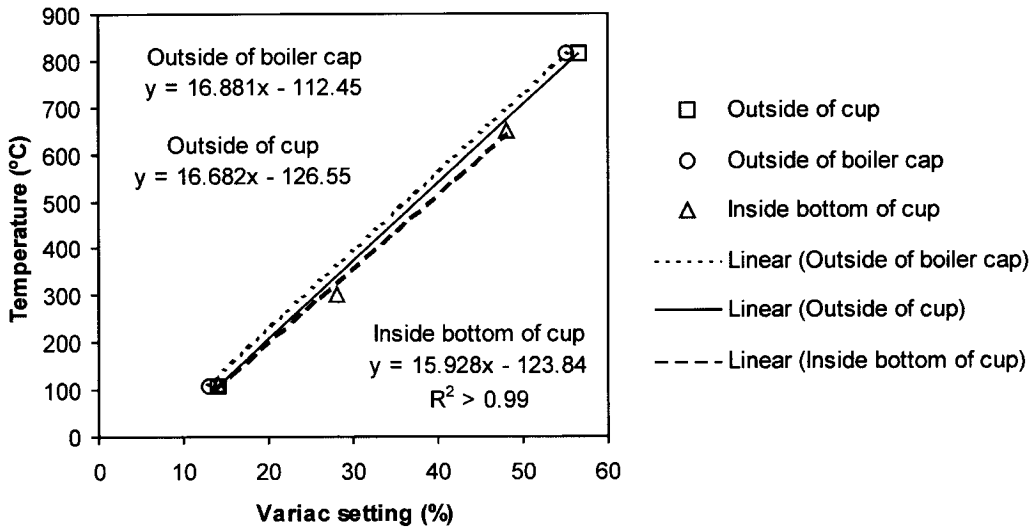

While the ranges of indicators used did not cover the full temperature range achieved by the cups, previous experiments using similarly shaped graphite cups and an IR thermocouple have shown that the temperature of the graphite cup is linear with respect to applied power from the range of 10% to 100% applied power. To calculate the maximum temperature reached by S-3 graphite cups, the same linear trend was assumed for these cups and the data in Figure 5-2 was extrapolated to the 100% Variac setting. The maximum temperature obtained at full RF power was approximately 1600°C outside of the cup and boiler cap, and 1400°C for the inside bottom of the cup where the sample is placed.

5.4.2 General observations of solid samples

Figure 5-3 shows the transient signals obtained from 0.62 mg of BCR 397 reference material. RF power was applied to the cups at the 10-second mark of the acquisition until the 70-second mark, giving a total heating time of 60 seconds. At an inside cup temperature of 1400°C, As, Hg, Cd, Pb and Zn appear to be completely vaporized from the powdered hair sample, while Cu does not appear to be vaporized.

It is also interesting that Zn, Cd, and Pb show multiple peaks in their transient profiles while Hg and As do not. Hg and As are the most volatile of the elements examined and the final inside temperature achieved by the graphite cup is sufficiently high to cause rapid vaporization of these elements. The remaining elements are less volatile in comparison. The multiple peaks may be the result of spatial temperature differences inside of the graphite cup. The inside walls of the cup probably heat up more quickly than the base of the cup, so any powdered sample adhered to the walls instead of the bottom of the cup is vaporized more quickly. A second explanation is that there could be multiple forms of the analyte present in the hair sample, each species producing a separate peak.

The transient signals for the same elements in NIES 13 and IAEA 086 reference materials showed the same profiles (Figure 5-4). Moreover, a 0.69 mg strand of hair from the author's head also showed the same general transient profiles (shown in Figure 5-5, elemental concentrations not known), indicating that powdered reference materials should be suitable for calibration of human hair strands.

Figure 5-3 Time profiles for powdered human hair (BCR 397, 0.62 mg)

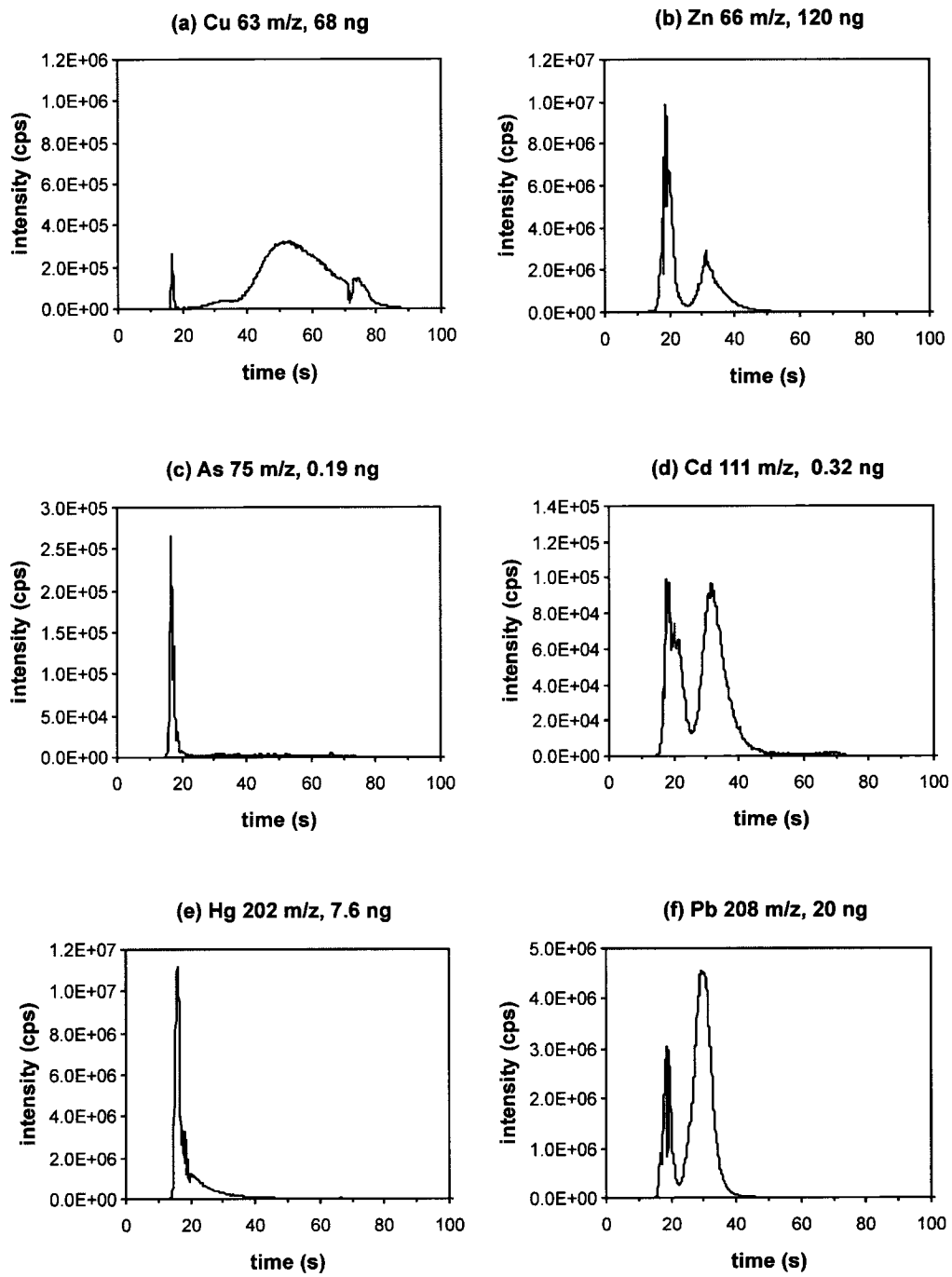

Figure 5-4 Time profiles for Zn (66 m/z) with three different hair reference materials. The data for IAEA 086 and NIES 13 are offset by $7.0*10^6$ and $1.6*10^7$ cps, respectively.

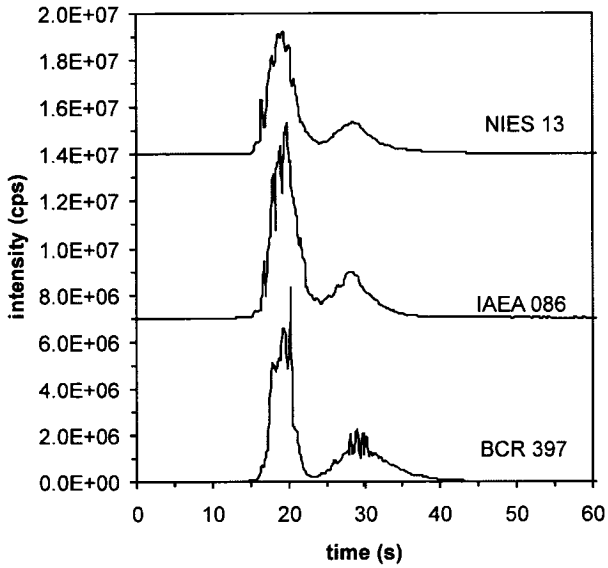

Figure 5-5 Time profiles for a single strand of human hair (0.69 mg)

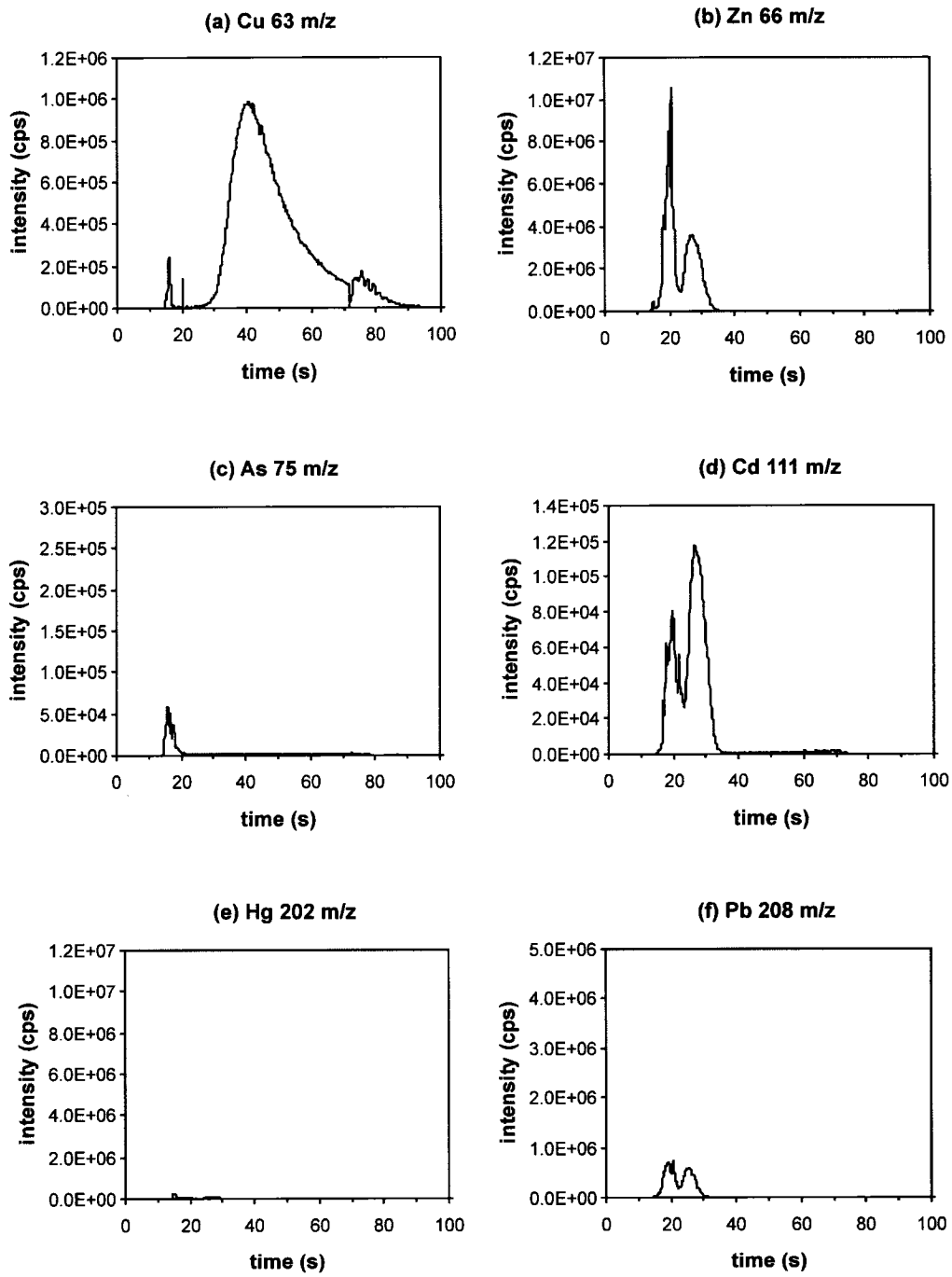

Some hair samples were ashed to investigate the effect of an ashing stage on the time profiles. The ashing stage consisted of heating the cup for 40 seconds at 500°C prior to the vaporization step. However, at that temperature, mercury vaporized easily while some of the other analytes also started to vaporize towards the end of the ashing stage. During the vaporization stage, there was no change in peak shape of the remaining analytes. Ashing under these conditions did not appear to offer any particular advantage and caused some premature loss of analytes, therefore only straight vaporization was used for subsequent analyses.

5.4.3 External standards calibration using powdered hair reference materials

Typical mass calibration plots using various amounts of both BCR 397 and NIES 13 SRMs and the integrated peak areas of the signals are shown in Figure 5-6. The peak areas were blank-corrected.

For arsenic, BCR 397 and NIES 13 show two different linear slopes. This is probably due to concentration values used to calculate the mass of arsenic present in the sample – the concentration values provided by the manufacturers for both of these materials are "indicative" values and are not certified values. While no arsenic value is supplied for IAEA 086, a four-point plot of integrated signal *vs.* sample mass also shows a straight line with $R^2 = 0.99$. The high linearity in the arsenic mass calibration plots indicates that it should be possible to accurately determine arsenic levels in hair samples by this method.

In Figure 5-6, Hg also shows a linear calibration plot as previous work has demonstrated, while Cd and Pb show some correlation. Zn and Cu plots show considerable scatter. This is probably due to incomplete vaporization of these elements from the hair matrix at 1400°C. Inhomogeneity of the sample is not a likely source of the scatter as one would expect poor correlation for all elements detected in that case.

Figure 5-6 Calibration plots using combination of BCR 397 and NIES 13 SRMs

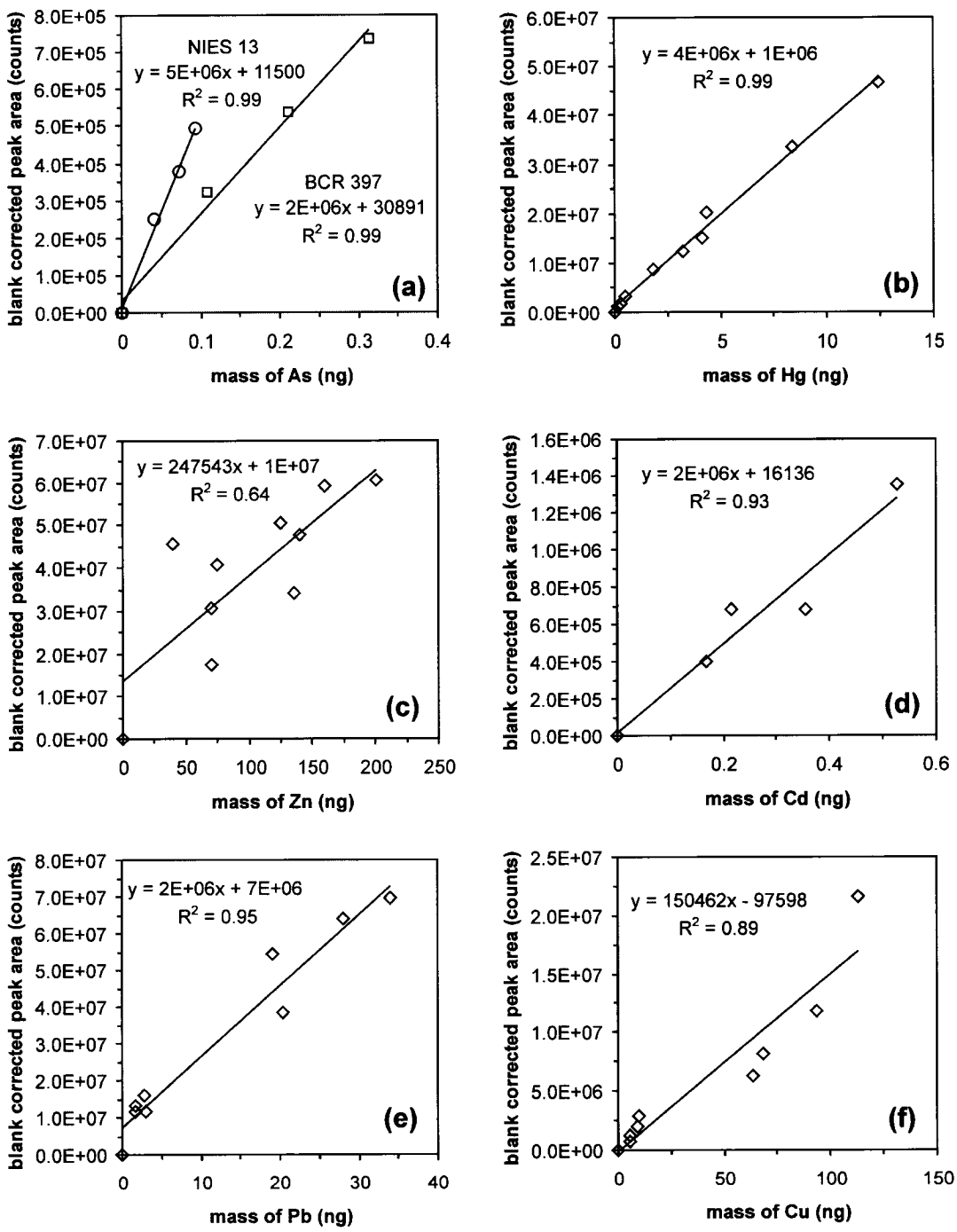

Varying masses of BCR and NIES were analyzed. In a set of samples containing both SRMs (4 of each SRM, total of 8 samples), one sample was treated as an "unknown" sample. The remaining samples (7 in this case) were then used to construct a mass calibration curve from which the concentration of the "unknown" was determined. This "leave-one-out" procedure was repeated for each sample in the set in order to determine its concentration.

This was repeated with a second set of samples (3 of each SRM, total of 6 samples). A pooled t-test at 95% confidence interval showed that there was no significant difference between the two data sets. The combined data from both sets (7 of each SRM, total 14 samples) is shown in Table 5-2. Note that the cadmium concentration was determined as a mean of two samples for each reference material as the remaining samples were near the detection limit. The results show agreement at a 95% confidence level with the certified values.

Table 5-2 Mean concentrations (± 95% confidence interval) as determined by external standards calibration using SRMs

Element	BCR 397 found ($\mu g\ g^{-1}$)	BCR 397 certified ($\mu g\ g^{-1}$)	NIES 13 found ($\mu g\ g^{-1}$)	NIES 13 certified ($\mu g\ g^{-1}$)
Hg	12 ± 1 (n=7, 9% RSD)	12.3 ± 0.5	4.5 ± 0.5 (n=7, 12% RSD)	4.4 ± 0.2
Cd	0.50 (n=2)	0.52 ± 0.02	0.27 (n=2)	0.23 ± 0.03
Pb	35 ± 9 (n=7, 29% RSD)	33 ± 1	6 ± 3 (n=7, 54% RSD)	4.6 ± 0.4
Zn	190 ± 80 (n=7, 47% RSD)	199 ± 5	190 ± 40 (n=7, 20% RSD)	170 ± 10

5.4.4 External standards calibration using multielement solutions

Even with the availability of several powdered reference hair materials, these reference materials may not necessarily be certified for the element of interest. The feasibility of using multielement solutions for calibration of hair samples was therefore examined.

The transient profiles of 10 µl of a multielement solution are shown in Figure 5-7. Arsenic was surprisingly not detected in the solution form. Aside from mercury, the peak shapes for solution form of the elements do not resemble those of the solid forms in Figure 5-3. In general, the solution forms of the elements vaporize more quickly than the solid form in the hair sample. The difference in volatility results from the form of the analytes, where in solution they are in an inorganic form when dried, while in the hair samples the analytes are likely bound to sulfur atoms in the cysteine residues of the hair's protein structure.

Figure 5-7 Transient profiles for a multielement standard solution (10µl)

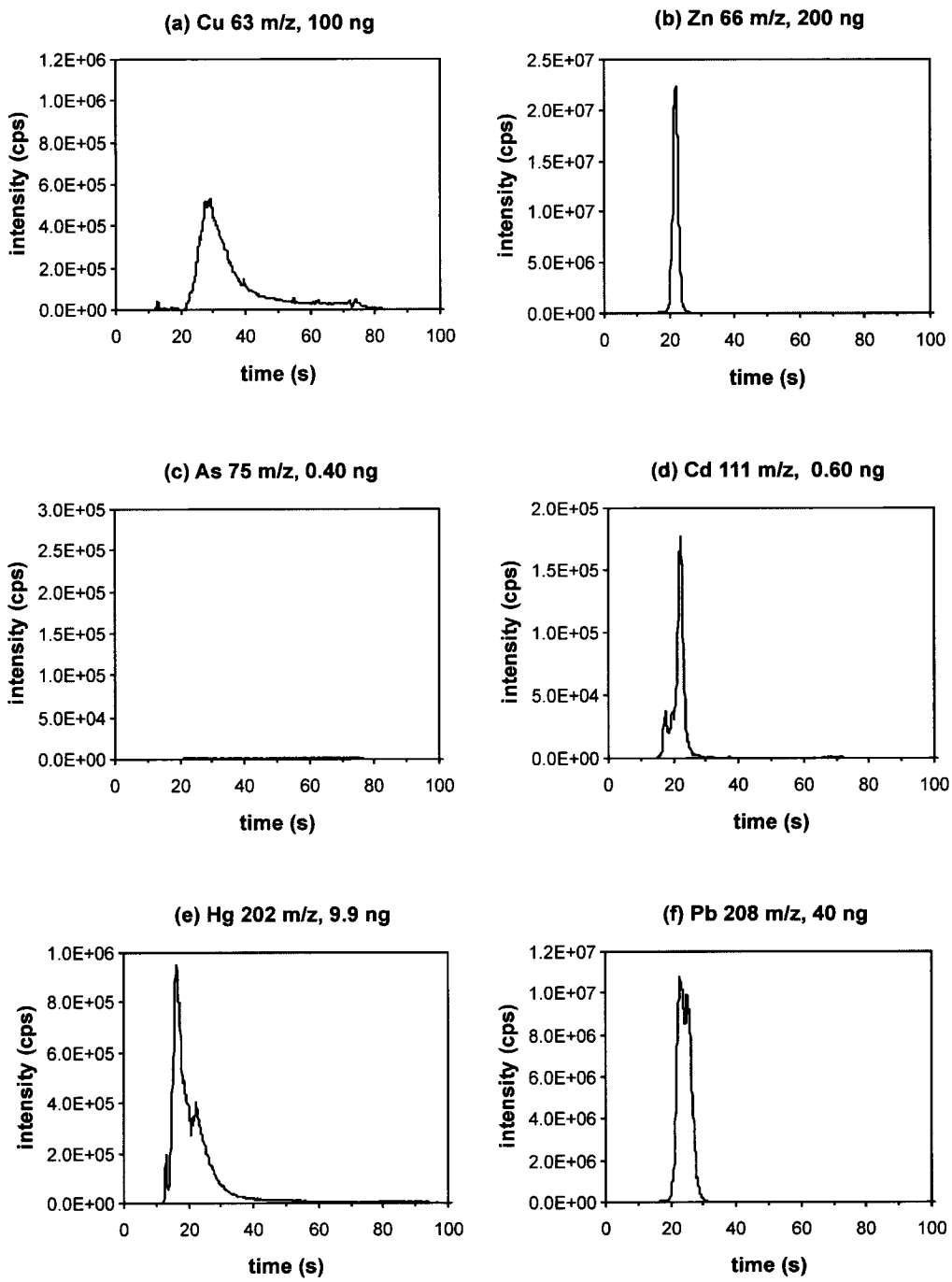

While the peak shapes are not the same for the solution and solid forms, it should not matter if the integrated peak areas are equivalent for the same mass of analyte. Calibration plots are shown in Figure 5-8. Arsenic is not shown since it was not detected in any solution, while mercury had the same time-dependent problem mentioned in previous mercury work (Chapter 4). With the exception of copper since it does not appear to be completely vaporized at this temperature, the plots are generally linear. However, the slopes of the plots show that the sensitivity (*i.e.* response/unit-mass) for solution samples is much lower than for solid samples. Concentration values for the powdered hair SRMs calculated using these regression values would then be greatly overestimated. The difference in sensitivities is likely due to the difference in transport efficiencies for liquid versus solid samples. It is possible that the particles from the hair matrix are acting as physical carriers for the vaporized analyte. Due to the difference in sensitivities, external standards by solution calibration is not suitable for direct multielement determination of hair samples.

Figure 5-8 Calibration plots for multielement solutions: (a) Cu 63 m/z, (b) Zn 66 m/z, (c) Cd 111 m/z, and (d) Pb 208 m/z

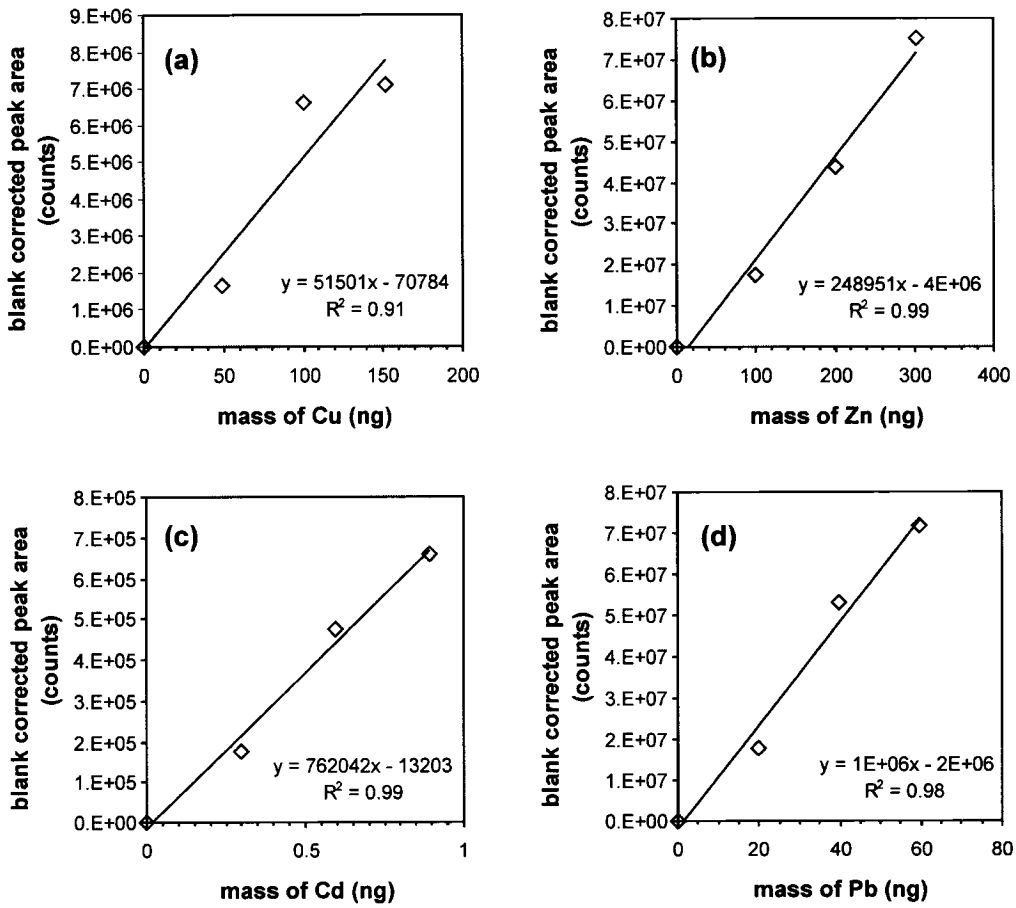

5.4.5 Standards addition calibration

A standard additions approach in which a small aliquot of standard solution is added to a solid sample has been described for ETV-ICP-MS work [14]. It is possible that the transport efficiency difference between the solid and solution sample may be overcome in this manner, allowing standard solutions to be used for calibration.

Figure 5-9 shows that the transient peak of Cd for powdered hair SRM spiked with 10 µl of standard solution (that is allowed to air-dry prior to vaporization) is merely the overlap of the transients seen for the solid and solution forms of Cd. The same observations can be made for the other elements that show multiple peaks in the solid transient profiles. This indicates that the added analyte from the solution spike is not interacting with the hair matrix the in the same manner as the analyte already present in the hair sample. Combined with the added difficulty of weighing replicate sub-microgram masses of hair sample, it is not surprising that the calculated elemental concentrations did not resemble the certified values. Therefore, a standard additions methodology using spikes of standard solution on the solid material is not a suitable approach for quantifying solid hair samples.

Figure 5-9 Cd 111 m/z time profiles in (a) powdered hair, (b) standard solution, and (c) powdered hair spiked with standard solution

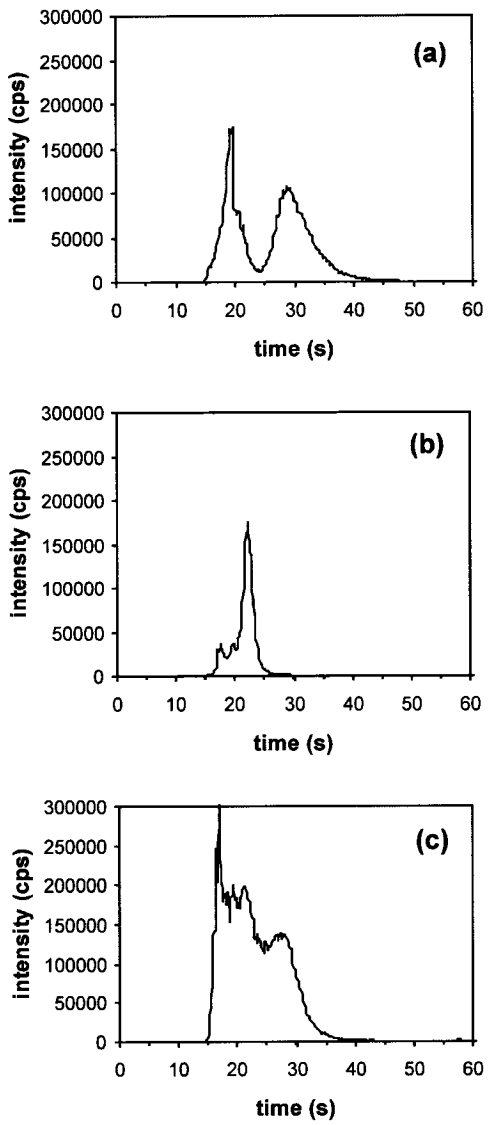

5.4.6 Limit of detections in hair

While a true blank was not available (*i.e.*, a hair sample that did not contain any of the elements monitored in this study), empty graphite cups were used to estimate a blank signal. The limit of detection (LOD) was then calculated using the following criteria:

Equation 5-1

$$LOD = 3\sigma_b / m$$

where σ_b is the standard deviation of the integrated blank signal and m is the slope of the calibration curve derived from the powdered hair SRMs. The results are presented in Table 5-3.

Table 5-3 Limits of detection (LOD) for various elements in hair for IH-ETV-ICP-MS

Element	Absolute LOD (ng)	Concentration LOD[a] ($\mu g\ g^{-1}$)	BCR 397 certified value ($\mu g\ g^{-1}$)
Cu	8	10	110[b]
Zn	0.8	1	199
As	0.01	0.02	0.31[b]
Cd	0.07	0.1	0.521
Hg	0.05	0.08	12.3
Pb	0.03	0.04	33.0

[a] based on a 0.6 mg sample (the average weight of a 12-cm strand of hair)
[b] indicative value, not certified value

If the certified concentration values for the SRMs are considered to be in the normal range for these elements in human hair, it is then apparent that a single human hair strand is sufficient to detect these elements by IH-ETV-ICP-MS. The LODs achieved are also comparable or up to two orders of magnitude better than those achieved for direct hair analysis by direct sample insertion or ETV with ICP-AES [12, 14].

5.5 Conclusions

Multielement analysis by IH-ETV-ICP-AES is possible, giving analyte detection limits below natural levels found in a single hair strand. Calibration by solid reference materials showed the most promise, while solution standards did not accurately quantify concentrations due to differences in transport efficiencies. Future work includes increasing the temperature achieved by the graphite sample cup in order to effectively vaporize less volatile analytes.

5.6 References

1. S. A. Katz and R. B. Katz, *Journal of Applied Toxicology*, 1992, **12**, 79-84.

2. W. Wasiak, W. Ciszewska and A. Ciszewski, *Analytica Chimica Acta*, 1996, **335**, 201-207.

3. X. Wang, Z. Zhuang, E. Zhu, C. Yang, T. Wan and L. Yu, *Microchemical Journal*, 1995, **51**, 5-14.

4. N. Miekeley, L. M. De Carvalho Fortes, C. L. Porto da Silveira and M. B. Lima, *Journal of Trace Elements in Medicine and Biology*, 2001, **15**, 46-55.

5. K. Sreenivasa Rao, T. Balaji, T. Prasada Rao, Y. Babu and G. R. K. Naidu, *Spectrochimica Acta, Part B: Atomic Spectroscopy*, 2002, **57B**, 1333-1338.

6. I. Rodushkin and M. D. Axelsson, *Science of the Total Environment*, 2000, **250**, 83-100.

7. H. Toyoda, H. Uchida and J. Takahashi, *Bunseki Kagaku*, 1986, **35**, T80-T85.

8. T. Y. Toribara and D. A. Jackson, *Analytical Chemistry*, 1982, **54**, 1844-1849.

9. I. Abugassa, S. B. Sarmani and S. B. Samat, *Applied Radiation and Isotopes*, 1999, **50**, 989-994.

10. S. F. Durrant and N. I. Ward, *Food Chemistry*, 1994, **49**, 317-323.

11. I. Rodushkin and M. D. Axelsson, *Science of the Total Environment*, 2003, **305**, 23-39.

12. C. V. Monasterios, A. M. Jones and E. D. Salin, *Analytical Chemistry*, 1986, **58**, 780-785.

13. J. F. Maurice, G. Wibetoe and K.-E. Sjastad, *Journal of Analytical Atomic Spectrometry*, 2002, **17**, 485-490.

14. F. Plantikow-Vossgaetter and E. Denkhaus, *Spectrochimica Acta, Part B: Atomic Spectroscopy*, 1996, **51B**, 261-270.

15. S. Chen, D. Lu, Z. Hu and Z. Wang, *International Journal of Environmental Analytical Chemistry*, 2005, **85**, 493-501.

16. J. P. Lafleur, R. Lam, H. M. Chan and E. D. Salin, *Journal of Analytical Atomic Spectrometry*, 2005, **20**, 1315-1317.

17. D. M. Goltz and E. D. Salin, *Journal of Analytical Atomic Spectrometry*, 1997, **12**, 1175-1180.

18. D. M. Goltz, C. D. Skinner and E. D. Salin, *Spectrochimica Acta, Part B: Atomic Spectroscopy*, 1998, **53B**, 1139-1147.

19. M. E. Rybak and E. D. Salin, *Applied Spectroscopy*, 2001, **55**, 816-821.

20. M. E. Rybak and E. D. Salin, *Spectrochimica Acta, Part B: Atomic Spectroscopy*, 2001, **56B**, 289-307.

Chapter 6 Induction-heating electrothermal vaporization for the direct analysis of analyte-laden chromatographic powder by inductively coupled plasma atomic emission spectroscopy

The IH-ETV is a unique sample introduction system for atomic spectrometry for the reasons listed in the introduction of this thesis. One of the important characteristics is its ability to handle large sample masses while providing excellent temperature control. We considered that it might be possible to combine the variable vaporization capability provided by the temperature control with the well known advantages of chemical chromatographic separation, thereby providing two "dimensions" of separation. Specifically, it was speculated that it might be possible to trap large amounts of isolated/separated analyte on a chromatographic stationary phase (or solid support) and then use the thermal control of the IH-ETV to vaporize just the trapped analyte (preferably just the analyte) and only small amounts of the chromatographic trapping material.

6.1 Abstract

The direct analysis of 8-hydroxyquinolate complexes adsorbed onto C_{18}-bonded silica gel using induction-heating electrothermal vaporization with inductively coupled plasma mass spectroscopy is described.

The 8-hydroxyquinolate complexes were adsorbed onto the silica gel support through a solid phase extraction procedure. Other elements present in the silica gel sample affected the shape of the Cd transient profile and may affect the magnitude of its signal. An external standards calibration curve constructed from various subsampled masses from the silica gel of one extraction did not produce a linear calibration curve. On the other hand, a calibration curve constructed from the same mass of several silica gel samples of varying concentration did give a linear correlation. Absolute detection limits of analytes studied ranged from 0.02–0.2 μg.

6.2 Introduction

The use of solid phase extraction for preconcentration and matrix separation is popular for trace metals determination, and continues to be an active field of research in atomic spectroscopy [1, 2].

For typical solution analysis by inductively coupled plasma atomic emission spectroscopy or mass spectrometry (ICP-AES or ICP-MS), an elution step is required to remove the bound analytes from the sorbent material. This elution step can lead to several problems. The sorbent used for extraction may not readily release the bound analyte with simple solvent elution, and may require a step to dissolve the sorbent instead [3, 4]. While some procedures suggest an organic solvent such as ethanol or methanol as the best way to elute the analytes from the sorbent, these solvents can negatively affect ICP performance [5, 6].

Direct analysis of the analyte-laden sorbents eliminates the elution step, and offers potential advantages. Higher preconcentration factors may be achieved, as analytes are deposited on less than one gram of sorbent versus being diluted in 5–10 ml of eluant. One might also expect better detection limits by direct analysis when compared to the low 1–3% efficiency of nebulizers. Rattray and Salin have suggested that by eliminating the elution step, it may be easier to design more selective sorbents [7]. In such a case, only the chemistry of retention, not both retention and elution, is of concern.

In spite of the popularity of solid phase extraction, there have been very few reports in the literature describing direct analysis of solid, analyte-laden sorbents or chelating agents. Metals extracted through various co-precipitation methods (*e.g.*, with a Ni–ammonium pyrrolidine dithiocarbamate complex) have been analyzed as solids by

graphite furnace atomic absorption spectroscopy (GF-AAS) [8-10]. Electrothermal vaporization (ETV) – ICP-AES has been used to analyze metals trapped with poly(dithiocarbamate) resin [11]. For the direct analysis of analytes bound to Chelex-100 resin (polystyrene-divinylbenzene iminodiacetate), methods using instrumental neutron activation analysis [12] and direct sample insertion with ICP-AES [7] have been described.

For aqueous samples, an extraction procedure where metals complexed with 8-hydroxyquinoline and trapped onto chromatographic packing (C_{18}-bonded silica gel) is commonly cited [13-18]. Silica gel-based sorbents are also frequently with other complexing agents or functionalized for trace metal solid phase extraction (SPE) applications [1, 19]. While dried precipitates of 8-hydroxyquinoline metal complexes have been directly analyzed by GF-AAS [20], the direct analysis of 8-hydroxyquinoline chelates (or any other metal chelates) laden on chromatographic powder has not yet been reported.

In this chapter, the use of induction-heating electrothermal vaporization (IH-ETV) for the direct analysis of 8-hydroxyquinoline complexes adsorbed onto C_{18}-bonded silica gel is discussed. The sorbent containing the trapped analytes is placed in a sample cup inside of the IH-ETV, where the analytes are vaporized from the sorbent matrix and detected with ICP-AES. ICP-AES was used rather than ICP-MS for these studies, as this technique is less prone to matrix effects and other problems that might emerge with the passage of large amounts of organics through the ICP.

6.3 Experimental

6.3.1 Reagents

Two brands of C_{18}-bonded silica gel were used as packing in the columns: Bondapak Porasil B (37–75 μm, Waters Corporation, Milford, MA, USA) and Chromabond Sorbenz (mean particle size of 45 μm, Macherey-Nagel, Düren, Germany). Neither material was treated prior to placement in the column.

Methanol (HPLC grade, Fisher Scientific, Nepean, ON, Canada) was used without further purification. An acidified methanol solution was made from 1 ml of concentrated HCl (Baker Instra-Analyzed, J.T.Baker, Phillipsburg, NJ, USA) in 125 ml of methanol.

A 2% NH_4OH solution was prepared from concentrated NH_4OH (ACS Plus, Fisher Scientific) diluted with distilled deionized water (Millipore Co., Bedford, MA, USA).

A 5% (w/v) solution of 8-hydroxyquinoline (99+% purity, Sigma-Aldrich Canada Ltd., Oakville, ON, Canada) in methanol was prepared fresh on the day of extraction.

All sample and reagent containers were conditioned in 10% HNO_3 (diluted in distilled deionized water from trace-metal grade concentrated HNO_3, Fisher Scientific) for at least 24 hours.

6.3.2 Column

The solid phase extraction column was constructed inside a micropipette tip (101–1000 μl Fisherbrand, Fisher Scientific). To act as a support for the packing, a plug of quartz wool was embedded in the pipette tip. Approximately 150 mg of C_{18}-bonded silica gel was slurried with 0.5 ml of methanol and loaded into the pipette tip, to give a packing

bed of about 1 cm in height. Tygon tubing (2.54 mm ID, Cole-Parmer, Anjou, QC, Canada) was attached to the end of the column, and a peristaltic pump (Gilson Inc., Middleton, WI, USA) was used to drive the solvents or sample through the column at a flow rate of about 5 ml min^{-1}. The configuration is illustrated in Figure 6-1.

Figure 6-1 Extraction set-up

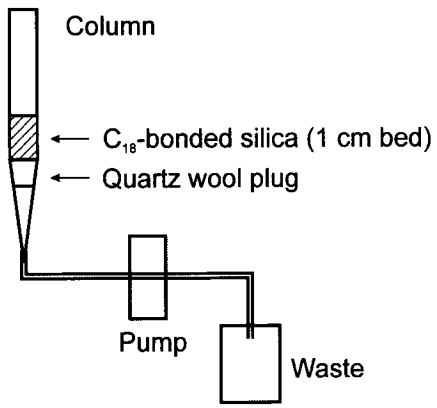

6.3.3 Samples

Aqueous samples (20 ml, elemental concentrations ranging from 0.25 – 1 μg g^{-1}) were prepared by diluting/mixing single-element reference solutions of Cd, Pb and Zn (stock concentration of 1000 μg g^{-1} in 2–5% HNO_3, Fisher Scientific) with distilled, deionized water in preconditioned polypropylene bottles. An equivalent volume of distilled, deionized water was prepared as a blank. Prior to the extraction, 0.5 ml of the 5% 8-hydroxyquinoline solution was added to the sample or blank. This was equivalent to 200–600 times the stoichiometric amount of 8-hydroxyquinoline required to chelate the analytes in a given sample. The sample was adjusted to pH 9.0 ± 0.1 with small additions

(less than 1 ml) of the 2% ammonium hydroxide solution and then manually shaken to ensure good mixing.

6.3.4 Extraction procedure

The basic extraction procedure used was modified from those described by Sturgeon *et al.* [14] and Skinner and Salin [17].

Solvents and samples were delivered to the top of the column manually by glass pipette. The column was washed with about 5 ml of acidified methanol at a flow rate of 5 ml min^{-1}, followed by 5 ml of methanol. The column was then conditioned with approximately 5 ml of distilled deionized water that was previously adjusted to a pH of 9.0 ± 0.1 with the 2% ammonium hydroxide solution.

The sample was then run through the column. The chelated analytes formed an easily observed thin green band on top of the column. The column was then rinsed with roughly 10 ml of deionized distilled water (previously adjusted to pH 9.0), and then air was pumped through for several minutes to remove most of the moisture. The column packing was allowed to air-dry overnight. Once dried, the silica gel was removed from the column, and transferred to a 1.5 ml microcentrifuge tube for storage in a dessicator. The analyte-laden silica gel samples were homogenized by manual shaking prior to being weighed for analysis.

6.3.5 Instrumentation and analysis

The IH-ETV system used in this study, a modified LECO Model 521 induction furnace with a full forward power of 1.5 kW (LECO, St. Joseph, MI, USA) and a quartz sample chamber, has been previously described in detail [21-24]. Commercially available

graphite sample cups (type S-3 cup with boiler cap BC-1, mounted on a separate S-1 pedestal, Bay Carbon, Bay City, MI, USA) were used. Their specifications can be found in Figure 5-1 of the previous chapter. To reduce the risk of arcing, a sparger was used to introduce water vapour in the argon carrier gas stream. Before use, new graphite cups were cleaned by heating at full RF power (approximately 1400°C inside the cup) for 60 seconds to remove any existing contamination.

Silica sample masses in the range of 5–50 mg were placed in the graphite cup. Ten seconds after the start of the data acquisition, power was applied to the IH-ETV to heat the cups for 45 seconds.

A 90 cm piece PTFE tubing (1/4" o.d., 1/8" i.d., Cole-Parmer, Anjou, QC, Canada was used to carry the vaporized analytes to a Thermo-Jarrell Ash IRIS ICP-AES system (Thermo Electron Corporation, Franklin, MA, USA). The peak areas of the transient signals were determined by the IRIS operating software (ThermoSPEC/CID, version 2.2.1). The operating conditions for the IRIS are shown in Table 6-1. With the exception of carbon, two wavelengths were monitored for each analyte in order to show that peaks were real and not due to spectral interferences. Comparison of the line intensity ratios is effective for that purpose.

Table 6-1 ICP-AES operating parameters

RF power	1350 W
Plasma gas flow rate	14 l min^{-1} Ar
Auxiliary gas flow rate	1 l min^{-1} Ar
Carrier gas flow rate	0.8 l min^{-1} Ar
Wavelengths monitored	C: 193.090 nm
	Si: 212.412 nm, 251.612 nm
	Zn: 206.200 nm, 213.856 nm
	Cd: 214.438 nm, 228.802 nm
	Pb: 220.353 nm, 261.418 nm
Number of time slices	500
Time per slice	0.2 s
Total acquisition time	100 s

6.4 Results and discussion

6.4.1 Preliminary studies

Initial experiments were performed to determine the amount of sample that could be placed and vaporized in the graphite cup without overloading the plasma of the ICP-AES. The maximum capacity of the commercial graphite cups was about 50 mg of C_{18}-bonded silica gel. It was discovered that the boiler cap alone was not sufficient to contain sample sizes ranging from 10–50 mg within the cup. After the vaporization step, white deposits of powder were seen in the sample chamber and transport tubing, indicating that some powder was ejected from the cup. Furthermore, an excessive number of particles entering the ICP can potentially clog the injector tip or extinguish the plasma.

To contain the sample inside of the cup, a plug of quartz wool was added as a filter inside of the boiler cap. Heating of empty graphite cups containing only the plug of quartz wool showed no silicon signal, indicating along with visual inspection, that the quartz wool was not breaking down at an inside cup temperature of 1400°C. With the quartz wool plug as a filter, minimal sample particles were seen in the sample chamber of the IHV or along the transport tubing.

Figure 6-2 Cd signal with different IH-ETV connections to ICP-AES

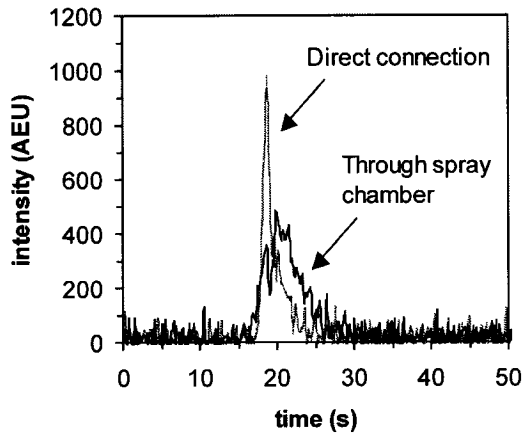

Some studies with samples of chelated cadmium adsorbed on Chromabond were performed to see if using a cyclonic spray chamber could potentially remove the remaining particles that the quartz plug could not contain for larger sample sizes. Figure 6-2 shows the transient signal of Cd when the transport tubing is directly connected to the injector of the ICP torch, and when the transport tubing is connected to a spray chamber attached to the injector. Visual inspection of the chamber showed that it did appear to remove some of the silica particles from the carrier stream, but the transient signal of the adsorbed Cd was broader and noisier than the one obtained with a direct connection. Therefore for all subsequent analyses, a direct connection from the IH-ETV to the torch of the ICP-AES was used along with caution to pack the plug of quartz wool in the boiler cap.

6.4.2 Time profiles of heated silica gel

In Figure 6-3, the time profiles of Cd (228.8 nm) are shown for samples of Chromabond and Porasil B silica gel used to extract an aqueous sample containing only

cadmium as the analyte. In both cases, heating of the sample begins at the 10-second mark, and the Cd is detected at around the 20-second mark. In general, the Cd signal from the Chromabond sample shows a narrow peak width while the Cd signal from the Porasil B sample is broader. This could mean that the Porasil B material may not be heating as quickly as the Chromabond material, or that the chelated analytes may be bonded more strongly to Porasil B.

Figure 6-3 IH-ETV-ICP-AES time profiles (a) 9.8 mg of Chromabond with 1.2 µg of Cd and (b) 10 mg of Porasil B with 0.80 µg Cd (data from 228.8 nm wavelength shown)

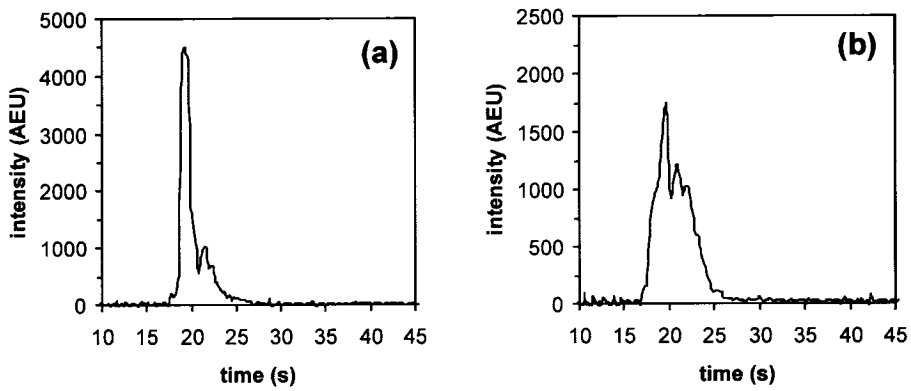

Figure 6-4 and Figure 6-5 show the time profiles of Chromabond and Porasil B used to extract multielement solutions containing Cd, Pb and Zn. The signals were obtained simultaneously; but are shown on separate plots due to scale differences.

Several differences between the profiles of the Chromabond samples and the Porasil B samples were noted. The Chromabond silica gel released a large amount of Si when heated, whereas the Porasil B released relatively little Si. The peak for Zn also consistently occurs a few seconds later in the Porasil B than in the Chromabond sample, indicating again that the Porasil B sample may be heating less quickly.

Interestingly, the Cd profile from the multielement samples was not the same as those from the single element samples shown in Figure 6-4. While not as apparent in Chromabond (Figure 6-4) when compared to Porasil B (Figure 6-5), the multielement samples of both show a second Cd peak that occurs at about the same time as the Zn peak. Both Cd emission lines monitored showed the double peaks.

Figure 6-4 IH-ETV-ICP-AES time profiles of Chromabond (10 mg) laden with Cd, Pb, and Zn.

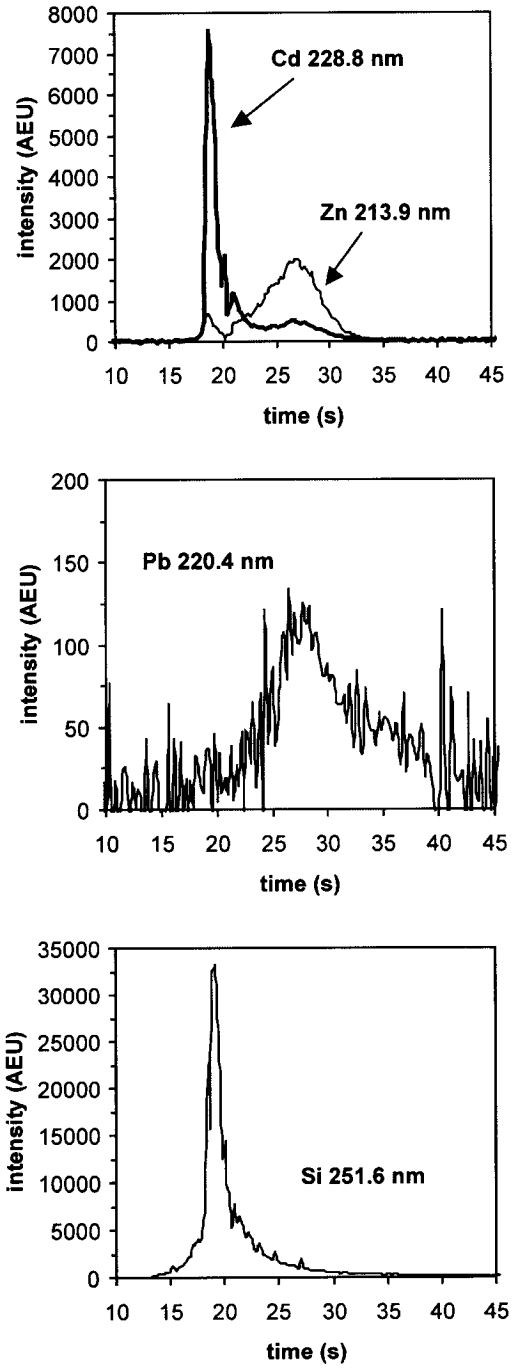

Figure 6-5 IH-ETV-ICP-AES time profiles of Porasil B (10 mg) laden with Cd, Pb, and Zn.

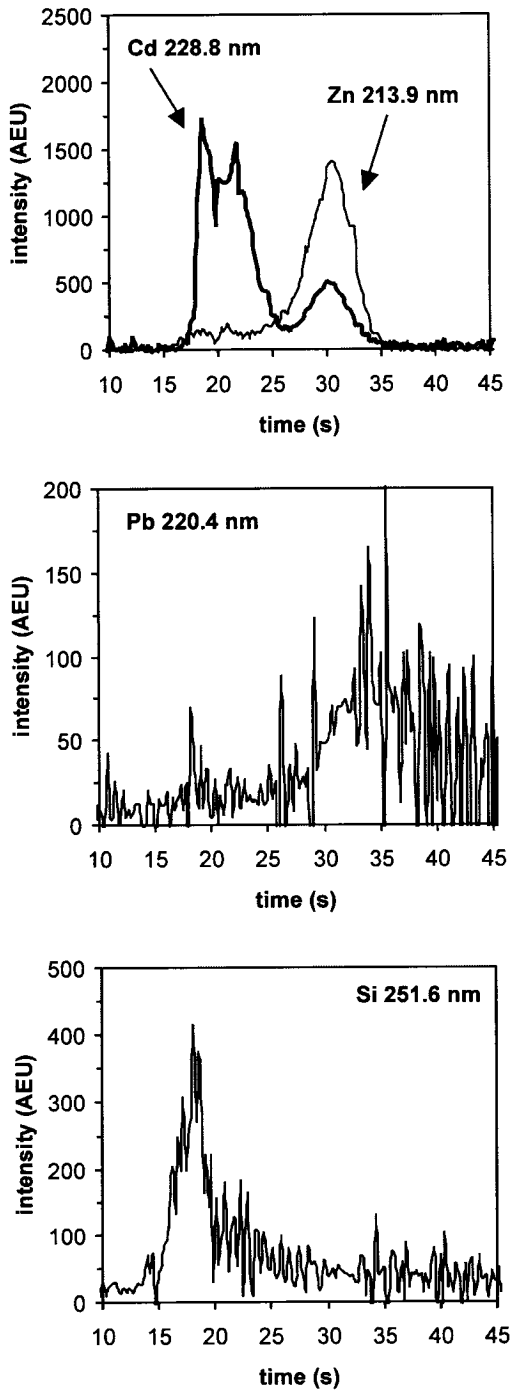

The carbon transient signals for an empty graphite cup and a cup containing a sample are shown in Figure 6-6. The empty cup shows that some carbon is lost during the latter part of the heating process. The additional peak(s) shown for carbon in the profile for the sample show that there is carbon coming from the C_{18}-bonded silica gel matrix and as well as any 8-hydroxyquinoline present. The shape and size of this profile is consistent across all samples and blanks analyzed.

Figure 6-6 Time profiles of carbon (193.1 nm)

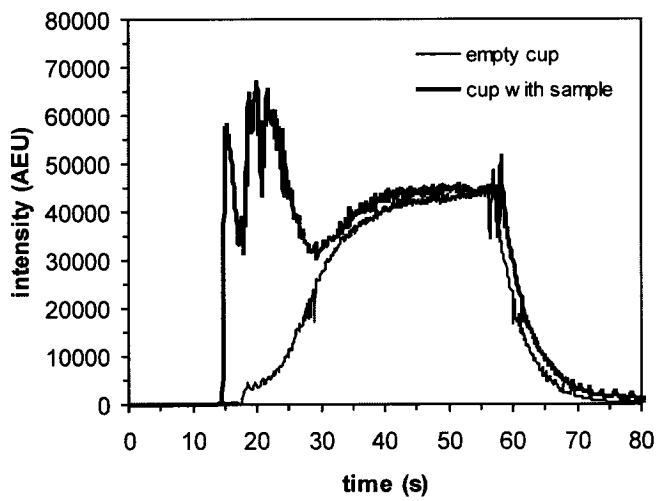

6.4.3 Calibration and detection limits

The waste collected from a few extractions was analyzed by ICP-AES. The measured signals did not vary from levels in waste collected from the blank extraction. Reported recoveries for similar extractions have been reported to be near 100% for Cd, Pb and Zn [13]. Subsequently, it was assumed when calculating the amount of analyte laden on the silica gel that the extraction efficiency was 100% for all samples.

A common approach in calibration by external standards with solid reference materials is to use a mass calibration curve whereby various masses of one reference material of known concentration are used. It is expected that the signal will increase linearly with increased mass of material.

Figure 6-7 Calibration curve obtained from varying the amount of analyte-laden silica from one extraction (Chromabond column)

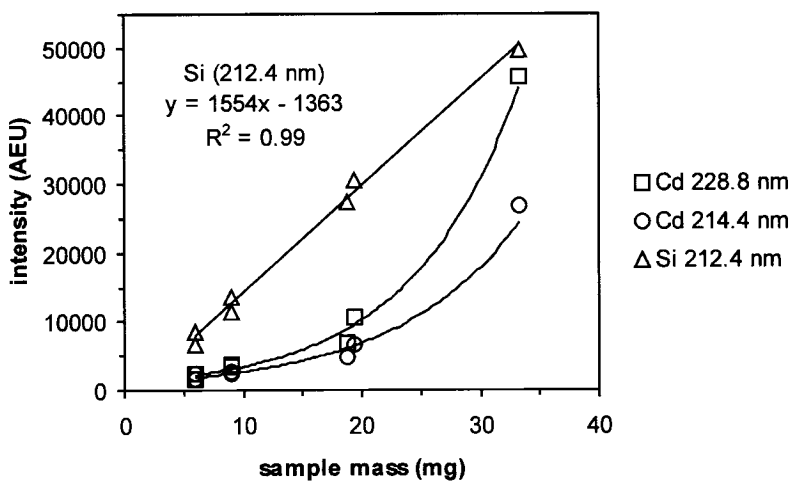

Figure 6-7 shows the results of using 6–33 mg of silica gel from the extraction of an aqueous sample containing 1 μg g^{-1} Cd (20 ml), using Chromabond packing. This sample mass range corresponds to approximately 0.4 to 2 μg of Cd. While the Si signal from the silica present in the sample is linear across the sample mass range, this method of calibration shows poor linear correlation in the Cd signal. In fact, replicate studies confirm a positive deviation from the expected linear response of all laden-analytes studied. This deviation was seen in samples extracted in both Porasil B and Chromabond, and in extractions of single element and multielement samples. The increasing signal with increased mass in the cup may be related to transport efficiency phenomena – when the

mass of sample is increased, so is the amount of silica matrix. The additional silica in the larger samples may be somehow enhancing the transport of the analytes. Mass transport effects in other solid matrices have been reported in the literature for ETV-ICP systems [25, 26].

A second approach in constructing an external standards calibration curve was taken. Figure 6-8 shows the results of analyzing a roughly 10 mg subsample of analyte-laden Porasil B from separate extractions of four solutions of differing concentrations (0.25, 0.5, 0.75, and 1 μg g^{-1} multielement aqueous standards containing Cd, Pb and Zn). A linear response is achieved in this method, showing good correlation for the analytes studied if the amount of matrix is kept the same for each standard.

Figure 6-8 Calibration curve obtained from four samples of different concentrations and a blank (Porasil B column)

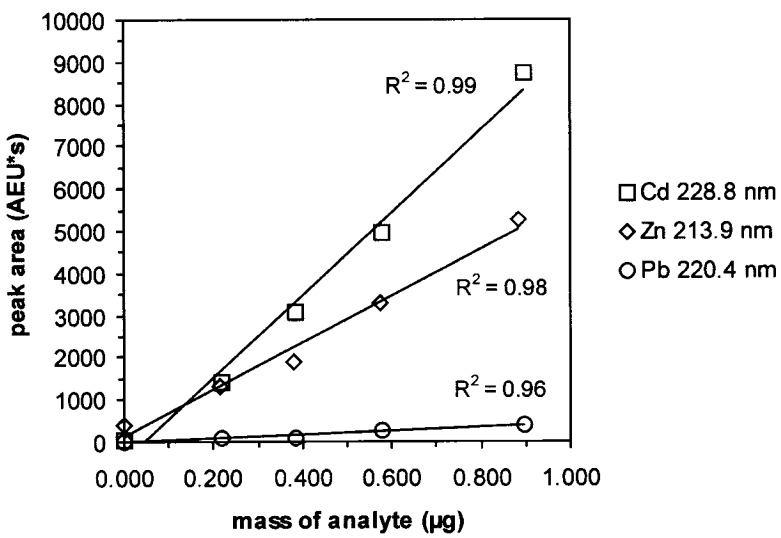

The detection limits (3σ) for Cd, Pb and Zn are shown in Table 6-2. Zn, in particular, has a higher detection limit than the others due to the relatively high blank. As a point of reference, to detect Cd in seawater reference materials (*e.g.*, about 0.03 ng g^{-1})

under these conditions, one litre of sample would be required. Except for Zn, the concentration detection limits are better than those obtained for solution nebulization for the same ICP-AES system (0.08 μg g^{-1} for Cd, 0.04 μg g^{-1} for Pb, and 0.002 μg g^{-1} for Zn). These detection limits could probably be improved if purified reagents are used, as well as optimization of carrier gas flow rate and ICP-AES conditions to improve the sensitivity of the method. The performance of the IH-ETV with an ICP-MS system would have to be tested, but complications might be expected due to the high levels of organics vaporized during the analysis.

Table 6-2 Detection limits of IH-ETV-ICP-AES of chromatographic material

Element (emission line)	Absolute detection limit (μg)	Concentration detection limit (μg g^{-1})*
Cd (214.4 nm)	0.02	0.001
Cd (228.8 nm)	0.02	0.001
Pb (220.4 nm)	0.07	0.004
Zn (206.2 nm)	0.2	0.01
Zn (213.9 nm)	0.2	0.01

* based on an aqueous sample size of 20 g (about 20 ml)

The concentration detection limit calculated in Table 6-2 assumes that the entire amount of sorbent used in the extraction is analyzed by IH-ETV-ICP-AES. If only a 10 mg subsample of the total 150 mg used in the extraction is vaporized in the IH-ETV (as was done in most experiments in this study), then we would expect the detection limit to be 15 times higher.

A "test" sample consisting of an aqueous solution of Cd was extracted in Porasil B. In 10 mg of Porasil B, the sample contained roughly 0.8 μg of Cd. A Cd calibration curve was constructed from the extraction of two multielement standard solutions and a

blank (equivalent to 0 μg, 0.5 μg and 1.1 μg of Cd in 10 mg of Porasil B) and using the integrated peak areas of both Cd peaks present. Each standard was analyzed twice. However, the integrated peak areas of the single Cd peak in the two replicates of the "test" sample were only about 80% of the expected peak area calculated from the calibration curve.

Recall that the single element Cd samples only produced a single peak that corresponded to the first of two Cd peaks seen in the multielement samples. If only the peak areas of the first Cd peak from the multielement standards were used to make the calibration curve, then measured peak area from the single Cd peak of "test" sample does match. This data is illustrated in Figure 6-9.

Figure 6-9 Cadmium calibration curves from multielement standards and a single element test sample (Porasil B column)

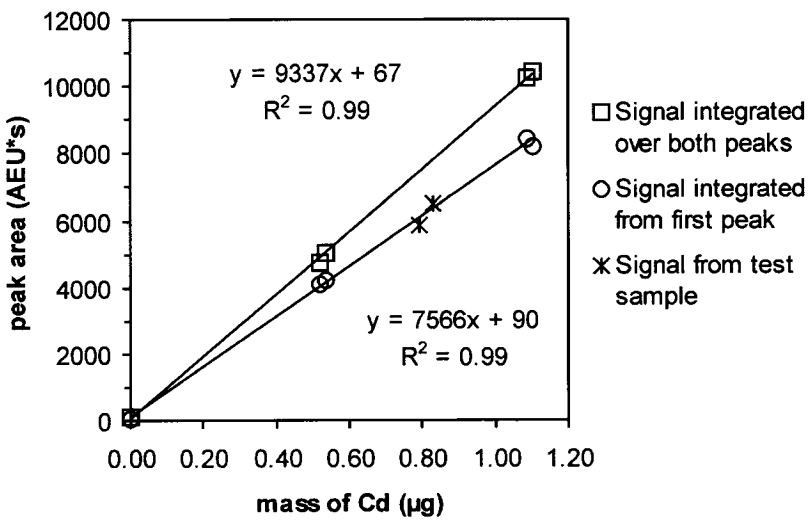

The same trend was seen when the Cd peak area from a 10 mg Chromabond sample containing about 1 μg of Cd was compared to the peak area of 10 mg Chromabond containing 1 μg of Cd, Pb and Zn. The value from the single element

standard was about 80% lower than the multielement sample, despite containing the same amount of Cd. However, the peak areas were similar if only the first Cd peak of the multielement sample was used.

Solutions of Pb and Zn were analyzed by ICP-mass spectrometry and were shown not to contain a different chemical form of Cd that might contaminated the sample and result in a second peak.

There are two possibilities for the discrepancies in the number of peaks and the integrated peak areas between the single element and multielement solution. In the first scenario, there may be a mass transport phenomenon occurring where some Cd is lost by condensation somewhere on the way to the ICP. The deposited Cd could then be picked up by the zinc as it travels to the ICP. In the second case, there may be a chemical conversion of Cd occurring in which the second form of Cd is only seen when other analytes are present.

6.4.4 Extractions in graphite cups

It was proposed that the solid phase extraction could be performed in the graphite sample cup itself. This would allow an easy analysis procedure whereby the extraction is done in the cup and then the cup containing the column packing with the laden analytes is simply transferred to the IH-ETV for direct analysis.

To test the feasibility of packing silica gel into a graphite cup, commercially-available graphite cups (type S-16 from Bay Carbon, specifications may be found in Appendix D) were modified by removing the base and drilling a hole through the stem and bottom of cup. A plug of quartz wool was added to support the silica, while the

peristaltic pump tubing was attached to the stem of the graphite cup. The configuration is shown in Figure 6-10.

Figure 6-10 Setup for extraction in a graphite cup (not to scale)

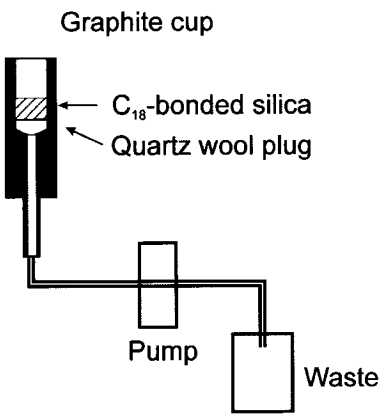

A problem was encountered in when trying to pack the column with a slurry of C_{18}-bonded silica in methanol. It was noticed that with some graphite cups, the methanol would seep into the graphite. The cups that appeared to have a smoother finish on the inside did not seem to have this problem. These graphite cups were also not large enough to contain much silica (roughly 50 mg dry silica capacity).

While the concept of using graphite cups is promising, the cups should have a coating on the inside to prevent intercalation of the solvents/sample into the graphite, as well as be large enough to accommodate the column packing and the stream of aqueous sample. The graphite cups could be pyrolytically coated, as has been done for graphite sample probes used in direct sample insertion into a plasma [27]. Graphite cups can also be machined in-house to obtain the necessary volume.

6.5 Conclusions

We have shown that the analysis of analyte-laden chromatographic material by IH-ETV-ICP-AES is feasible. The detection limits obtained are useful for many applications. The experiments indicate that it may be possible to making sampling systems which treat the sample on-site and then preserve the sample the sample on-column for storage, followed by direct analysis by IH-ETV-ICP-AES later in the laboratory. Experiments would certainly be necessary to determine the effects of other matrix species.

6.6 References

1. V. Camel, *Spectrochimica Acta, Part B: Atomic Spectroscopy*, 2003, **58B**, 1177-1233.

2. E. H. Evans, J. A. Day, C. Palmer, W. J. Price, C. M. M. Smith and J. F. Tyson, *Journal of Analytical Atomic Spectrometry*, 2006, **21**, 592-625.

3. R. S. S. Murthy, Z. Horvath and R. M. Barnes, *Journal of Analytical Atomic Spectrometry*, 1986, **1**, 269-272.

4. R. M. Barnes and J. S. Genna, *Analytical Chemistry*, 1979, **51**, 1065-1070.

5. J. W. Olesik and A. W. Moore, Jr., *Analytical Chemistry*, 1990, **62**, 840-845.

6. T. W. Avery, C. Chakrabarty and J. J. Thompson, *Applied Spectroscopy*, 1990, **44**, 1690-1698.

7. R. Rattray and E. D. Salin, *Journal of Analytical Atomic Spectrometry*, 1995, **10**, 1053-1058.

8. Q. Zhang, H. Minami, S. Inoue and I. Atsuya, *Fresenius' Journal of Analytical Chemistry*, 2001, **370**, 860-864.

9. Q. Zhang, H. Minami, S. Inoue and I. Atsuya, *Analytica Chimica Acta*, 2000, **407**, 147-153.

10. Q. Zhang, H. Minami, S. Inoue and I. Atsuya, *Analytica Chimica Acta*, 1999, **401**, 277-282.

11. W. W. Van Berkel and F. J. M. J. Maessen, *Spectrochimica Acta, Part B: Atomic Spectroscopy*, 1988, **43B**, 1337-1347.

12. J. E. Milley and A. Chatt, *Journal of Radioanalytical and Nuclear Chemistry*, 1987, **110**, 345-363.

13. R. E. Sturgeon, S. S. Berman and S. N. Willie, *Talanta*, 1982, **29**, 167-171.

14. R. E. Sturgeon, S. S. Berman, S. N. Willie and J. A. H. Desaulniers, *Analytical Chemistry*, 1981, **53**, 2337-2340.

15. H. Watanabe, K. Goto, S. Taguchi, J. W. McLaren, S. S. Berman and D. S. Russell, *Analytical Chemistry*, 1981, **53**, 738-739.

16. S. N. Willie, R. E. Sturgeon and S. S. Berman, *Analytica Chimica Acta*, 1983, **149**, 59-66.

17. C. D. Skinner and E. D. Salin, *Journal of Analytical Atomic Spectrometry*, 2003, **18**, 495-500.

18. J. Otero-Romani, A. Moreda-Pineiro, A. Bermejo-Barrera and P. Bermejo-Barrera, *Analytica Chimica Acta*, 2005, **536**, 213-218.

19. M. Zougagh, J. M. Cano Pavon and A. Garcia de Torres, *Analytical and Bioanalytical Chemistry*, 2005, **381**, 1103-1113.

20. K. Akatsuka and I. Atsuya, *Fresenius' Zeitschrift fuer Analytische Chemie*, 1987, **329**, 453-456.

21. D. M. Goltz and E. D. Salin, *Journal of Analytical Atomic Spectrometry*, 1997, **12**, 1175-1180.

22. D. M. Goltz, C. D. Skinner and E. D. Salin, *Spectrochimica Acta, Part B: Atomic Spectroscopy*, 1998, **53B**, 1139-1147.

23. M. E. Rybak and E. D. Salin, *Applied Spectroscopy*, 2001, **55**, 816-821.

24. M. E. Rybak and E. D. Salin, *Spectrochimica Acta, Part B: Atomic Spectroscopy*, 2001, **56B**, 289-307.

25. R. D. Ediger and S. A. Beres, *Spectrochimica Acta, Part B: Atomic Spectroscopy*, 1992, **47B**, 907-922.

26. D. C. Gregoire, M. Lamoureux, C. L. Chakrabarti, S. Al-Maawali and J. P. Byrne, *Journal of Analytical Atomic Spectrometry*, 1992, **7**, 579-585.

27. M. E. Rybak and E. D. Salin, *Journal of Analytical Atomic Spectrometry*, 1998, **13**, 707-713.

Chapter 7 Conclusion

7.1 Summary of thesis work

The work presented in this thesis shows that it is possible to use laser ablation and thermal vaporization with inductively coupled plasma instruments to directly analyze biological, environmental, and pharmaceutical samples in the solid form.

In Chapter 2, the first application of LA-ICP-AES to pharmaceutical tables was presented. The precision of LA-ICP-AES of pharmaceutical tablets depended on the laser parameters and could be improved using signal ratios. Detection limits and precision were satisfactory for trace level analysis.

In Chapter 3, we demonstrated that we could detect natural levels of mercury using LA-ICP-MS to analyze spots along a single hair strand. The spatial resolution of 50 μm (less than a day's growth) achieved by the laser was one that was not previously matched by other techniques for hair analysis. The Hg concentrations along the length of the hair could potentially be monitored using sulfur as an internal standard.

For the first time, the IH-ETV with ICP-MS was successfully used to quantify levels of mercury in single human hair strands, using powdered hair reference materials for calibration. This work was presented in Chapter 4. In Chapter 5, the application of IH-ETV-ICP-MS was expanded to included multielement analysis of powdered hair. Data showed that the method works well for relatively volatile elements using powdered hair reference materials for calibration. Detection limits of all analytes studied were below their natural levels in a single strand of human hair.

The IH-ETV-ICP-AES direct analysis of chromatographic material showed the potential of this technique. Excellent detection limits were obtained using the trapping capability of the material and lower detection limits, by several orders of magnitude appear possible by trapping within the cup (discussed in the next section) and using larger sample volumes.

7.2 Suggestions for future work

Other capabilities of a laser ablation system can be exploited to include other potential applications in the pharmaceutical industry. For example, analysis of layers in metal samples has been performed by depth profiling with the laser [1]. We speculate that layers of coated pharmaceutical tablets could be similarly analyzed by LA-ICP-AES or LA-ICP-MS. With the high sensitivity of ICP-MS, it may be possible to probe tablets for trace metal contamination that can be left in the manufacturing process.

With the multielement capability of LA-ICP-MS, other elements of toxic or nutritional interest (in addition to Hg) can be monitored in hair – an aspect not investigated in the work presented. Due to the technical limitations of our first-generation laser ablation system, we were restricted to ablating numerous spots along the hair strand in order to build the history of Hg along the length of the hair. A more efficient way of profiling the history of Hg exposure would be to continuously ablate along the hair strand. Current laser ablation systems have the necessary control of the sample stage and laser to move along a hair strand without breaking it. Since the publication of the manuscript in Chapter 3, some work in this vein has been continued by another research group [2]. Accurate quantification also remains a problem for the analysis of hair strands

by LA-ICP-MS. Future work could focus on finding or making appropriate matrix-matched reference materials.

While the calibration of IH-ETV-ICP-MS for hair analysis using solid hair reference materials was successful, these expensive materials could be avoided if solution standards can be used instead. As mentioned in Chapter 4 and Appendix D, the main problem preventing the use of solution standards for mercury analysis appears to be the volatility of mercury solutions at room temperature. Trapping the mercury into solution form by binding it to a molecule like cysteine may help.

The ultimate success of using IH-ETV for multielement hair analysis seems to be limited by the temperature achieved by the graphite cup. A moderately volatile analyte such as copper does not appear to completely vaporize at the temperature used (1400°C for the inside of the sample cup). Conventional ETV systems are capable of temperatures of 2500–3000°C. Graphite cups with thinner walls may increase the vaporization temperature by a few hundred degrees, but a more powerful induction furnace than the once used in these studies may be required to achieve the higher temperatures necessary to vaporize other elements.

Future work on the analysis of analyte-laden chromatographic powder by IH-ETV-ICP-AES should focus on determining the effects of other matrix species. Some of these effects were apparent in the results of Chapter 6, for example, as in the analysis of Cd. If a real sample such as seawater is to be analyzed, the effect of ions such as Na, Mg and Ca, that may not be completely removed in the extraction process, should be examined. This method is also not limited to using silica gel as a support. We speculate that the analysis of other extraction/trapping resins should also be feasible by IH-ETV-ICP-AES.

Performing the extraction inside of the graphite sample cup itself is an attractive possibility. It is envisioned that a graphite cartridge containing trapping material could be developed. This graphite cartridge could then be placed directly into the IH-ETV for analysis after the analyte is collected. The graphite would need to be coated (such as a pyrolitic coating [3]) to prevent the solvents/sample from intercalating into the graphite.

7.3 References

1. D. Bleiner, A. Plotnikov, C. Vogt, K. Wetzig and D. Gunther, *Fresenius' Journal of Analytical Chemistry*, 2000, **368**, 221-226.

2. C. Stadlbauer, T. Prohaska, C. Reiter, A. Knaus and G. Stingeder, *Analytical and Bioanalytical Chemistry*, 2005, **383**, 500-508.

3. M. E. Rybak and E. D. Salin, *Journal of Analytical Atomic Spectrometry*, 1998, **13**, 707-713.

Appendix A Experimental design and construction of an electrothermal vaporizer system for direct thermal speciation analysis of mercury in solid samples

A.1 Introduction

A.1.1 Importance of speciation analysis

The mobility, biological availability and toxicity of trace metals in the environment depend not only on their concentrations but also on their chemical form (species). For example, chromium(III) is an essential nutrient required by the body for sugar metabolism, while chromium(VI) is a carcinogen.

As defined by the International Union of Pure and Applied Chemistry, the term "speciation" refers to the distribution of an element's species within a sample [1]. Changes in the environment, whether natural or anthropogenic, can alter the speciation of a metal. Performing speciation analysis to determine the different species of an element within a sample as well as their concentrations can help us understand which chemical and physical transformations are likely to occur in the environment or a biological system. Additionally, pathways of metals in the environment can be determined, as well as their sources and sinks.

A.1.2 Speciation of mercury

Mercury is released into the environment from both natural and anthropogenic sources. Major anthropogenic sources of mercury include mining and smelting, industrial

processes and the combustion of coal. Mercury is released naturally into the environment as elemental mercury or inorganic forms from volcanic activity or the weathering of mercury containing ores. Bacteria present in soil or water can methylate Hg^{2+}, giving methylmercury.

The speciation of mercury, particular between organic forms and inorganic forms of mercury, is of great interest in both environmental and toxicological fields. First, the toxicological profiles of inorganic and organic forms of mercury are different. Organic forms such as dimethylmercury are readily absorbed by the gastrointestinal tract and can easily cross the blood-brain barrier or the placenta by complexation with proteins in the blood. In contrast, inorganic forms are not absorbed to the same extent and do more damage to the kidneys. Second, the form of mercury can dictate where it travels in the environment. The organic forms of mercury can quickly enter and bioaccumulate in the aquatic food chain. This has prompted several organizations, such as Health Canada and the U.S. Environment Protection Agency, to set limits on the consumption of certain species of fish that have accumulated potentially harmful levels of mercury [2, 3].

A.1.3 Methods for speciation analysis of mercury

Analytical techniques commonly used for trace metal determinations such as inductively coupled atomic emission spectroscopy (ICP-AES) and inductively coupled plasma mass spectrometry (ICP-MS) only allow the determination of the total concentration of all species of an element without distinguishing between their different complexes or compounds. Consequently, an additional step is required to separate the elements of their various forms before their quantification in speciation analysis.

A careful choice of solvents can be used to selectively remove species of an element from a sample matrix. The concentrations of the element in the fractions can then be determined by conventional trace metal methods. For example, organic mercury can be removed from a sediment sample using chloroform while HgO can be separated from HgS using different mixtures of acids [4]. Mercury species can also be extracted from sediment samples according to geochemical groups such as water soluble mercury species and organo-chelated species rather than as individual compounds [5]. In both cases, the multi-step extraction process offers the disadvantages of general sample extraction/digestion outlined in Chapter 1.

Chromatographic methods such as gas chromatography (GC) and liquid chromatography (LC) can be used for separating species of an element [6, 7]. Both gas and liquid chromatographs can be coupled to detectors or detection systems suitable for quantifying trace levels of mercury compounds, such as fluorescence detectors [8], microwave-induced plasma atomic emission detectors [9] or ICP instruments [10].

While chromatographic methods are the most common approach for speciation analysis, they have their disadvantages. First, the analytes need to be removed from the sample matrix (using methods such solvent extraction [11], pervaporation [12], or solid phase extraction [13]) prior to injection into a GC or LC system. Depending on the sample, a preconcentration step may be needed to produce concentrations above the detection limit [14]. The extracted analytes usually require a laborious and time-consuming derivatization step to improve their chromatographic characteristics (*e.g.*, peak shape) [15]. The extraction and derivatization steps can also result in species transformation during these steps, leading to errors in determination. While derivatization

can be avoided with LC methods, high amounts of organic solvents in the mobile phase of LC can adversely affect the plasma of an ICP instrument or form carbon deposits on the cones of an ICP-MS.

A.1.4 Proposed method

The solvent leaching protocols and chromatographic hybrid methods both involve using the chemical properties of the compounds of interest in order to perform the speciation analysis.

Alternatively, it is proposed that the physical properties of the species of interest could be exploited to separate them. The boiling points of some common forms of mercury and tin are listed in Table A-1. Considering the range of boiling points of these compounds, it should be possible to separate them using differential vaporization.

The electrothermal vaporizer was discussed in Chapter 1 as a solid sample introduction system for ICP instruments. Hybrid ETV-ICP-AES or ETV-ICP-MS systems combine the advantages of ETV (demonstrated solid sample capabilities, commercially available) with ICP instruments (low detection limits, large linear range). The ETV is temperature-controllable and should be able to perform thermal vaporization of soil or sediment samples in order to differentiate the organic and inorganic forms of mercury.

Table A-1 Physical properties of selected Hg compounds

Element / Compound	Melting Point (°C)	Boiling Point (°C)
Hg	-39[a]	357[a]
$HgCl_2$	276[a]	304[a]
Hg_2Cl_2	sublimates 400[a]	n/a
$(CH_3)_2Hg$	-43[b]	93[b]
CH_3HgCl	170[c]	volatile
HgO	decomposes 500[a]	n/a
HgS	sublimates 584[a]	n/a

a. CRC Handbook 2006
b. National Institute for Occupational Safety and Health
c. Sigma Aldrich

Previous reports in the literature show the potential of a thermal vaporization for the speciation analysis of toxic metals. Both Bombach *et al.* and Windmöller *et al.* showed that a linearly heated soil sample could give off several mercury peaks, though they did not identify or quantify all of the peaks seen [16, 17]. In analyses using graphite furnace atomic absorption spectroscopy, the appearance of two peaks due to different species has been speculated [18]. In ETV-ICP-MS analyses of waste oils, organic and inorganic chlorine has been thermally differentiated and semi-quantified [19]. At the start of this project, there were no published papers in the literature on the use of ETV with ICP for direct thermal speciation analysis of mercury in solid samples. Consequently, the goal of this project were to develop a system using ETV and ICP to study the feasibility of measuring spectrometry organic forms of mercury in soil and sediment samples by differential temperature programming.

A.2 First generation instrument results

Figure A-1 First generation thermal speciation setup

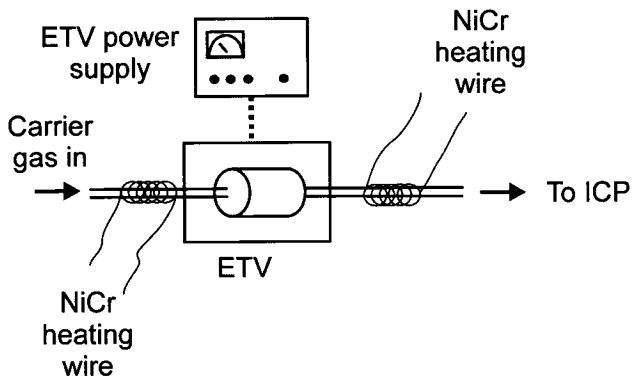

The first instrument setup (shown in Figure A-1) using an ETV coupled to an ICP-AES, was tested by previous members (J. Ren and J. Asselin) of the lab group. They modified the fittings of a graphite furnace designed for an atomic absorption spectrometer (model HGA 2200, Perkin-Elmer, Norwalk, CT, USA) so that it could be coupled to an ICP-AES system (TJA IRIS, Thermo Electron Corp., Franklin, MA, USA) using PTFE tubing. This ETV unit used a a traditional tubular graphite tube. Ni-Cr wire connected to a power supply was wrapped around the transport tubing in order to heat it. The tube transporting the Ar carrier gas (flow rate of 0.7 l min^{-1}) to the ETV was heated to an inside temperature of 130°C so that the Ar would not cool the graphite tube in the ETV, while the transfer tubing between the ETV and the ICP was maintained at an inside temperature of 260°C to prevent condensation of the volatile analytes.

Due to the safety concerns of handling highly toxic organomercury compounds, they tested this system using less toxic halides of similar boiling points as surrogate compounds. Concentrated $NbCl_5$ and $ZrCl_4$ (Sigma Aldrich, Oakville, ON, Canada)

solutions were prepared in anhydrous ethanol (Commercial Alcohol Inc., Brampton, ON, Canada) and injected by syringe.

Their unpublished work showed some flaws with the design. It was found that the reproducibility in the signal was poor for injections of the individual compounds, and that in general they evolved at lower temperatures than their boiling points (254°C for $NbCl_5$, $ZrCl_4$ sublimes at 331°C). The two compounds also could not be temporally resolved with a temperature program when injected as a mixture. It was concluded that poor temperature control of the ETV was the major flaw in the experiment.

A.3 Second generation instrument results

Figure A-2 Second generation thermal speciation setup with second surface trap

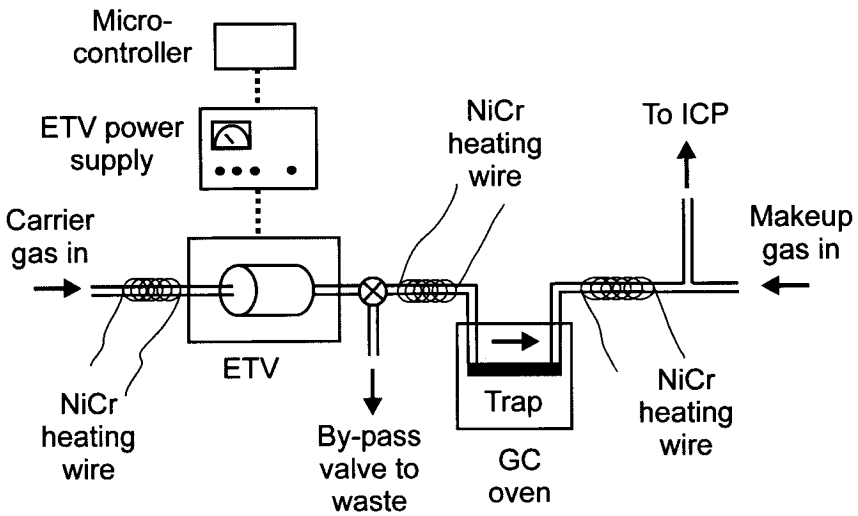

The work described from here on was carried out by the thesis author. New modifications to the system were proposed and are shown in Figure A-2.

One factor leading to poor temperature control was the original interface on the ETV's power supply. The temperature program of the ETV was set by the user via knobs. It was found that the manual positioning of the knobs themselves could result in a temperature discrepancy of ± 50°C. Therefore, modification of the ETV power supply to add a digitally-controlled interface was needed to improve its accuracy and precision.

The knobs of the power supply turned potentiometers in the power supply's circuit. Turning these potentiometers varied the voltage of the circuit, which correlated to the temperature of the ETV during a heating stage, as well as the heating time. These manual potentiometers were replaced with digital potentiometer chips (AD7376, Analog Devices, Norwood, MA, USA). The digital potentiometers were set by micro-controller

(BASIC Stamp SX, Parallax Inc, Rockland, CA, USA). A computer program (example shown in Figure A-3) stating the desired temperatures and heating times of the temperature program for the ETV was stored in the microcontroller's memory. The circuit diagram of the complete digital control unit (built-in house by the author and I. Levesque) for the ETV power supply is shown in Figure A-4.

Figure A-3 Sample code for controlling the digital ETV controller

```
'{$STAMP BS2e}
'Digital potentiometer for ETV temperature control

SIGdry VAR Word
SIGchar VAR Word
SIGatom VAR Word

SDIdry CON 2
'CLKdry con 3
'CSdry con 4
'low CSdry

SDIchar CON 6
'CLKchar con 7
'CSchar con 8
'low Cschar

SDIatom CON 10
CLK CON 11
CS CON 12
LOW CS

'Signal for drying cycle
'Possible values are 0-128, which corresponds to 0-3000 degC
SIGdry=5
SHIFTOUT SDIdry, CLK, MSBFIRST,[SIGdry\7]
PULSOUT CS, 150

'Signal for charring cycle
SIGchar=20
SHIFTOUT SDIchar, CLK, MSBFIRST,[SIGchar\7]
PULSOUT CS, 150

'Signal for atomizing cycle
SIGatom=100
SHIFTOUT SDIatom, CLK, MSBFIRST,[SIGatom\7]
PULSOUT CS, 150
```

Figure A-4 Circuit diagrams of the digital control of the ETV power supply

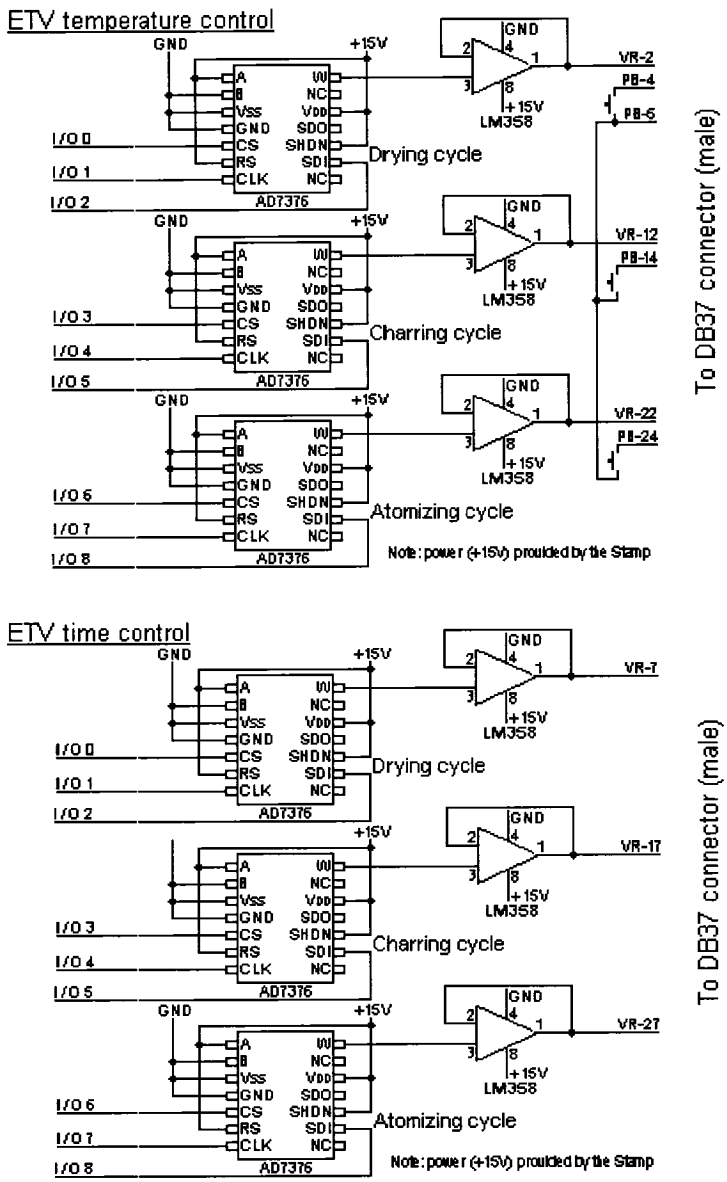

It was also speculated that an even heating process for a solid sample such as soil might not be possible given the narrow range of temperatures seen between some species in Table A-1. The graphite tube itself may not be evenly heated. Furthermore, even if one knew the surface temperature, this did not mean that this temperature would be transferred uniformly through the solid material, especially given that the gas flowing over the sample might act as cooling mechanism.

If that is the case, an additional component is needed – an analyte trap. In this configuration, the sample placed in the ETV would be gently heated at a temperature high enough to vaporize all mercury species from the sample matrix. The vaporized analytes would then be trapped on a second surface (such as a cooled segment of fused silica tubing). This concept of second surface trapping for ETV has been demonstrated in the literature [20-22]. The adsorbed mercury species could then be selectively vaporized from the trap and then detected by ICP. The trap could be housed in a GC oven (HP5700, Hewlett-Packard, USA), which was found to have suitable temperature control in the range required (Figure A-5).

Figure A-5 Calibration of the GC oven

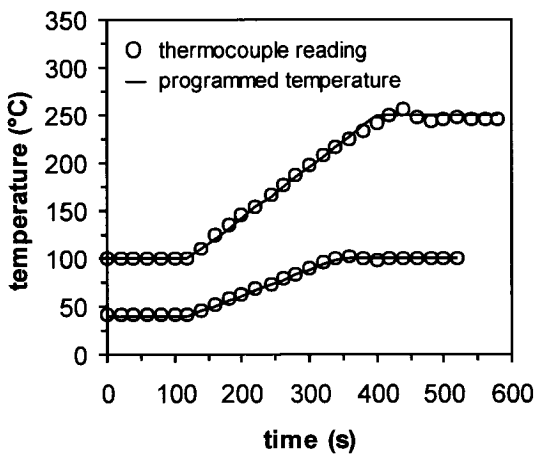

The transient profiles of the mercury species as they evolved from the trap could potentially be modelled using desorption kinetics according to the Polanyi-Wigner equation:

Equation A-1

$$\frac{dM_{gas}}{dt} = -\frac{d\theta_M}{dt} = \nu_{des}\theta^n \exp\left(-\frac{E_{des}}{RT}\right)$$

where:
M_{gas} = the number of molecules in the gas phase
t = time (t)
T = temperature (K)
υ_{des} = pre-exponential factor of desorption from the surface (s^{-1})
θ = number of molecules
n = order of reaction
E_{des} = activation energy of desorption ($kJ \cdot mol^{-1}$)
R = gas constant ($kJ \cdot mol \cdot K^{-1}$)

Equation A-1 is used to describe the transient profile of desorbed analytes in thermal desorption spectroscopy (also known as temperature programmed desorption) [23-25]. Holcombe *et al.* have also modeled desorption of analytes in a graphite tube furnace based on this equation [26-29].

While this designed provided considerable improvements in temperature control, further problems were encountered in preliminary experiments with soil samples. First, the original "dosing hole" of this ETV system was designed for syringe or micropipette delivery of solution samples and was not large enough to accommodate a spatula of solid sample. Also, it was difficult to reproducibly place a solid sample within the furnace via insertion of a spatula through the end of graphite tube of this system. Secondly, the age of the commercial ETV system had become a problem. The precision-machined graphite

components of the system that required replacement on this system (such as the contact electrodes) were no longer available from suppliers.

A.4 Third generation instrument results

Figure A-6 Schematic of the induction-heating electrothermal vaporizer

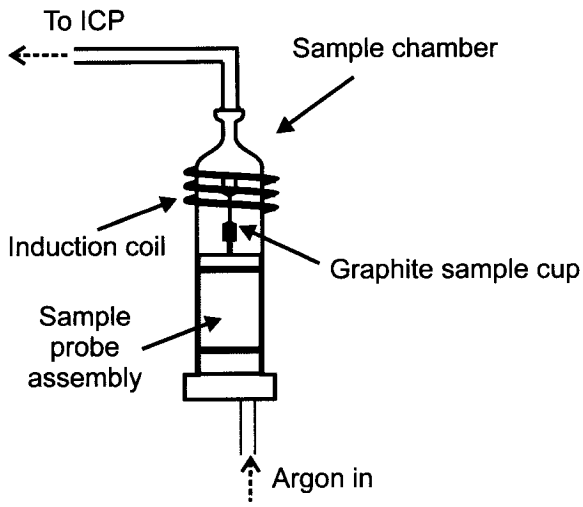

While the use of a commercial ETV was attractive in that the developed setup would potentially be easy for other labs to adopt using their own ETV systems, it was obvious that the traditional graphite tube design of the ETV in our lab was not convenient for solid sample analysis. Therefore the ETV was replaced with an IH-ETV system (modified Leco 521 Induction furnace, LECO, St. Joseph, MI, USA) developed in-house [30, 31]. A schematic of this system is shown in Figure A-6. The design of the sample holder assembly and the graphite cups that hold the sample allowed easy insertion of a solid sample into the system. It could also hold larger samples (up to one gram versus mg size in the ETV), thereby also potentially improving detection limits. This device has been used for soils analysis in a slurry form although at much higher temperatures and for the determination of different analytes than those proposed in this project.

Preliminary work by the author of this thesis while studying reference material BCR 580 (Estuarine soil, 132 ppm total Hg, 75 ppb methyl-Hg, IRMM, Belgium) by IH-ETV coupled to an ICP-MS (Perkin Elmer Elan 5000, SCIEX, Concord, Ontario, Canada) showed that total Hg could be determined with isothermal heating of 6 mg of soil at 750°C (Figure A-7).

Figure A-7 ^{202}Hg signal from BCR 580 heated at 750°C

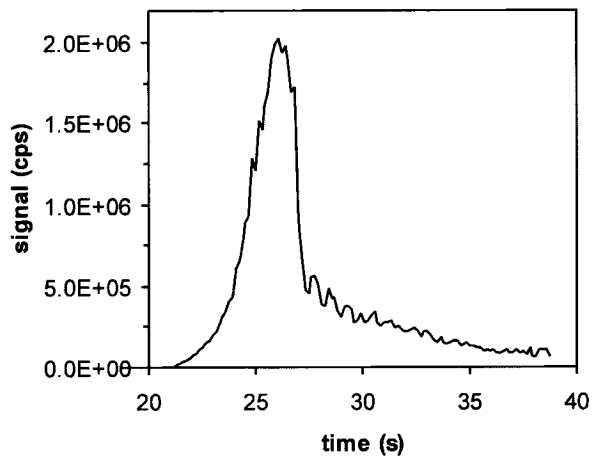

When a temperature program (200°C between 5 s and 65 s, 800°C between 85-145 s, no heat applied to the cup during other times in the acquisition) was applied to attempt to differentiate the volatile organic forms from the less volatile inorganic forms of mercury, several peaks were seen (Figure A-8). Due to their boiling points and the relative concentrations, we would expect a small peak for methyl-Hg when 200°C is applied, followed by a larger peak(s) for the inorganic Hg at 800°C. The study shows that there may be other forms of Hg coming off the sample at the lower temperature.

Figure A-8 ^{202}Hg signal from BCR 580 heated with a temperature program

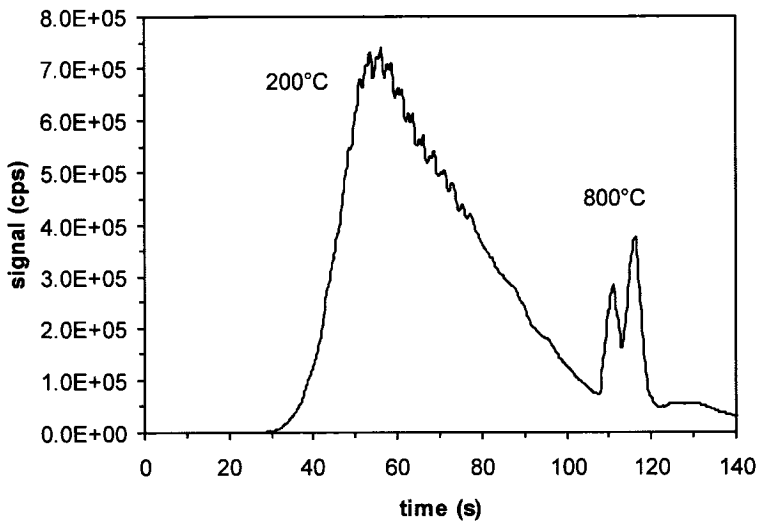

During the undertaking of this project in late 2002, another research group published a paper on thermal vaporization for speciation analysis of mercury [32]. Gelaude *et al.* reported the use of ETV-ICP-MS for direct determination of methylmercury and inorganic mercury in biological reference materials. They had already investigated several calibration techniques, and were successful in quantification using a gas phase isotope dilution technique. The similarity between the proposed project and their research led us to abandon this aspect of our studies.

A.5 References

1. D. M. Templeton, F. Ariese, R. Cornelis, L.-G. Danielsson, H. Muntau, H. P. Van Leeuwen and R. Lobinski, *Pure and Applied Chemistry*, 2000, **72**, 1453-1470.

2. Health Canada, *Information on mercury levels in fish (2002-41)*, 2002, available at http://www.hc-sc.gc.ca/ahc-asc/media/advisories-avis/2002/2002_41_e.html, accessed on August 23, 2006

3. U.S. Food and Drug Administration and U.S. Environmental Protection Agency, *2004 EPA and FDA Advice For: Women Who Might Become Pregnant, Women Who are Pregnant, Nursing Mothers, and Young Children (EPA-823-R-04-005)*, 2004, available at http://www.cfsan.fda.gov/~dms/admehg3.html, accessed on August 23, 2006

4. H. Sakamoto, T. Tomiyasu and N. Yonehara, *Analytical Sciences*, 1992, **8**, 35-39.

5. N. S. Bloom, E. Preus, J. Katon and M. Hiltner, *Analytica Chimica Acta*, 2003, **479**, 233-248.

6. C. F. Harrington, *TrAC, Trends in Analytical Chemistry*, 2000, **19**, 167-179.

7. R. Lobifiskia and F. C. Adams, *Spectrochimica Acta, Part B: Atomic Spectroscopy*, 1997, **52B**, 1865-1903.

8. E. Bramanti, C. Lomonte, M. Onor, R. Zamboni, A. D'Ulivo and G. Raspi, *Talanta*, 2005, **66**, 762-768.

9. I. R. Pereiro and A. C. Diaz, *Analytical and Bioanalytical Chemistry*, 2002, **372**, 74-90.

10. P. Jitaru, H. Goenaga Infante and F. C. Adams, *Analytica Chimica Acta*, 2003, **489**, 45-57.

11. I. R. Pereiro, A. Wasik and R. Lobinski, *Journal of Analytical Atomic Spectrometry*, 1998, **13**, 743-747.

12. D. W. Bryce, A. Izquierdo and M. D. Luque de Castro, *Analytical Chemistry*, 1997, **69**, 844-847.

13. J. Munoz, M. Gallego and M. Valcarcel, *Journal of Chromatography, A*, 2004, **1055**, 185-190.

14. H. Emteborg, D. C. Baxter and W. Frech, *Analyst (Cambridge, United Kingdom)*, 1993, **118**, 1007-1013.

15. E. Bulska, D. C. Baxter and W. Frech, *Analytica Chimica Acta*, 1991, **249**, 545-554.

16. G. Bombach, K. Bombach and W. Klemm, *Fresenius' Journal of Analytical Chemistry*, 1994, **350**, 18-20.

17. C. C. Windmoeller, R. D. Wilken and W. d. F. Jardim, *Water, Air, and Soil Pollution*, 1996, **89**, 399-416.

18. D. C. Hassell, T. M. Rettberg, F. A. Fort and J. A. Holcombe, *Analytical Chemistry*, 1988, **60**, 2680-2683.

19. P. Richner and S. Wunderli, *Journal of Analytical Atomic Spectrometry*, 1993, **8**, 45-49.

20. A. J. Scheie and J. A. Holcombe, *Journal of Analytical Atomic Spectrometry*, 1994, **9**, 415-417.

21. P. Hocquellet, *Spectrochimica Acta, Part B: Atomic Spectroscopy*, 1992, **47B**, 719-729.

22. T. M. Rettberg and J. A. Holcombe, *Analytical Chemistry*, 1986, **58**, 1462-1467.

23. D. H. Parker, M. E. Jones and B. E. Koel, *Surface Science*, 1990, **233**, 65-74.

24. A. M. De Jong and J. W. Niemantsverdriet, *Surface Science*, 1990, **233**, 355-365.

25. X. Zhao, R. A. Outlaw, J. J. Wang, M. Y. Zhu, G. D. Smith and B. C. Holloway, *The Journal of chemical physics*, 2006, **124**, 194704.

26. O. A. Guell and J. A. Holcombe, *Journal of Analytical Atomic Spectrometry*, 1992, **7**, 135-140.

27. T. E. Histen, O. A. Guell, I. A. Chavez and J. A. Holcombe, *Spectrochimica Acta, Part B: Atomic Spectroscopy*, 1996, **51B**, 1279-1289.

28. G. Ertas and J. A. Holcombe, *Journal of Analytical Atomic Spectrometry*, 2005, **20**, 687-695.

29. J. A. Holcombe, G. D. Rayson and N. Akerlind, Jr., *Spectrochimica Acta, Part B: Atomic Spectroscopy*, 1982, **37B**, 319-330.

30. D. M. Goltz and E. D. Salin, *Journal of Analytical Atomic Spectrometry*, 1997, **12**, 1175-1180.

31. M. E. Rybak and E. D. Salin, *Spectrochimica Acta, Part B: Atomic Spectroscopy*, 2001, **56B**, 289-307.

32. I. Gelaude, R. Dams, M. Resano, F. Vanhaecke and L. Moens, *Analytical Chemistry*, 2002, **74**, 3833-3842.

Appendix B Additional figures for the LA-ICP-AES and LA-ICP-MS of pharmaceutical tablets

A simplified schematic of the laser ablation system used is shown in Figure B-1.

Figure B-1 Schematic of the CETAC LSX-100 laser ablation system

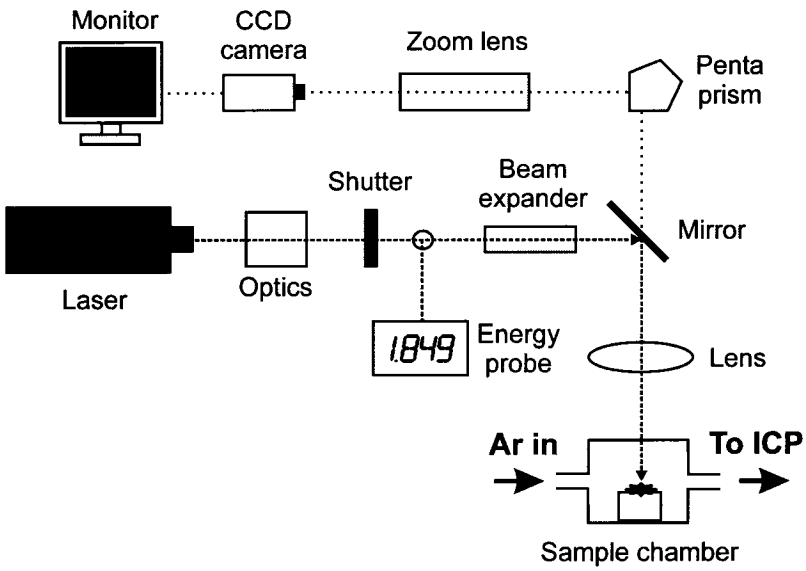

The following data (Figure B-2 and Figure B-3) was made available with the manuscript in Chapter 2 as "Electronic Supplementary Information". This data can be accessed from the website of the "Journal of Analytical Atomic Spectrometry" at:

http://www.rsc.org/suppdata/ja/b3/b314732k/

Figure B-2 Images of ablation craters. (a) tablet surface showing ablation sites, (b) the laser is focused on the surface, (c) the laser is focused 2 mm below the surface (E = 1.8 mJ, 50 shots per site in all cases)

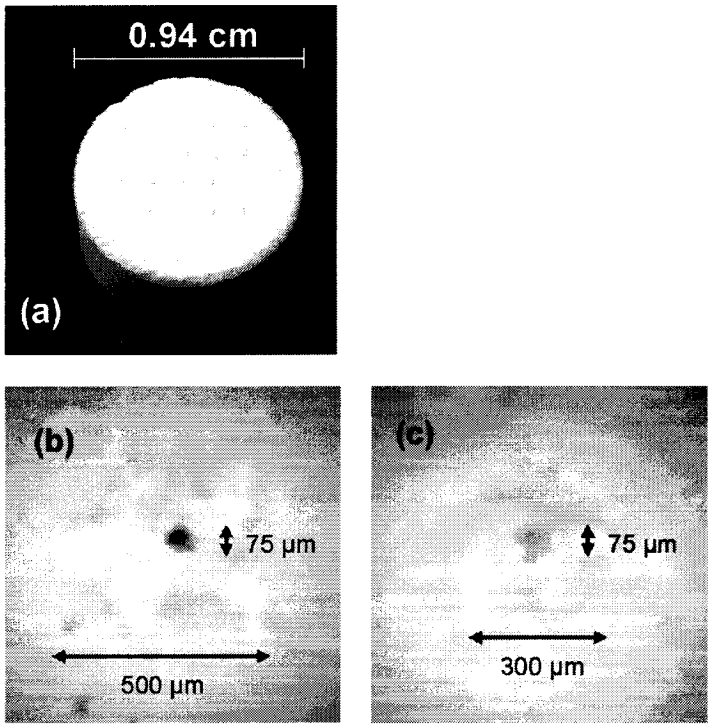

Figure B-3 Ablation trenches formed by the continuous scanning method with scan rates of (a) 10 μm s^{-1}, (b) 20 μm s^{-1}, (c) 50 μm s^{-1}, and (d) 150 μm s^{-1}. The trench width is approximately 75 μm wide. All photos are to the same scale.

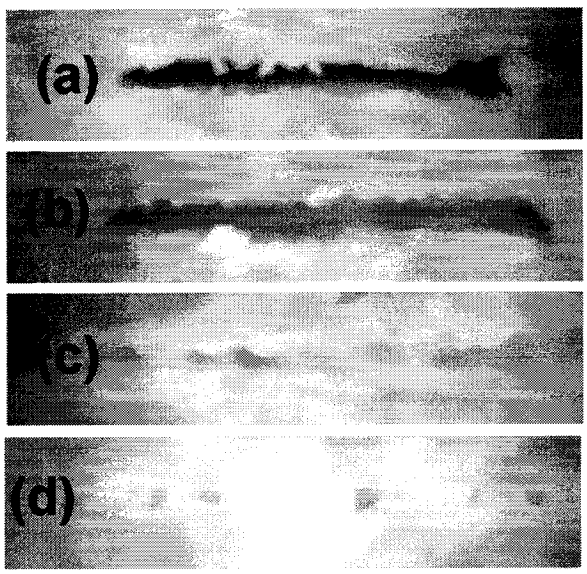

Appendix C Additional experimental details for the detection of mercury in human hair by LA-ICP-MS

The operating conditions of the ICP-MS are shown in Table C-1.

Table C-1 Instrument operating parameters

ICP-MS	
RF power	1000 W
Sampling and skimmer cones	Nickel
Plasma gas flow rate	15 l min^{-1} Ar
Auxiliary gas flow rate	1.2 l min^{-1} Ar
Carrier gas flow rate	0.8 l min^{-1} Ar
Signal measuring parameters	
Detector mode	Pulse
Acquisition mode	Peak hopping
Sweeps per reading	1
Readings per replicate	1000
Replicates	1
MCA channels	1 for each isotope
Dwell time	22-30 ms for each isotope
Total acquisition time	100 s

Appendix D Additional experimental details for direct mercury analysis of human hair by IH-ETV-ICP-MS

D.1 The IH-ETV system and sample cups

Detailed schematics showing the set-up of the IH-ETV instrumentation are shown in Figure D-1 and Figure D-2. These images were modified from the original figures that appear in the paper describing the characterization of this IH-ETV system by Rybak and Salin [1]. Dimensions of the Bay Carbon graphite electrodes used as sample cups can be found in Figure D-3. (Note that these three figures are not drawn to scale.)

Figure D-1 Set-up of the IH-ETV system with the water sparger

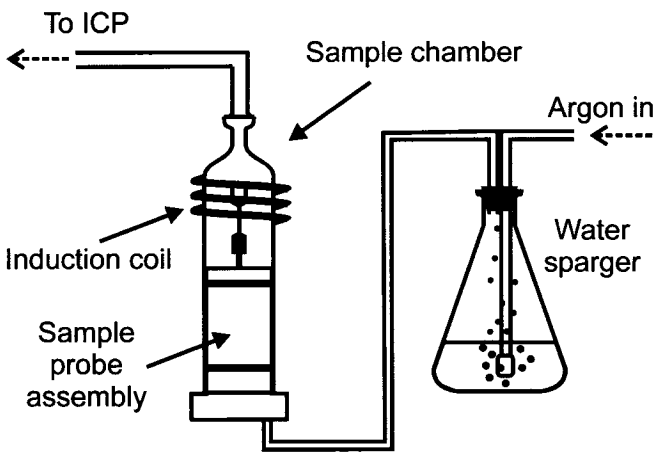

Figure D-2 Details of the sample probe assembly

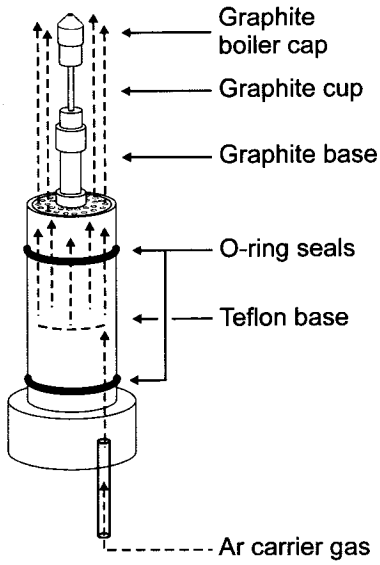

Figure D-3 Dimensions of (a) the S-16 graphite cup and (b) the BC-1 boiler cap

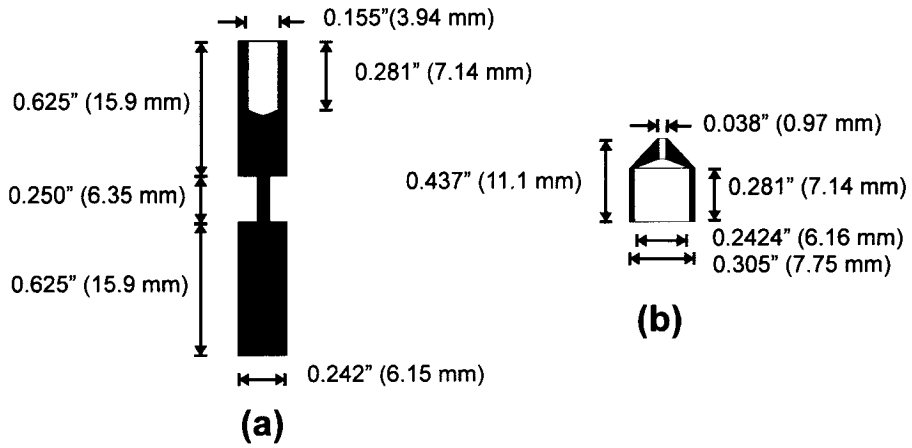

D.2 Instrument parameters

The operating parameters for the Elan 6000 ICP-MS system can be found Table D-1. ^{34}S was monitored as a potential internal standard but was not ultimately used in any final calculations.

Table D-1 ICP-MS operating parameters

ICP-MS	
RF power	1100 W
Sampling and skimmer cones	Nickel
Plasma gas flow rate	15 l min^{-1} Ar
Auxiliary gas flow rate	1.2 l min^{-1} Ar
Carrier gas flow rate	0.5 l min^{-1} Ar
Signal measuring parameters	
Detector mode	Analog
Acquisition mode	Peak hopping
Sweeps per reading	1
Readings per replicate	500
Replicates	1
MCA channels	1
Dwell time	50 ms per isotope
Total acquisition time	100 s
Isotopes measured	^{34}S, ^{197}Au, ^{200}Hg and ^{202}Hg

D.3 Boiler caps

Previous applications of this IH-ETV system where a graphite cup was used to hold a liquid or slurried sample have not required a boiler cap [1-4]. Initially, the same approach was tried for hair samples. However, several problems were encountered.

First, even relatively small amounts of loose powdered hair samples (less than one milligram) placed in an open graphite cup often caused the plasma of the ICP-MS to extinguish when power was applied to the IH-ETV. When the gas present inside the cup was heated, it underwent expansion. This gas expansion likely expelled the powder from the cup, where it traveled to the plasma mostly as a solid instead of vaporized material. This caused the plasma to overload and extinguish. It is not possible to record any signal when the plasma is doused during the data acquisition. It is only occasionally that a powdered hair sample did not extinguish the plasma and a transient signal could be measured.

Figure D-4 shows the transient peaks of powdered hair samples in graphite cups with and without a graphite cup. While the signals in part (a) and (b) were obtained from different powdered hair reference materials, they illustrate the typical peaks seen for all powdered hair samples. A broad peak covering a time span of over 100 seconds is observed when a boiler cap is not used. A small initial peak is the result of material expelled when power is initially applied to the cup. The rest of the powder sample gradually made its way to the ICP-MS. A disadvantage of the wide peak width is that it increases the analysis time required per sample. The increased peak width also results in lower peak heights, which can potentially degrade detection limits if peak heights are used for calibration. In contrast, when a boiler cap covers the graphite cup, a sharp

transient peak with a peak width of about five seconds is seen. In this case, the bulk of the sample is contained in the cup while the Hg is vaporized and transported to the ICP-MS as a discrete "plug" to give an excellent transient peak shape.

Figure D-4 Transient signal for ^{202}Hg of a powdered hair sample placed in (a) an open graphite cup and (b) a graphite cup closed with a boiler cap.

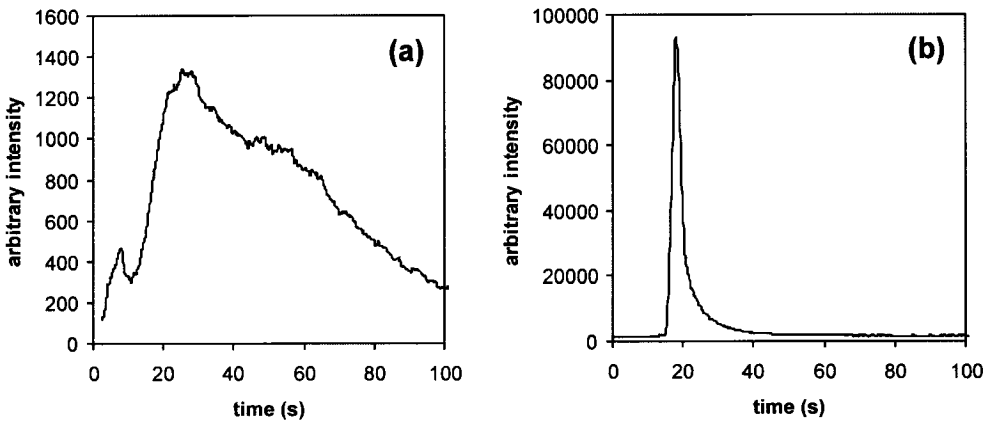

The boiler cap is also necessary when hair strands are used. To be placed in the graphite cup, the individual 12-cm hair strands were usually coiled or rolled into a loose ball. When power was applied to the RF coil to heat the cup, the coiled or balled-up hair strand could be ejected from the graphite cup before analyte vaporization can occur. In this case, no signal was seen and the hair strand sample was found at the bottom of the sample chamber. The boiler cap was therefore necessary to keep the hair strand inside of the graphite cup during the complete heating process.

D.4 Hg solutions

A volume of 10 µl was chosen for the solution samples as it was the smallest amount that did not cause the boiler cap to blow off from the sample cup upon heating. The amount of water in 25, 50 and 100 µl volumes would boil violently, causing the boiler cap to eject and the sample to splatter. While slowly drying the larger solution volume in the cup was considered (*e.g.*, offline in a drying oven, a hot plate or online using the IHV), there were concerns of analyte loss due to the volatility of mercury.

External standard calibration was attempted using mercury calibration solutions (10 µl of 0.5, 1.0 or 1.5 µg g^{-1} of Hg in 1% HNO_3). Lower mercury signals (or sometimes no signal at all!) were usually observed in comparison to solid samples containing an equivalent amount of mercury. Poor precision for replicates (*e.g.*, 41% RSD, n=9) and poor linearity for calibration plots ($R^2 < 0.90$) were also noted.

The precision of the micropipette was measured, to determine if it was a major contributor to the imprecision of the Hg solution analyses. Five replicate 10 µl volumes of 1% HNO_3 dispensed from the micropipette were weighed. The relative standard deviation was determined to be 1.6%. Therefore, the pipette is not the major source of imprecision.

It was observed that the solution would sometimes seep into the walls or the bottom of the graphite cup. It was possible that mercury was being absorbed and trapped by the graphite, and might require a higher heating temperature to be released. After cups containing mercury solution underwent the analysis at 800°C, the cups were reheated at maximum power (outside wall temperature = 1400°C, inside temperature = 1600°C). During these reheating stages at higher temperature, no further mercury signal was seen. Therefore it is unlikely that Hg was still present in the inner portion of the cup.

It was also possible that the 8.8 mm thickness at the bottom of the cup's well, where the sample is placed, might make it difficult for any seeped mercury to escape. However, experiments using graphite cups with a much thinner wall/base thickness (about 0.25 mm) showed the same trend of lower or no mercury signals. It was concluded that mercury leaching into the cup was not a factor, though a comparison between these graphite cups with graphite cups with a less porous surface (such as those that are pyrolytically coated) would confirm this conclusion.

Since the samples are placed in the graphite cup *ex-situ* of the actual IH-ETV system, samples can be prepared ahead of time and be allowed to sit on a lab bench prior to analyses. An additional experiment was performed to determine if the mercury was simply evaporating from the sample cups prior to the analyses. Replicates of 10 µl of 1.0 µg g^{-1} of Hg solution (10 ng Hg) were analyzed with different waiting times prior to analysis. During the wait period, the graphite cups containing the solution were left exposed to the atmosphere. Figure D-5 shows the relationship between the measured Hg signal with relation to the waiting time for the sample. A decay in the measured mercury signal is seen over time.

Figure D-5 Loss of mercury over a period of time

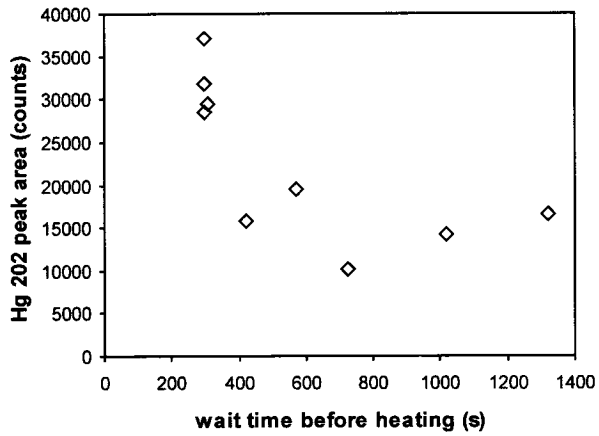

The use of Hg solutions for calibration may be possible if the evaporation of the Hg from the solution could be prevented. For solutions analyzed as quickly as possible, the measured peak area was almost the same as the peak area for a powdered hair sample containing the same amount of mercury. A possible approach is to add a substance to the calibration solutions that will bind to the mercury, making it less likely to evaporate from the solution. Cysteine is a potential candidate, as the sulfur group in its structure is known to bind effectively to mercury. Due to its bonding capabilities, it is often used in merury extraction procedures to reduce the memory effect of mercury in ICP instruments [5-7]. Cysteine is an attractive candidate as it is also likely a binding site for mercury in hair.

D.5 References

1. M. E. Rybak and E. D. Salin, *Applied Spectroscopy*, 2001, **55**, 816-821.

2. D. M. Goltz and E. D. Salin, *Journal of Analytical Atomic Spectrometry*, 1997, **12**, 1175-1180.

3. D. M. Goltz, C. D. Skinner and E. D. Salin, *Spectrochimica Acta, Part B: Atomic Spectroscopy*, 1998, **53B**, 1139-1147.

4. M. E. Rybak and E. D. Salin, *Spectrochimica Acta, Part B: Atomic Spectroscopy*, 2001, **56B**, 289-307.

5. L. Magos, *The Analyst*, 1971, **96**, 847-853.

6. W. Chen, P. Wee and I. D. Brindle, *Journal of Analytical Atomic Spectrometry*, 2000, **15**, 409-413.

7. Y. Li, C. Chen, B. Li, J. Sun, J. Wang, Y. Gao, Y. Zhao and Z. Chai, *Journal of Analytical Atomic Spectrometry*, 2006, **21**, 94-96.

Appendix E Waivers from co-authors of published manuscripts

This appendix contains copies of waivers from manuscript co-authors, as well as permission from the Royal Society of Chemistry to include to following manuscripts in this thesis:

"Analysis of pharmaceutical tablets by laser ablation inductively coupled plasma atomic emission spectrometry and mass spectrometry (LA-ICP-AES and LA-ICP-MS)", **Rebecca Lam** and Eric D. Salin, *Journal of Analytical Atomic Spectrometry*, 2004, 19(7), 938-940.

"Direct detection of mercury in single human hair strands by laser ablation inductively coupled plasma mass spectrometry (LA-ICP-MS)", Melissa Legrand, **Rebecca Lam**, Madeleine Jensen-Fontaine, Eric D Salin, and Hing Man Chan, *Journal of Analytical Atomic Spectrometry*, 2004, 19(10), 1287-1288.

"Induction heating-electrothermal vaporization for direct mercury analysis of a single human hair strand by inductively coupled plasma mass spectrometry", Josiane P. Lafleur, **Rebecca Lam**, Hing Man Chan, and Eric D. Salin, *Journal of Analytical Atomic Spectrometry*, 2005, 20(12), 1315-1317.